

SEASONAL CHANGES IN THE GLOBAL ATMOSPHERIC
ENERGY BALANCE AND RESULTS FOR RESTRICTED REGIONS

by

DAYTON G. VINCENT
A.B., University of Rochester
(1958)
M.Sc., University of Oklahoma
(1964)

SUBMITTED IN PARTIAL FULFILLMENT
OF THE REQUIREMENT FOR THE
DEGREE OF DOCTOR OF
PHILOSOPHY
at the
MASSACHUSETTS INSTITUTE OF TECHNOLOGY

(November 12, 1969)
i. e. Feb. 1970

Signature of Author

Department of Meteorology, 12 November 1969

Certified by

Thesis Supervisor

Accepted by

Chairman, Departmental Committee on Graduate
Students

Lindgren

WITHDRAWN

MASS. INST. TECH.

FROM
JAN 20 1970

SEASONAL CHANGES IN THE GLOBAL ATMOSPHERIC
ENERGY BALANCE AND RESULTS FOR RESTRICTED REGIONS

by

Dayton G. Vincent

Submitted to the Department of Meteorology on 12 November
1969 in partial fulfillment of the requirements for the
degree of Doctor of Philosophy

ABSTRACT

An observational approach is used to investigate seasonal changes in the atmospheric energy balance. Results are given for 1000-100 mb for the globe, Northern Hemisphere, Southern Hemisphere, tropics and extratropical Northern Hemisphere. In the latter region the data was sufficient to extend the analyses up to 10 mb. Factors governing the temperature distribution are also discussed as they form an integral part of the investigation and provide a check on the consistency of the results.

The vertical distribution of latent heat release is estimated, based on a cloud weighting scheme at middle and high latitudes and theoretical studies near the equator. Net diabatic heating rates are obtained by combining the latent heat release with radiative heating rates presented by Rodgers and boundary layer heating given by Budyko. A dominant feature in all seasons is the maximum heating in the middle troposphere near the equator which is associated with latent heat release in the ascending branch of the Hadley circulation.

Diabatic heating rates are used to compute the generation of zonal available potential energy (AZ). Global values indicate that over the long run radiation destroys AZ while latent heat release and boundary layer heating produce AZ. In the tropics the destruction of AZ due to radiative processes is balanced by a production due to latent heat release; boundary layer heating, although comparatively small, is essentially responsible for the net generation. In middle

and high latitudes radiation produces AZ in all seasons except summer; the other components are small and the net generation is approximately equal to that given by radiative heating alone. In the Northern Hemisphere it appears that the generation of eddy available potential energy (AE) is much smaller than the generation of AZ, although daily fluctuations of the former were not available.

The conversion from available potential energy to kinetic energy is primarily due to eddy processes. AZ is converted to AE in all seasons and almost all of the conversion takes place outside the tropical regions. The conversion from AE to eddy kinetic energy (KE) was not computed, but values given by Jensen suggest that most of the AE is converted to KE. There is also a conversion from KE to zonal kinetic energy (KZ) in all seasons. Mean motions, although secondary, are a significant factor in seasonal changes in the energy budget, particularly at low latitudes in the winter hemisphere where the Hadley circulation converts AZ to KZ. The Ferrel cell causes a conversion from KZ to AZ in middle latitudes.

Frictional losses appear to occur mainly through dissipation of KE. There is reasonable compatibility between the generation rates computed herein and the dissipation rates estimated from conversions to KE and KZ.

Thesis Supervisor: Reginald E. Newell
Title: Professor of Meteorology

ACKNOWLEDGEMENTS

The author is most grateful to his advisor, Professor Reginald E. Newell, for his advice and enthusiasm during the research. He is also grateful to his former colleague, Dr. John W. Kidson, who processed the tropical data and whose helpful suggestions were always available. In addition he wishes to thank Captain Thomas G. Dopplick and Major David Ferruzza for their contributions to the discussion of the atmospheric energy balance. He specifically thanks Captain Dopplick for his formulation of Sections 6.3 and 6.4 which will appear in a future publication.

The research was supported by the United States Atomic Energy Commission under contract AT (30-1) 2241. The manuscript would have been difficult to accomplish without considerable technical assistance for which the writer is most thankful to Mrs. Susan Ary who helped prepare the data at middle and high latitudes and who plotted most of the results. He also thanks Mrs. Dorothy Berry and Miss Susan Davis for their kind assistance. He extends his appreciation to Miss Diane Lippincott who typed the manuscript and to Miss Isabelle Kole and Mr. Steven Ricci who prepared the figures.

Finally the author expresses his deepest affection to his wife and children for their understanding and endurance while he was a student.

TABLE OF CONTENTS

CHAPTER 1:	INTRODUCTION	9
CHAPTER 2:	DATA SOURCES AND PROCESSING	
	2.1 Data Sources	12
	2.2 Data Processing	14
CHAPTER 3:	DIABATIC HEATING	
	3.1 Radiative Heating Rates	16
	3.2 Latent Heat Release	17
	3.3 Boundary Layer Heating	23
CHAPTER 4:	GLOBAL CIRCULATION	
	4.1 Temperature Field	28
	4.2 Zonal Wind Field	32
	4.3 Mean Meridional Circulations	35
	4.4 Horizontal Eddy Transport of Momentum	40
	4.5 Horizontal Eddy Transport of Sensible Heat	42
CHAPTER 5:	TEMPERATURE CHANGES	
	5.1 Diabatic Heat Sources	57
	5.2 Adiabatic Subsidence	59
	5.3 Eddy Heat Flux Convergence	62
	5.4 Atmospheric Heat Balance	63
CHAPTER 6:	ATMOSPHERIC ENERGY BUDGET	
	6.1 Available Potential Energy	83
	6.2 General Equations for Energy Balance	85

	6.
6.3 Treatment of Restricted Regions	90
6.4 Zonal and Eddy Forms of Energy	92
6.5 Global Energy Budget	96
6.6 Northern Hemisphere vs Southern Hemisphere	106
6.7 Tropics vs Higher Latitudes	111
6.8 Extratropical Troposphere vs Stratosphere	115
CHAPTER 7: CONCLUDING REMARKS AND UNRESOLVED PROBLEMS	135
TABLES 3.1-4.4	139
REFERENCES	166
BIOGRAPHICAL NOTE	174

DEFINITION OF SYMBOLS

a	radius of earth, assumed to be 6.378×10^8 cm
c_p	specific heat at constant pressure
f	$2\Omega \sin \phi$, Coriolis parameter
g	acceleration due to gravity
p	atmospheric pressure
p_0	pressure at 1000 mb
t	time
u	east-west wind component, positive eastwards
u_g	geostrophic east-west wind component, positive eastwards
v	north-south wind component, positive northwards
w	vertical velocity, positive upwards
z	geopotential height
D_H	eddy diffusion of heat
F_p	frictional force per unit mass vector on a constant pressure surface
F_λ, F_ϕ	frictional force per unit mass in eastward, northward directions
N	$1 - p^k P^k$, efficiency factor
P_r	reference pressure, global mean pressure on an isentropic surface
Q	total diabatic heating
R_d	gas constant for dry air
T	temperature
V_p	horizontal wind vector on a constant pressure surface

dm	$g^{-1} a^2 \cos \phi d\phi d\lambda dp$, an element of mass
dS	$a^2 \cos \phi d\phi d\lambda$, an element of horizontal area
α	specific volume
β	stability parameter, defined in Eq. (5.1)
γ	stability factor, defined in Eq. (6.14)
θ	potential temperature
κ	R_d/c_p
λ	longitude, positive eastwards
ρ	atmospheric density
ϕ	latitude, positive northwards
ω	vertical velocity, dp/dt , in a pressure coordinate system
Γ	existing lapse rate of temperature
Γ_d	dry adiabatic lapse rate of temperature
ϕ	gz
Ω	earth's angular velocity
∇_p	horizontal gradient on a constant pressure surface
overbar	time average
prime	deviation from time average
[]	average around a latitude band
asterisk	longitudinal deviation from []
[\sim]	global average on a constant pressure surface
[]''	latitudinal deviation from [\sim]
[$\overline{x'y'}$]	transient eddy
[$\overline{x^*y^*}$]	standing eddy

CHAPTER 1
INTRODUCTION

There have been numerous articles in the literature concerned with the general circulation and heat and energy balances of the atmosphere. A monograph published by the World Meteorological Organization and written by Lorenz (1967) offers one of the more comprehensive reviews on these subjects. Lorenz discusses the problem of explaining the observed circulation, not only as seen today but as noted over 200 years ago by Edmund Halley (1686) and George Hadley (1735). He includes discussions of observational, theoretical and numerical model aspects of the circulation, processes which maintain it and the energetics of the atmosphere. Another notable contribution based mainly on observational studies is a collection of 76 papers on the momentum, energy and water vapor budgets of the atmosphere, edited by Starr and Saltzman (1966).

Not until recently have sufficient data become available in the tropics and data paucity has always been a problem in extratropical regions in the Southern Hemisphere because of the vast ocean areas. Recent research programs, such as the Line Islands Experiment and the Barbados Oceanographic and Meteorological Experiment (BOMEX), have stressed tropical circulations over ocean areas and air-sea interactions. Riehl (1969) compares the role of the tropics in the general circulation of the atmosphere, as he sees it today, with his views on the same subject nearly 20 years ago (Riehl, 1950). His

discussion includes comments on the interactions between middle latitude and low latitude circulations. Currently there are many efforts to blend the knowledge on tropical circulations, now forthcoming at an accelerating pace, with the more established knowledge on extratropical circulations to obtain the global picture. The Global Atmospheric Research Program (GARP) has this task as one of its main objectives.

The purpose of the present study is to use the observational approach to investigate seasonal changes in the general circulation and heat and energy budgets of the atmosphere. In the chapters which follow, consideration is given to changes in the global patterns, as well as those in regions of limited volume. In previous studies there have been no attempts to use observations to calculate seasonal variations in the global energy budget and therefore no basis for comparing results obtained for restricted regions. There have also been no attempts on a global scale to compute seasonal changes in the vertical distribution of heat released in precipitation processes; hence, for example, estimates of the generation of potential energy, which depend on total diabatic heating rates, have been scarce. To date, only Dutton and Johnson (1967) have computed hemispheric generation rates and their values are based on a two-layer model and represent the mean annual conditions for the Northern Hemisphere.

In this thesis an attempt is made to estimate seasonal changes in the vertical distribution of latent heat release and the subsequent generation of zonal available potential energy. The time and

space scales are small enough to incorporate and illustrate some of the larger synoptic scale circulation patterns, such as the Indian summer Monsoon; yet they appear to be large enough so that sufficient data is available for statistically significant results. The main objective in the thesis is to arrive at a better understanding of the atmospheric energy balance. To achieve this it is necessary to consider the factors involved in the energy budget calculations; these are discussed in Chapters 2-5. In Chapter 2 the data sources are given. In Chapter 3 the diabatic heat sources are presented and the methods used to derive vertical profiles of latent heat release and boundary layer heating are discussed. In Chapter 4 the global circulation patterns are presented and particular attention is given to the tropical and subtropical regions. In Chapter 5 the factors governing the temperature distribution are discussed as this is an integral part of the investigation and provides a check on the consistency of the results. Finally in Chapter 6 seasonal changes in the atmospheric energy balance are presented. Results are given in the form of energy box diagrams for the globe, the Northern Hemisphere, the Southern Hemisphere, the tropics and the extratropical Northern Hemisphere. Energy transports between different regions, such as tropics and higher latitudes are also inferred.

CHAPTER 2
DATA SOURCES AND PROCESSING

This chapter describes the sources of data used in deriving global values of wind, temperature and eddy transports of momentum and heat. For each quantity there is a list of references which states where the data are either given or can be found. If the quantity was calculated this is noted also. The procedures used to process these data are given after the data references. A description of the data sources and methods used to derive the components of diabatic heating is given in Chapter 3.

2.1 Data Sources

1. Zonal wind \bar{u}

- (a) Crutcher (1961, 1966): seasonal averages were extracted for 90N-40N, 1000-100 mb.
- (b) Newell and Richards (1969): three months averaged together using IQSY data for 90N-20N, 100-10 mb.
- (c) Newell et al. (1970a): seasonal averages based on 7 1/2 years data for 40N-30S, 1000-10 mb.
- (d) Heastie and Stephenson (1960): one month averages were extracted for 30S-60S, 1000-100 mb.
- (e) Schwerdtfeger and Martin (1964): seasonal averages were extracted from 40S-90S, 1000-30 mb.
- (f) U.S. Navy Marine Climatic Atlas of the World, Vol. VII,

Antarctic (1965): seasonal averages were extracted for stations in the Antarctic sector, 1000-30 mb.

2. Meridional wind \bar{v}

- (a) same as 1(a).
- (b) same as 1(b).
- (c) same as 1(c).
- (d) Vincent (1968): three months averaged together using IQSY data to compute $[\bar{v}]$ for 90N-20N, 100-10 mb.
- (e) Holopainen (1967): seasonal averages of $[\bar{v}]$ extracted for 90N-30N, 1000-100 mb.
- (f) Vernekar (1966, 1967): one month averages of $[\bar{v}]$ extracted for 90N-30N, 1000-100 mb.

3. Temperature \bar{T}

- (a) Goldie et al. (1958): one month averages were extracted for 90N-40N, 40S-50S, 700-100 mb.
- (b) Hann and Süring (1943): one month averages were used for January and July and their average was used for April and October; extracted for 90N-40N, 40S-50S, surface.
- (c) same as 1(b).
- (d) same as 1(c).
- (e) Weyant (1966): one month averages were extracted for 60S-90S, 700-100 mb.
- (f) Morin (1966): one month averages were extracted for 60S-90S, 200-100 mb.

4. Momentum fluxes $[\overline{u'v'}]$, $[\overline{u^*v^*}]$
- (a) same as 1(a) for both $[\overline{u'v'}]$ and $[\overline{u^*v^*}]$.
 - (b) same as 1(b) for both $[\overline{u'v'}]$ and $[\overline{u^*v^*}]$.
 - (c) same as 1(c) for $[\overline{u'v'}]$; $[\overline{u^*v^*}]$ for 1000-100 mb only.
 - (d) U.S. Navy Marine Climatic Atlas of the World, Vol. VII, Antarctic (1965): seasonal values of $[\overline{u'v'}]$ calculated from wind statistics.
5. Heat fluxes $[\overline{v'T'}]$, $[\overline{v^*T^*}]$
- (a) Wiin-Nielsen (personal communication): three months averaged together of total heat flux used for 90N-40N, 1000-100 mb.
 - (b) Oort and Rasmussen (personal communication): seasonal averages for total heat flux used for 90N-40N, 1000-100 mb.
 - (c) same as 1(b) for $[\overline{v'T'}]$ and $[\overline{v^*T^*}]$.
 - (d) same as 1(c) for $[\overline{v'T'}]$; $[\overline{v^*T^*}]$ for 1000-100 mb only.
 - (e) J. B. Robinson (personal communication): six month averages used for 30S-90S, 1000-100 mb.

2.2 Data Processing

From 90N-30S values of \bar{u} were taken at each 20 degrees of longitude, each 10 degrees of latitude and for the pressure levels 1000, 850, 700, 500, 400, 300, 200, 150, 100 and 70 mb and zonal averages were then computed. Because of data paucity above 70 mb and in the region 30S-90S from 1000-100 mb, only zonal averages were computed. The same procedure was used to obtain values of \bar{v} but, with the

exception of the region 20N-20S, 1000-100 mb, zonal averages were not used in any further calculations. In the Northern Hemisphere values of $[\bar{v}]$ computed by Holopainen (1967), Vernekar (1966, 1967) and Vincent (1968) using "indirect" methods were adopted. In the Southern Hemisphere $[\bar{v}]$ was computed from

$$Z[\bar{v}] = - (a^2 \cos^2 \phi)^{-1} \frac{\partial}{\partial \phi} ([\bar{u}'v'] \cos^2 \phi)$$

where

$$Z = f - (a \cos \phi)^{-1} \frac{\partial}{\partial \phi} ([\bar{u}] \cos \phi)$$

together with the continuity equation. The values of $[\bar{v}]$ thus obtained were used to compute vertical motion, mass flux, temperature advection and terms in the energy budget.

Temperature data were processed in the same manner as zonal wind data with two exceptions. First, no upper air data below 700 mb were available outside the tropical region; vertical cross sections of \bar{T}^* were analyzed using surface temperatures taken from maps presented by Hann and Süring (1943) and values of \bar{T} at 850 mb were thereby deduced. Secondly, temperature data as a function of longitude were available on a global basis.

CHAPTER 3

DIABATIC HEATING

Diabatic heating in a column of air occurs as a result of radiative flux convergence, phase changes and heat exchange between the earth's surface and atmosphere. Solar radiation is the ultimate source of radiative energy in the atmosphere while thermal (terrestrial) radiation provides the energy sink. There is net radiative cooling in most of the region studied (1000-10 mb) with the exception of the tropical region above 150 mb. Latent heat release is the predominant diabatic heating source in the troposphere above the atmospheric boundary layer. The turbulent heat exchange near the earth's surface, henceforth called boundary layer heating, is generally from the earth to the atmosphere because the ocean surface temperatures are usually warmer than the air above. In addition at low latitudes and in the summer hemisphere at middle latitudes the underlying land surfaces are relatively warm.

3.1 Radiative Heating Rates

Net radiative heating rates in pressure layers from 1000-10 mb at intervals of 10 degrees latitude between the equator and 70°N for January, April, July and October were taken from Rodgers (1967). His heating rates were derived from visible and near infrared solar flux and long wave thermal flux. For atmospheric data he used the following: temperatures based partly on a 5-year sample taken from the

MIT General Circulation Library data and partly on the sources presented in Chapter 2 (Data Sources 3a and 3c); cloud statistics given by London (1957); water vapor data up to 400 mb provided by Dr. E. G. Rasmusson; and ozone cross sections from Hering and Borden (1964). For the concentration of tropospheric water vapor above 400 mb an interpolation scheme was devised and the stratospheric content was assumed to be constant at 0.002 g/kg. The concentration of carbon dioxide was also assumed to be constant with a mixing ratio of 0.49 g/kg. Unfortunately radiative heating rates as a function of pressure were not available in the Southern Hemisphere and it was necessary to assume seasonal symmetry about the equator, e.g. values at 30N in January were substituted for those at 30S in July. Values were extrapolated from 70N to the pole and a smoothed set of results for the Northern Hemisphere is given in Table 3.1.

3.2 Latent Heat Release

For an entire latitude band mean monthly amounts of surface precipitation are good indicators of the total columnar latent heat release since they represent the excess heat available to the atmosphere by cloud generative and dissipative processes. The vertical distribution of latent heat release is the most difficult part of the diabatic heating to assess as no direct measurements are available. In the tropics it is generally agreed that the major rain producing process is coalescence; therefore the main phase change is from vapor to liquid. As a consequence the most important source of latent

heat release is condensation. At higher latitudes the Bergeron-Findeisen ice crystal process becomes an important precipitation mechanism. It has been known for some time that both ice crystal formation and coalescence are required in middle latitudes to produce raindrops of the observed size (see, for example, Houghton, 1950). Recently, Houghton (1968) has suggested that the ice crystal process is more important in middle latitude precipitation. Ice crystal growth occurs most rapidly at temperatures between -10°C and -15°C (Mason, 1962) and is mainly due to direct sublimation of water vapor onto crystals and collisions with supercooled water droplets. In the former process latent heat release takes place above the freezing level. In the latter process water vapor may condense above the freezing level or it may condense below the freezing level and be lifted to temperatures colder than 0°C .

In the present work the level of maximum latent heat release outside of the tropical regions was assumed to occur near 0°C or at temperatures slightly below freezing. Condensational heating was considered to be the primary source of latent heat release and the latent heat of vaporization was used to convert zonally-averaged surface rainfall amounts to values of total columnar latent heat release. A small addition was made to the columnar latent heat release at higher latitudes to allow for precipitation reaching the ground in solid form such as snow. Also final values in the vertical distribution of latent heat release were adjusted to allow for a small percentage of heating due to fusion above the melting level.

For the most part past studies on the atmospheric heat balance have included only annual averages of each of the budget components as a function of latitude and investigations into the heat budget of the Southern Hemisphere are particularly lacking. Davis (1963) in an analysis of the atmospheric heat budget calculated the seasonal changes of latent heat release for different vertical layers (his lowest single layer was 1010-500 mb) but his results were only available from 70N-20N. Budyko and Kondratiev (1964) give latitudinal distributions of total condensational heating for both hemispheres, based on surface rainfall amounts, but their results include only annual means. For the present investigation the annual average values of total latent heat release by Budyko and Kondratiev were plotted on a graph together with Davis' values in the Northern Hemisphere for January, April, July and October. Curves of the meridional distribution of total latent heat release were then estimated for each of the four 3-month seasons centered about Davis' months (see Fig. 3.1). The latitude of maximum latent heat release was assumed to occur where the maximum upward motion in the Hadley circulations was observed (see Chapter 4). The seasonal trend of maximum values was also found to be in good agreement with the monthly distributions of precipitable water presented by Tuller (1968).

The scheme used for distributing latent heat release in the vertical was based on northern hemisphere cloud statistics at middle and high latitudes and model profiles of vertical motion in the vicinity of the equator, where the cloud statistics did not appear to be

as reliable. A method similar to that of Davis (1963) was used to estimate latent heat release profiles for latitudes from 80N-30N. Zonal averages of percentage of sky cover for each of six cloud types (cirrus, altocumulus-altostratus, stratus, cumulus, nimbostratus and cumulonimbus), as well as mean bases and tops are given in a report by Telegades and London (1954) for the northern hemisphere winter and summer. Weighting factors, based on liquid water content, drop size distribution and the average depth over which precipitation occurs (Davis, 1961), were applied to each cloud type in pressure layers of 100 mb thickness and a weighted percentage of each type was derived. From the normalized weighted percentages the fraction of latent heat released within each layer was estimated (see Table 3.2). These values were then applied to the total columnar latent heat shown in Fig. 3.1 between 80N and 30N for the periods December-February and June-August.

This cloud weighting scheme was also tried at low latitudes but the absence of convective clouds in the statistics used, particularly cumulonimbus (Cb) above 450 mb, lead to insufficient heating in the upper troposphere and the scheme could not be used. The reason for such low mean cloud tops in Telegades and London's tropical data is not known but we can be certain that a few relatively large Cb, such as those in the Intertropical Convergence Zone, were present (see for example, Malkus and Riehl, 1964). Perhaps these were included in the original data set and lost in the averaging process or they may not have been observed due to lack of stations in the tropical

network. Because Davis' weighting factor for Cb is .75 a cloud cover of less than one percent would be sufficient to produce the latent heat release required in the upper tropical troposphere to compensate for the radiational cooling.

According to Riehl (1950) the tropical upper troposphere receives most of its latent energy supply from a few tall cumulonimbus clouds. Malkus and Ronne (1954) used cameras to investigate the growth of convective towers at the tops of large Cb. Their results showed that Cb, which averaged 9 km in width, could produce towers at heights of 10-12 km (250 mb) within 20 minutes. These "bubbles" had an average diameter of 1.3 km and lasted approximately 5 minutes. Vertical velocities within the bubbles were estimated at about $10-12 \text{ m sec}^{-1}$. Using their observational evidence as a guide, Malkus and Ronne estimated the amount of latent heat release from large Cb of this type. They assumed that a Cb, 2 km on a side, embedded in an environment, 30 km on a side, had an average upward vertical velocity of 10 m sec^{-1} . From mass continuity considerations, the downdraft in the environment was 4 cm sec^{-1} which is in agreement with computed values of synoptic-scale vertical velocities. Using water vapor contents of 3 g/kg and 0.5 g/kg in the rising and sinking air they calculated a net upward vapor transport of $6 \times 10^7 \text{ g sec}^{-1}$ which produced a latent heat transport of $3.6 \times 10^{10} \text{ cal sec}^{-1}$. Averaged over a 10 degree latitude belt centered on the equator this gives a latent heat release of approximately $400 \text{ cal cm}^{-2} \text{ day}^{-1}$, a value which compares favorably with Budyko and Kondratiev's value of 300

cal $\text{cm}^{-2} \text{ day}^{-1}$, derived from Fig. 3.1. Thus, if the estimates of Malkus and Ronne are correct, it appears that less than 1% of active Cb coverage is required in the equatorial zone to maintain a heat balance. In a later investigation, Riehl and Malkus (1958) estimated that active giant clouds, reaching heights of 40,000-50,000 ft (150 mb) would have to occupy approximately 1% of the area in the 10 degree equatorial latitude belt to maintain a heat balance. The finding herein that only a few tenths of a percent of Cb in the tropical upper troposphere would be sufficient to produce net heating is in good agreement with the results of both Malkus and Ronne and Riehl and Malkus.

The adopted values of latent heat release near the equator were based on the results of a theoretical study by Malkus and Williams (1963). They used a numerical model, based on buoyancy considerations, to compute ascent rates as a function of altitude for different tropical environments. One group of vertical velocity profiles was derived for a mean tropical atmosphere (with respect to temperature and humidity) consisting of large convective cloud elements of radii 1-3 km. A profile was selected from this group corresponding to cloud elements of radius 1.5 km ascending through a saturated environment, since it appeared to represent the best average conditions according to results described above (e.g. Malkus and Ronne, Riehl and Malkus). This choice ensured that condensation was occurring and that latent heat release was accompanying the strong updrafts. It was assumed that the distribution of latent heat release was

proportional to the vertical profile of ascent rates. The values of vertical velocity were normalized so that a percentage of the total latent heat release could be calculated for each pressure layer of 100 mb thickness. This procedure was only applied at latitude bands centered at the equator and at 10 degrees latitude in the summer hemisphere where the strongest rising motions in the Hadley circulations occurred. Profiles of the normalized ratios at these latitudes were blended with those at 30N to give the profiles at intermediate latitudes for the periods December-February and June-August.

Values of the ratios for the periods March-May and September-November were obtained by taking the average of the profiles from the other two seasons. All profiles except those at the equator and 10 degrees latitude in the summer hemisphere were adjusted, as noted previously, to allow for some latent heat release due to fusion. Since no cloud statistics were available for the Southern Hemisphere northern hemisphere ratios for the corresponding seasons were used. In each latitude band values of total latent heat release, shown in Fig. 3.1 were multiplied by the corresponding ratios for each pressure layer and vertical distributions of latent heat release were obtained. Meridional cross sections for each season were plotted, analyzed and smoothed, and the results are given in Table 3.3.

3.3 Boundary Layer Heating

Boundary layer heating (BLH) is confined mainly to the lowest one or two kilometers; in the present investigation it is assumed

that all of the BLH takes place from 1000-700 mb with the largest contribution occurring below 900 mb. Under the present assumption there are only two pressure levels, 1000 mb and 850 mb, at which BLH can be distributed. The adopted values of BLH are presented in Table 3.5 and were computed as follows. Analyzed maps presented in the Budyko Atlas (1963) were used to compute zonally-averaged values of total columnar BLH in each 10 degree latitude band from 60N-60S for January, April, July and October. Values given by Davis (1963) for the same months from 70N-20N were also used. Polewards of 60 degrees latitude reliable values were not available but approximate values were obtained by extrapolation based mainly on the Budyko Atlas. Curves illustrating the total columnar BLH are given in Fig. 3.2

Approximately two-thirds of the total heating was assigned to the lower half of the boundary layer and the remaining portion was assigned to the upper half. The boundary layer over which the heating was distributed varied in depth, increasing from 1000-900 mb at high latitudes to 1000-700 mb near the equator. This latitudinal distribution was selected so that the boundary layer extended up to at least the level of the mean convective cloud base. Ratios of the total columnar BLH were derived for pressure layers of 50 mb thickness and the results are given in Table 3.4. Cross sections were analyzed and the values obtained at 1000 mb and 850 mb are presented in Table 3.5. Although the adopted values of BLH are only rough approximations their contribution to the heat budget of the atmosphere

is comparatively small. For example, the annual average value of total BLH given by Budyko and Kondratiev (1964) for the globe is only about 22% of the condensational heating. Comments concerning the patterns of BLH, radiative heating and latent heat release are given in Chapter 5 where their effects on temperature changes are discussed.

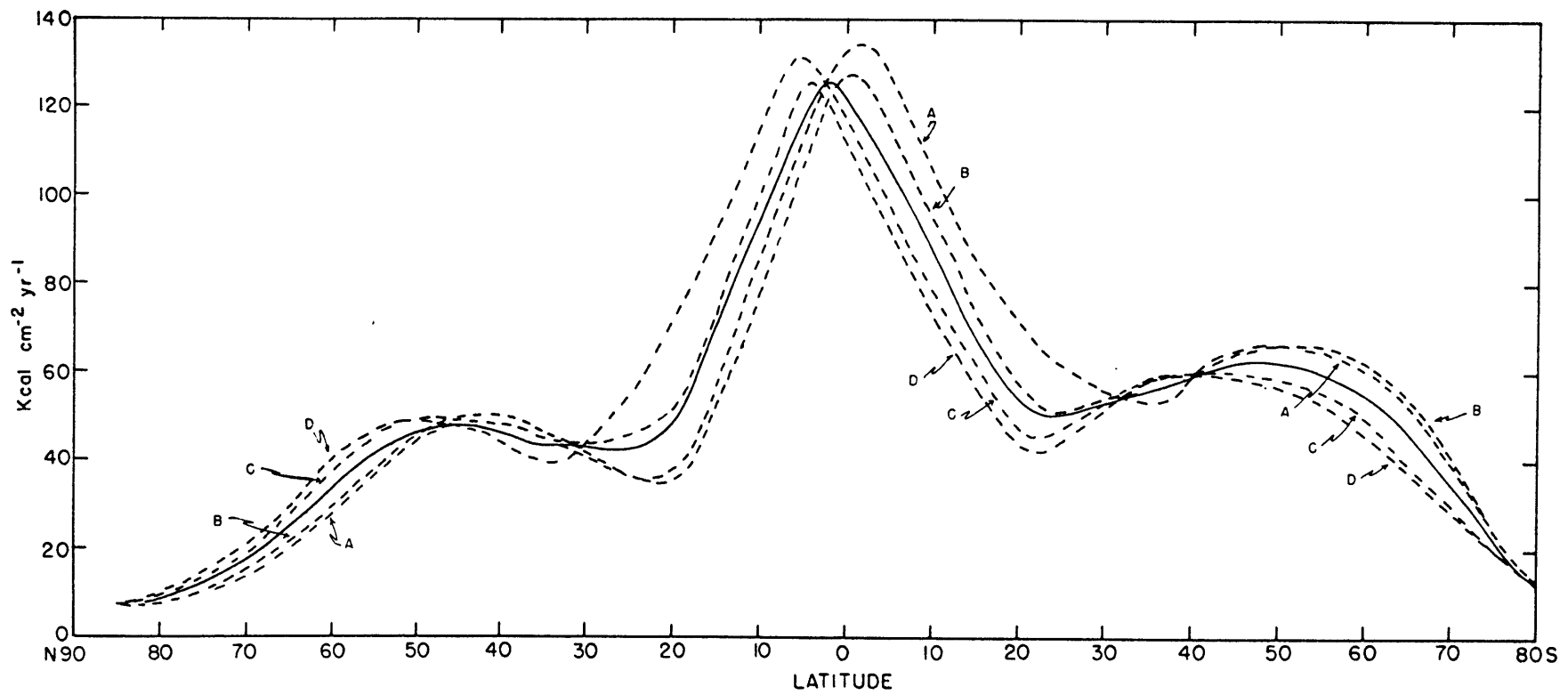


Fig. 3.1: Total columnar latent heat release: (A) Dec-Feb, (B) Mar-May, (C) Jun-Aug, (D) Sep-Nov, solid line is annual mean.

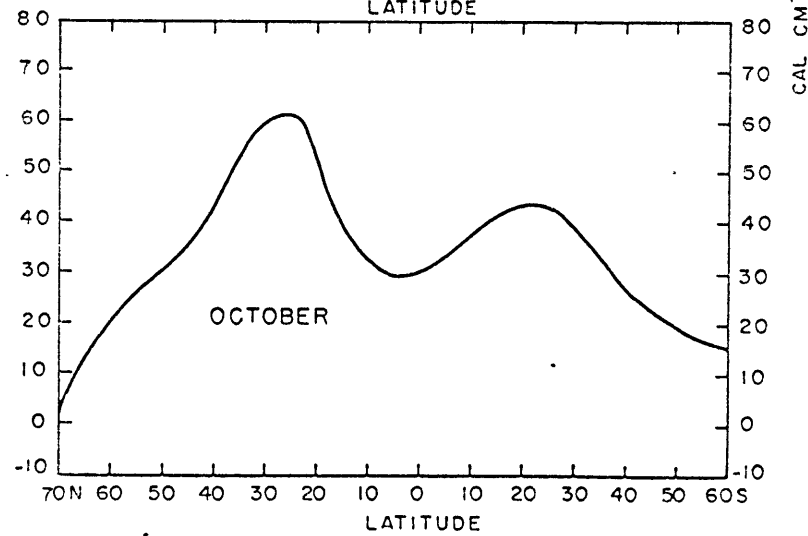
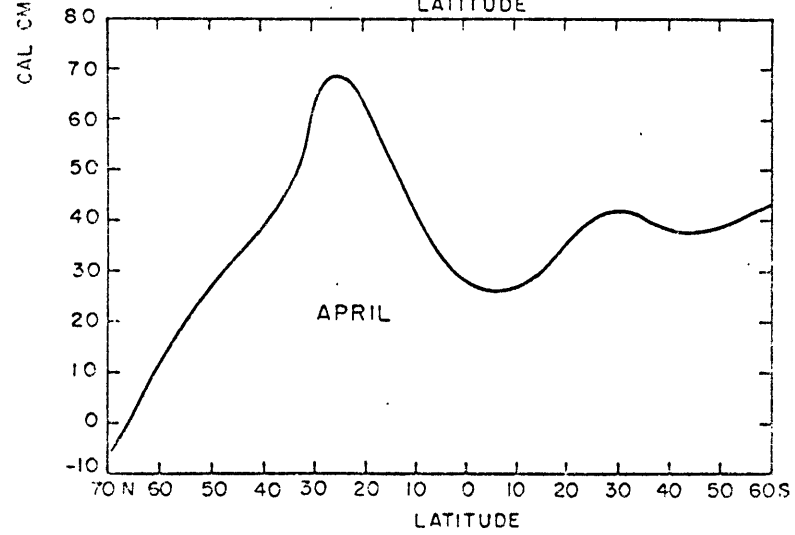
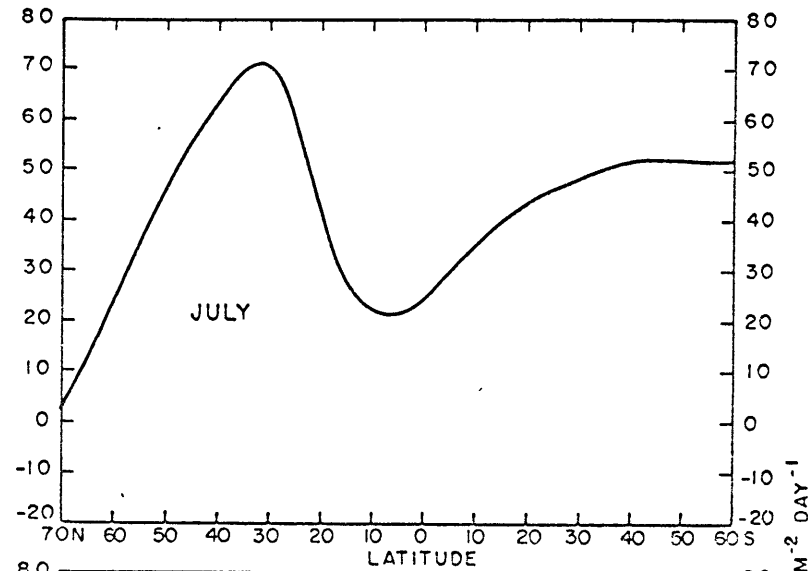
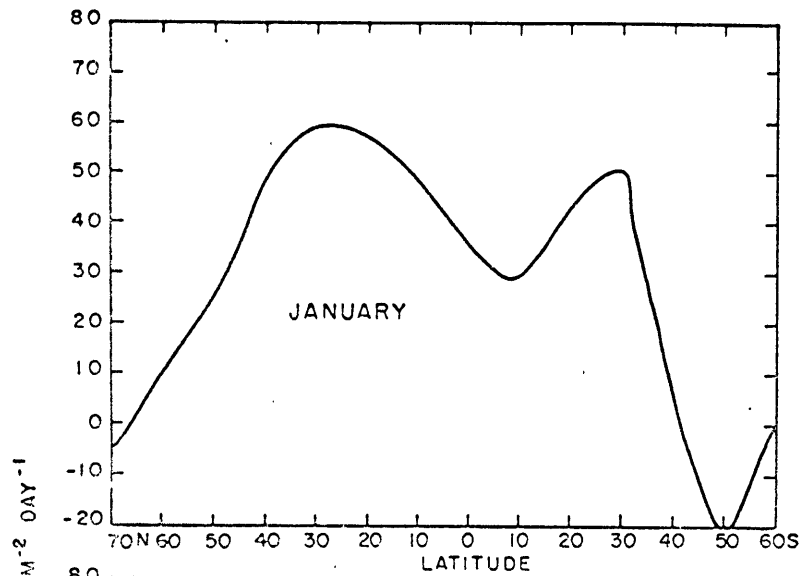


Fig. 3.2: Total boundary layer heating.

CHAPTER 4
GLOBAL CIRCULATION

In this chapter the quantities $[\bar{T}]$, $[\bar{u}]$, $[\bar{v}]$, $[\bar{w}]$, mass flux, $[\bar{u}'v']$, $[\bar{u}^*v^*]$, $[\bar{v}'T']$ and $[\bar{v}^*T^*]$ are presented; these quantities provide the basic information used in Chapters 5 and 6.

4.1 Temperature Field

The most comprehensive study of upper air temperature over the world is the Geophysical Memoir by Goldie, Moore and Austin (1958). It contains meridional cross sections, mean soundings and a large selection of maps for the months of January, April, July and October. In the present study temperature maps for each season at all of the mandatory pressure levels between 1000 mb and 70 mb were analyzed by hand for the region 40N-40S using station data. Above 70 mb, year to year differences, data paucity and instrumental inaccuracies precluded long term map analyses and only zonal averages, based on latitude band means (Kidson et al., 1969) were obtained. The maps are not presented as they will soon appear in a monograph by Newell et al. (1970a).

When the tropical data were combined with data at other latitudes (see Chapter 2) a coherent temperature pattern was observed for each season. The features most significant to discussions in Chapters 5 and 6 were:

- (1) longitudinal temperature variations in the troposphere were

- larger at middle latitudes than at low latitudes in all seasons, hence AE (see Eq. 6.13) is larger in the former region;
- (2) a very warm region was found in the middle and upper troposphere in June-August over India and China, presumably due to latent heat release in the summer Monsoon rains;
 - (3) lowest temperatures occurred near 100 mb in December-May; according to Reed and Vleck (1969) and Newell et al. (1969) a stronger Hadley circulation in January-February is responsible for intensified upward vertical velocities and, hence, increased cooling aloft due to adiabatic expansion;
 - (4) at the equator the highest temperatures in the middle and upper troposphere were located near 180 degrees longitude and are probably due to latent heat release in the rising branch of the "Walker Circulation" which is discussed in detail by Bjerknes (1969); relatively colder air was found directly above the warm air, again suggesting cooling due to adiabatic expansion.

There appear to have been no previous attempts other than the referenced work by Goldie et al. to map the global temperature field on both sides of the equator. A comprehensive study of the field over the Northern Hemisphere for the year 1950, divided into two six-month seasons, has been performed by Peixoto (1960a) and will be referred to later. For the Africa-Indian Ocean region the most recent study is that by Thompson (1965). In discussing the energy budget (Chapter 6) it is desirable to have temperature values for the entire field.

Zonal mean temperatures derived for the globe, using techniques

described in Chapter 2, are shown in Table 4.1 for the four seasons. Some of the characteristics of the temperature patterns are, of course, eliminated by the spatial averaging. Table 4.1 shows that the highest tropospheric temperatures in June-August are located near 20N, whereas maximum diabatic heating (see Chapter 5) was found near 5N. Our tropical map analyses (Newell et al., 1970a) suggest that the high temperatures at 20N are caused by two effects, heating over the desert regions of North Africa and Saudi Arabia supplied to the lower levels and latent heat release over the Bay of Bengal and India supplied to the middle and upper levels during the summer Monsoon. Meridional cross sections of temperature based on the map analyses are presented at 20E and 80E in Fig. 4.1 for June-August and illustrate this point. The cross sections were obtained by subtracting the meridional average of the temperature (derived for each pressure surface from values at increments of 10 degrees latitude between 40N-40S inclusive) from the values at each latitude. The maps of Africa and the Indian Ocean region presented by Thompson (1965) show maximum temperatures located along 20N in July at all pressure levels. In compiling zonal averages this region represents nearly one-third of the distance around a latitude circle and is sufficient, therefore, to produce the highest zonal mean temperature. On the other hand the location of maximum diabatic heating in the tropics is mainly a reflection of the region having the most latent heat release.

In the Northern Hemisphere, vertical cross sections of net radiative heating at each 10 degrees of latitude are presented by Katayama

(1967) for January and July. In addition he presents maps for both months showing total columnar latent heat release due to condensation. His values of latent heat release were vertically distributed using the ratios given in Table 3.2 and they were combined with his radiative heating rates to give values of diabatic heating. His results show maximum latent heat release of $800 \text{ cal cm}^{-2} \text{ day}^{-1}$ near India; however, his zonally-averaged net diabatic heating rates were a maximum near 10N. Thus, the present results are in general agreement with those of Katayama.

Zonally-averaged temperatures were used to construct the mean profiles given in Fig. 4.2 at 80N, 60N, 40N, 20N and the equator for December-February and June-August. At low latitudes in January the mean tropopause height is located near the 90 mb level and is characterized by the coldest temperatures. The temperatures decrease (increase) below (above) the tropopause at a nearly uniform rate. At high latitudes the tropopause is near 300 mb; the temperatures above this level are nearly isothermal and the lapse-rates below are approximately the same as at low latitudes. From 200-40 mb the highest temperatures are near 55N. The same remarks are essentially true in June-August, except that the tropical tropopause heights are lower (100 mb) and the middle latitude sounding at 40N lies between those at 20N and 60N so that there is no reversal in the temperature gradient in the lower stratosphere. In addition the subtropical temperatures in the troposphere are higher than the tropical temperatures. Note that in both periods at all latitudes, with the possible exception

of the winter pole, the temperature is essentially the same near the 200 mb level. This feature actually occurs at 190 mb in December-February where the temperature is -58°C and near 240 mb in June-August where it is -42°C . Maps of the tropopause pressure and temperature are presented by Goldie et al. (loc. cit.); they also reproduce a number of mean temperature soundings for typical stations which illustrate the variety of tropopause found.

4.2 Zonal Wind Field

Buch (1954) presented maps of mean wind components based on observed winds for the year 1950 divided into two six-month seasons for levels 850-100 mb for the Northern Hemisphere. Heastie and Stephenson (1960) present global maps based on winds calculated from mean contour heights for the four months January, April, July and October for levels 700-100 mb. Crutcher (1959) prepared a set of maps for mean wind components and other wind statistics for levels 850-100 mb for the Northern Hemisphere. Three-month seasons were used corresponding to the present combinations. For most stations at least 5 years of data were used. From these Crutcher (1961) subsequently compiled a set of meridional cross sections for each 10 degrees of longitude from which zonal means can easily be obtained. Crutcher's data were mainly based on observed winds although occasionally in data-poor ocean areas the gradient wind relationship (although not the geostrophic approximation) was used. More recently Crutcher (1966) has prepared monthly maps for the wind components for 1000 mb. Surface

wind data were used when 1000 mb was below the land or sea surface. As noted in Chapter 2, wind data from Heastie and Stephenson (loc. cit.) and Crutcher (1961, 1966) were used in conjunction with our tropical data (Newell et al., 1970a) to obtain global wind fields. Other references include Obasi (1963a) who presented wind component maps from 850-50 mb for the Southern Hemisphere for two six-month periods during the International Geophysical Year (IGY) and Riehl (1954) who presented maps of streamlines (paralleling the direction of wind flow) for the surface (January and July) and for 700 mb and 300 mb (two three-month seasons centered on January and July) for the tropical region.

In the present work the zonal wind component showed the following general features:

- (1) in middle latitudes there were essentially westerlies at all levels;
- (2) in the subtropics there were low level easterlies and middle and upper level westerlies;
- (3) in the equatorial zone the wind regimes seemed to be a function of longitude rather than latitude; the western hemisphere was characterized by upper level westerlies with easterlies below while the eastern hemisphere was characterized by upper level easterlies with westerlies below.

A dominant feature in the circulation pattern was the strong easterly maximum which occurred in June-August in the upper troposphere over southern India. Peak velocities of more than 30 m sec^{-1}

were attained between 150 mb and 100 mb. In the lower troposphere weak westerly winds were observed over India and our analyses at the intermediate levels show a latitudinal increase of temperature accompanying the vertical wind shear (see Fig. 4.1b).

Meridional cross sections of the zonal wind component along 75W and 80E are presented from 40N-40S for December-February and June-August in Figs. 4.3 and 4.4. They represent typical wind patterns in the Western and Eastern Hemispheres and illustrate the differences between the tropical circulations in each hemisphere. In compiling zonal averages for energy budget calculations this feature is obviously significant.

Mean zonal winds were obtained on a global basis in the same manner as temperature, using the data sources and techniques outlined in Chapter 2. The values are given in Table 4.2. An important difference between December-February and June-August is that the northern hemisphere jet core weakens considerably in June-August whereas the southern hemisphere jet core has almost the same central speed in both seasons. In the southern hemisphere winter there is evidence of a secondary maximum near 50S in addition to the main subtropical jet at 30S. The data coverage in the Southern Hemisphere is not very extensive but indicates that the jet stream meanders more than its counterpart in the Northern Hemisphere which may account for the double maximum in the zonal averages. Streten (1969), in an investigation of extratropical cyclones and anticyclones in the southern hemisphere winter of 1962, found that cyclone frequencies at 700 mb

appeared to have maxima near 40S and 60S. This is not inconsistent with the present analyses of a double wind maximum at 30S and 50S in southern winter. In another study Solot and Angell (1969) using "ghost" balloons at 200 mb in the Southern Hemisphere also found a double jet. Their annual mean values of the zonal wind maxima were 35 m sec^{-1} at 20S and 29 m sec^{-1} at 45S and they noted that the double maximum was most pronounced in spring and summer. In contrast, the present analyses suggest that the double jet structure is most pronounced in winter and spring, that it is about 10 degrees latitude further south and that no double maximum occurs in the summer season.

Zonally-averaged values of \bar{u} in the equatorial upper troposphere are relatively small because, as already noted, there are generally easterlies in the Eastern Hemisphere and westerlies in the Western Hemisphere. Only in northern summer when the zonal wind component is near zero in the Western Hemisphere, concomitant with strong easterlies in the Eastern Hemisphere, are the zonally-averaged easterlies very extensive in the tropics. Thus it appears that longitudinal asymmetries are very important near the equator.

4.3 Mean Meridional Circulations

In contrast to the temperature and zonal wind component, the meridional wind component is very difficult to obtain from the direct wind measurements. Essentially the problem is that the day-to-day variations are often larger than the long term mean; at higher levels, this difficulty is enhanced by instrumental errors, tidal effects, etc.

The situation is particularly bad at middle latitudes where the winds are most intense and the day-to-day fluctuations are several meters per second compared with a mean of about one meter per second or less. The fluctuations generally diminish towards low latitudes except in the upper troposphere. Notwithstanding the difficulty the importance of north-south transports of water vapor, mass, heat, momentum and energy at various levels by mean motions is so great that each independent effort to appraise them has some value.

The significant features in the meridional wind component were:

- (1) evidence of a three wave pattern in the troposphere at middle latitudes in both hemispheres except during the summer season;
- (2) the familiar pattern of northeast and southeast trade winds in the subtropical Northern and Southern Hemispheres;
- (3) cellular motions in meridional planes in the tropics which appear to have systematic seasonal variations.

The tropical circulations were dominated by low level convergence into a region south of the equator in December-February and north of the equator in June-August. The upper level maps showed divergence from a region a little south of the equator in December-February and a little north of the equator in June-August. In the middle troposphere, magnitudes of \bar{v} were very weak and it was difficult to distinguish a coherent pattern. In March-May and September-November a similar pattern was evident but the corresponding convergent and divergent regions were located approximately over the equator.

Meridional cross sections of the north-south component of the

wind at 80E are presented for December-February and June-August in Fig. 4.5. In December-February cellular circulations are implied in both hemispheres with low level convergence and upper level divergence in the vicinity of 10S. The northern hemisphere cell appears to be stronger. In June-August a cellular structure is not evident, presumably because of the Monsoon Circulation. The pattern of \bar{v} in the upper troposphere is the same as that presented by Keshava Murty (1968) for the Indian summer Monsoon. Further discussion of this point is given in Chapter 6.

Because of the difficulties noted at the beginning of this section observed values of the meridional wind component were not generally used to obtain zonal averages; instead, $[\bar{v}]$ computed by "indirect" methods was used. Only in the tropical region 20N-20S, where direct values were found to satisfy the momentum budget (Kidson et al., 1969; Newell, et al., 1970a), were observed values of $[\bar{v}]$ used. In the Northern Hemisphere, as noted in Chapter 2, values of $[\bar{v}]$ were based on the results of Holopainen (1967), Vernekar (1966, 1967) and Vincent (1968). Holopainen calculated indirect values of $[\bar{v}]$ from 1000-100 mb using the angular momentum and continuity equations, assuming that vertical eddy fluxes of zonal momentum were negligible in the free atmosphere. Vernekar obtained mean meridional velocities in the same region using the vorticity and thermodynamic equations, forcing the circulation from observed eddy transports of heat and momentum. Vincent used the zonal momentum and continuity equations in an iteration process to compute values of $[\bar{v}]$ and $[\bar{w}]$ in the stratosphere which

were forced from momentum and heat sources. Unfortunately in the Southern Hemisphere no comparable three month seasonal studies were available and the expression given in Chapter 2 was used to approximate values of $[\bar{v}]$. For comparison there is an investigation by Gilman (1965) who used momentum and mass balance considerations to infer indirect mean meridional circulations from 1000-75 mb for two six month periods during the IGY. The present results for three month winter and summer seasons are in good agreement with those of Gilman with respect to sign; only in the extratropical boundary layer is there a disagreement in magnitudes, with the present values being smaller. This is probably because Gilman included vertical eddy momentum transports in his calculations, whereas they were excluded in the present study.

The adopted values of $[\bar{v}]$ are given in Table 4.3 for the four seasons along with the vertical averages for each latitude. Tucker (1959) evaluates the vertical average of $[\bar{v}]$ and applies this as a correction to the values at each level. The resulting velocities automatically satisfy the condition that there is no mass flux through the latitude circle; this is not strictly true as there are mean pressure changes in latitude belts caused by net mass transports, but these changes (see Gordon, 1953) may be used to show that vertical averages do not normally exceed a few millimeters per second. Most of the vertical averages in the present work were less than 10 mm sec⁻¹. Values of $[\bar{w}]$, derived from continuity, assuming $\omega = -\rho g w$ and applying the equation of state appear in Table 4.4.

Mean meridional circulation patterns were derived from Eq.

(4.1).

$$\psi = \frac{2\pi a \cos \phi}{g} \int_p^{1000} [\bar{v}] dp \quad (4.1)$$

The results are shown in Fig. 4.6 for four seasons and illustrate the following features:

- (1) at low latitudes there is one large thermally direct (Hadley) cell in December-February and June-August, centered in the winter hemisphere and spanning the whole of the tropical region; a small weak direct cell is centered in the subtropical summer hemisphere and has apparently been distorted in the Northern Hemisphere, presumably by the strong Monsoon circulation;
- (2) at low latitudes in the intermediate seasons there are two Hadley cells, one in each hemisphere, with rising motion near the equator; in September-November the circulation is strongest in the southern hemisphere cell, while in March-May the two cells are about equal in strength;
- (3) at middle latitudes there are indirect (Ferrel) cells in both hemispheres during all seasons; the southern hemisphere cells are generally weaker but this may be due in part to the assumptions used to compute $[\bar{v}]$;
- (4) at high latitudes there are polar direct cells in both hemispheres except during northern summer;
- (5) in December-February and September-November the tropospheric

cells (in the Northern Hemisphere) extend into the stratosphere and show a poleward tilt with height above the tropopause at least up to 30 mb.

The mass circulation of the northern winter Hadley cell is approximately $1.5 \times 10^{14} \text{ g sec}^{-1}$ and for the southern winter cell is about $1.9 \times 10^{14} \text{ g sec}^{-1}$. These compare with values of 2.3 and $1.8 \times 10^{14} \text{ g sec}^{-1}$ obtained by Palmen and Vuorela (1963) and Vuorela and Tuominen (1964), respectively, using Crutcher's northern hemisphere data. Manabe and Smagorinsky's (1967) model experiment gives $1.4 \times 10^{14} \text{ g sec}^{-1}$. In March-May the strengths of both the northern and southern hemisphere Hadley cells are the same while in September-November the southern cell is twice as strong as the northern cell. It is interesting to note that the total mass circulation in the two Hadley cells is roughly the same in each season. Viewed collectively the mean meridional circulation patterns show a seasonal variation which is very important in the heat and energy balances of the atmosphere. These effects are discussed in detail in Chapters 5 and 6.

4.4 Horizontal Eddy Transport of Momentum

In the present formulation of the energy budget only zonal averages of the eddy momentum transport are needed, whereas for temperature and wind components both longitudinal variations and zonal averages are required. Zonal averages of transient and standing eddies were obtained using the same data as for wind components (see Chapter 2). From 30S-90S, only the contribution due to transient eddies was

available. Currently maps of \bar{u} and \bar{v} are being analyzed at middle and high latitudes in the Southern Hemisphere and the standing eddy contribution to the momentum flux should be available in the near future. Cross sections of $[\overline{u'v'}]$ are given in Fig. 4.7 for December-February and June-August and show a strong middle latitude poleward flux in both hemispheres and a cross-equatorial flux in the upper troposphere from the winter to the summer hemisphere. The latter flux was noted by Obasi (1963b) and stressed by Tucker (1965) who did a detailed study of momentum flux near the equator based on seven stations. The cross sections also show equatorward fluxes at high latitudes in the troposphere and strong poleward fluxes in the winter stratosphere. The poleward fluxes in the southern hemisphere troposphere are larger than those in the Northern Hemisphere and they are comparable in both seasons whereas the fluxes in northern winter are larger than those in northern summer.

The standing eddy fluxes usually had the same sign as the transient eddy fluxes except in the southern hemisphere tropical-upper troposphere in June-November; magnitudes were generally smaller except in the tropical upper troposphere where they were frequently comparable and in northern hemisphere middle latitudes above 500 mb where they were approximately one-half as large as the transient eddies in September-February.

When the sum of the transient and standing eddy terms is considered, the patterns for the troposphere in middle latitudes are similar to the results obtained by Starr and White (1954) and Buch (1954)

for the Northern Hemisphere and Obasi (1963b,1965) for the Southern Hemisphere. These studies used station data plotted on maps as a base, rather than geostrophic winds, and may therefore be compared with the present work although the year was divided into two, rather than four, seasons. The significance of many of the factors noted above will become evident in the discussion of the energy balance in Chapter 6.

4.5 Horizontal Eddy Transport of Sensible Heat

The earliest measurements of eddy heat fluxes on a hemispheric basis were made by White (1954) who calculated values for the Northern Hemisphere for the year 1950 using stations grouped into latitude bands from 31N to 70N. His results showed a strong poleward flux at 850 mb with a secondary peak near the tropopause; both maxima occurred at about 55N. He also found that the middle latitude flux in the lower stratosphere was poleward; with minimum temperatures observed in the tropics this poleward flux was directed towards warmer temperatures or against the gradient. This was the first discovery of the stratospheric countergradient heat flux on a hemispheric basis although it had been noted by Priestley (1949) in the data for a single station. Later investigations by Murakami (1962) and Peng (1963, 1965) for the 18 months of the IGY period showed that the stratospheric heat flux by transient eddies was predominantly poleward except at high latitudes. The implications of this countergradient flux will be discussed in Chapter 6.

The Northern Hemisphere data for 1950 have been examined in greater detail by Peixoto (1960a) whose results also include the tropical regions. Statistics were obtained from grid point values read from analyzed maps for six month winter and summer seasons as well as for the complete year. The results obtained did not differ greatly from White's but the tropical analyses showed the transient eddy flux to be predominantly equatorward south of 30N. The winter fluxes were approximately twice as strong as those in the summer.

The equatorward heat fluxes in the tropical troposphere have been discussed in more detail by Peixoto (1960b) and Starr and Wallace (1964). Peixoto was first to suggest that this equatorward flux was countergradient. His conclusion was based on annual averages of temperature and sensible heat flux data for the year 1950 and the equatorward flux was strongest in the middle and upper troposphere, extending as far polewards at 28N at 500 mb. Starr and Wallace re-examined Peixoto's data (1960a) for the winter and summer seasons (six months each) and noted that, with the exception of the upper and lower levels of the tropical troposphere in summer, the sensible heat transport by transient eddies was countergradient. The standing eddy contributions were available only for the winter season and showed the same general pattern as that by transient eddies. It should be noted that these results need not necessarily apply to shorter climatological periods such as individual months or even three-month seasons. For example, zonal mean temperature cross sections for January and July presented by Goldie et al. (1958) show the tropospheric latitu-

dinal temperature maxima to be near the equator and 30N, respectively. Thus, if the tropical heat fluxes were equatorward for each month, the term "countergradient" would not apply to July.

In the present work zonal averages of the total eddy heat flux were obtained on a seasonal basis from 90N-30S, 1000-10 mb using data sources given in Chapter 2. From 30S-90S only six-month averages of the transient eddy component were available; hence the values in southern winter have undoubtedly been underestimated. The latter values were extracted from maps and are currently being updated by Professors J. Peixoto and V. P. Starr using additional data sources.

The total heat flux patterns are illustrated in Fig. 4.8 for December-February and June-August. The general features of the earlier studies are evident; there are poleward fluxes at middle and high latitudes with maxima at 850 mb and near the tropopause at about 50 degrees latitude in both hemispheres, and there are equatorward fluxes in the tropics. Note that there is a flux convergence near the equator in the summer hemisphere. It appears to be associated with the maximum rising motion in the main winter Hadley cell. The poleward limit of the equatorward fluxes in the winter hemisphere is found in the descending branch of the Hadley cell. With the lapse rate being less than dry adiabatic, ascending motion corresponds to cooling while descent is associated with heating. The effect of the equatorward fluxes, therefore, is to conduct heat away from the source regions in the descending branch and toward the heat sink in the ascending branch.

The standing eddy fluxes are generally smaller than the transient eddy fluxes. They are most prominent in the tropical and subtropical upper troposphere in the Northern Hemisphere where they often oppose the equatorward flux due to the transient eddies; otherwise the pattern of the total eddy flux is the same as for the transient eddy flux alone. Although the zonally-averaged horizontal temperature gradients are weak in the tropics (see Table 4.1) the equatorward heat flux in the troposphere is not countergradient throughout the entire year. In June-August when the temperature maximum in the middle and upper troposphere moves to about 20N the northern hemisphere flux is actually down a weak temperature gradient. The factors noted above will become more meaningful in Chapters 5 and 6 where the atmospheric heat and energy balances are discussed.

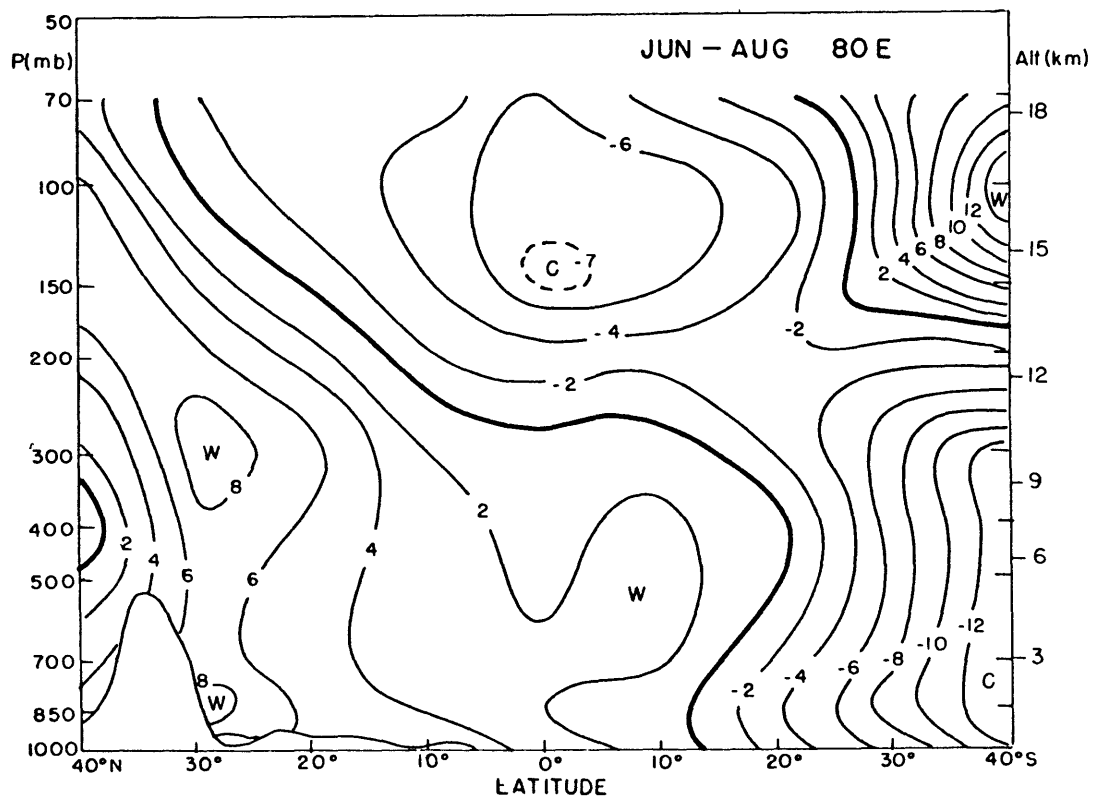
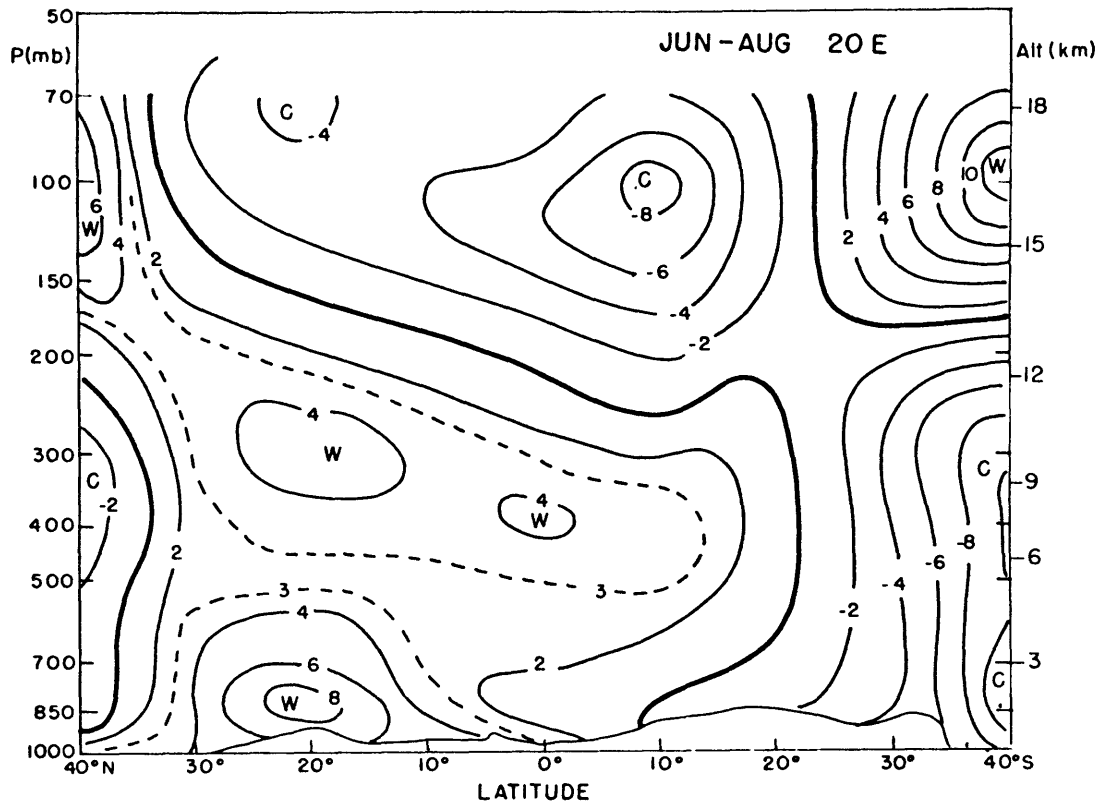


Fig. 4.1: Temperature pattern, ΔT , in $^{\circ}\text{C}$ for June-August:
 (a) 20E, (b) 80E (see text for explanation of isopleths)

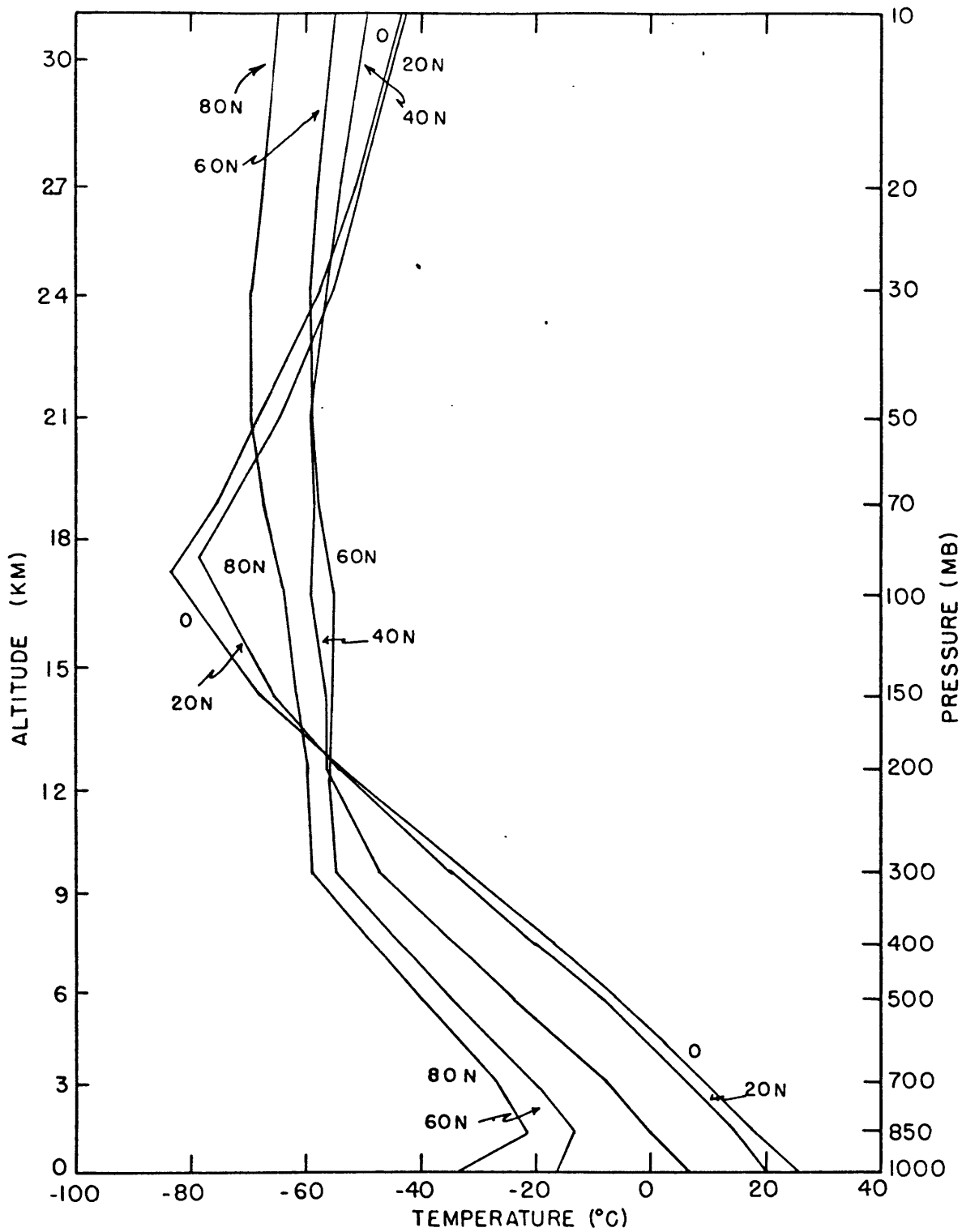


Fig. 4.2a: Temperature profiles in Northern Hemisphere for December-February.

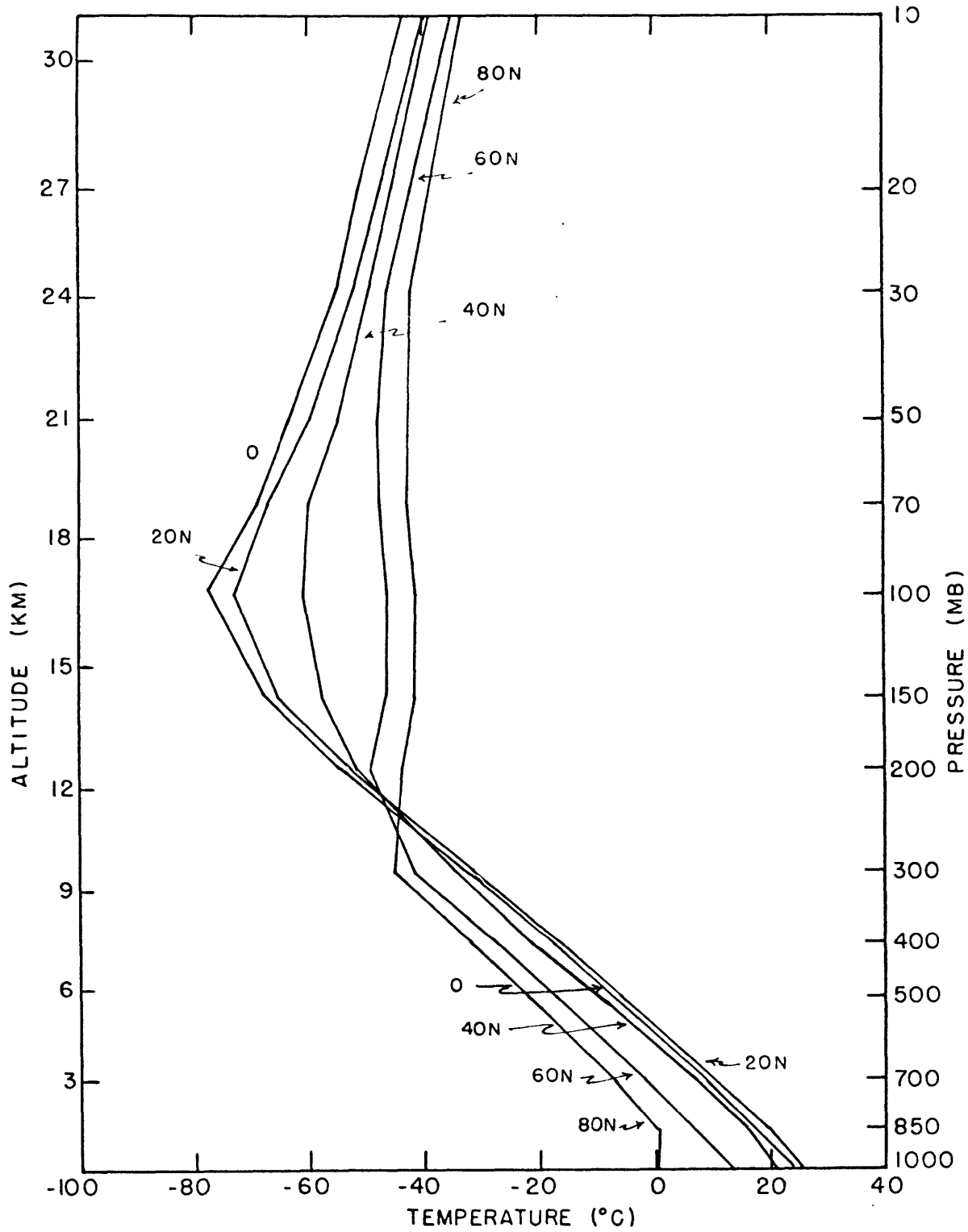


Fig. 4.2b: Temperature profiles in Northern Hemisphere for June-August.

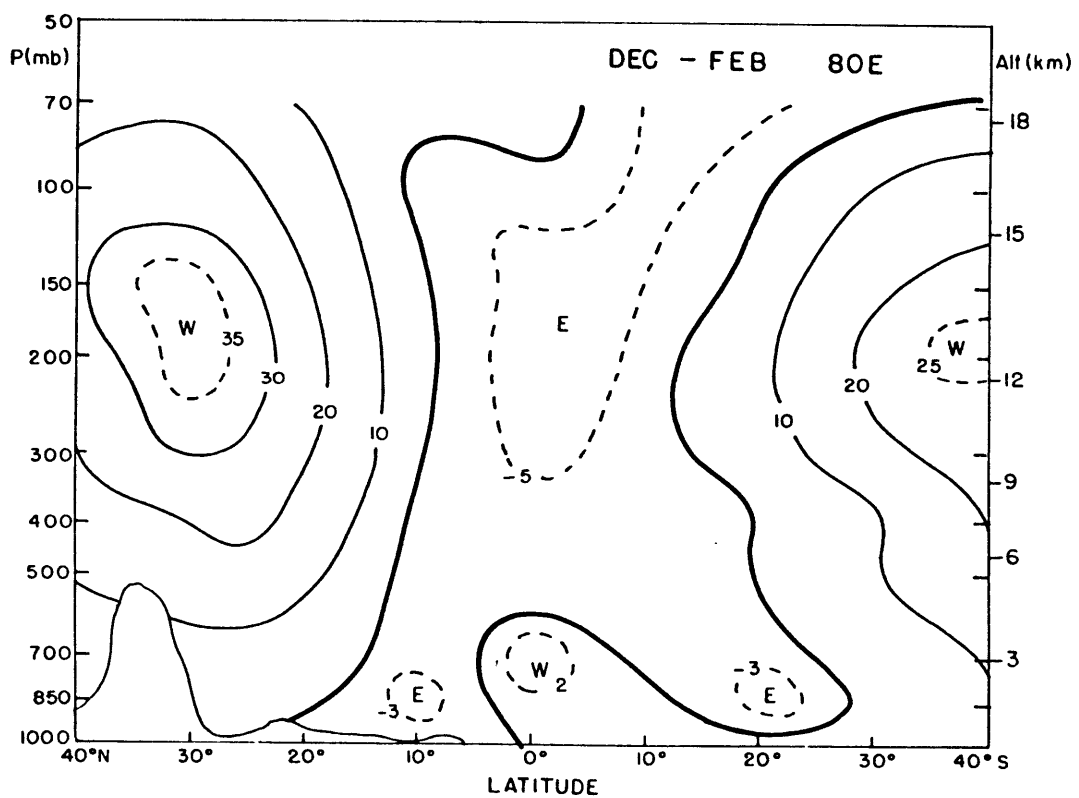
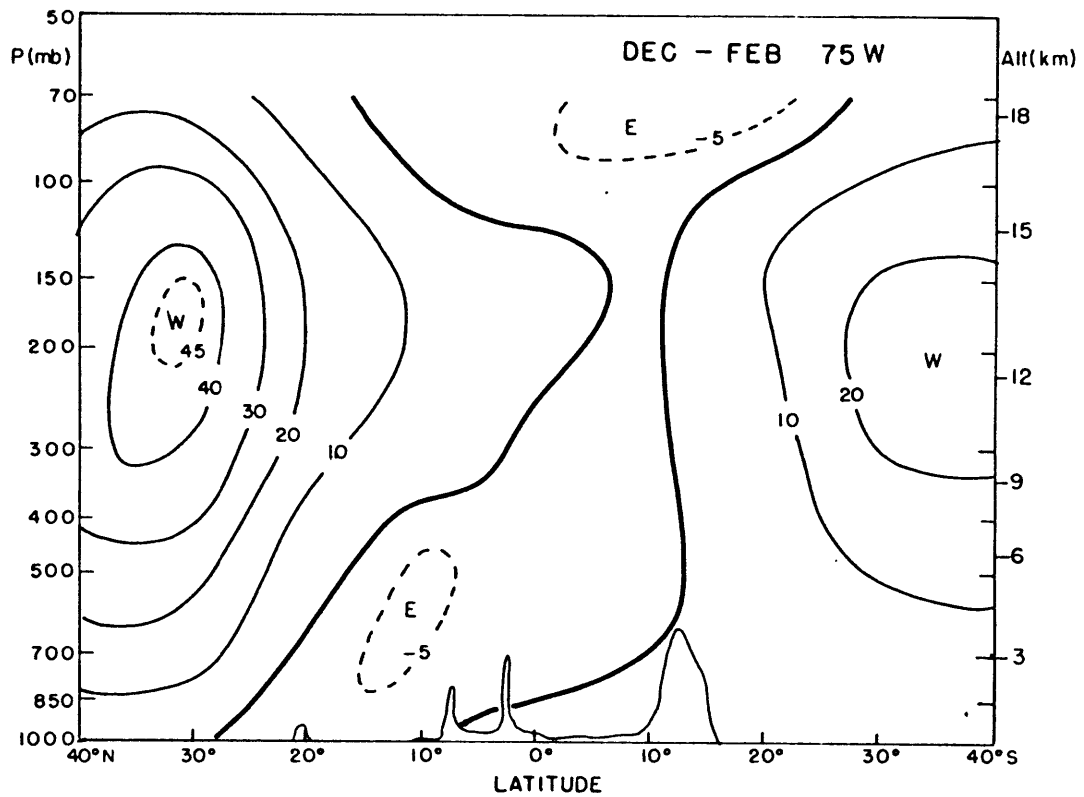


Fig. 4.3: Zonal wind velocity in m sec^{-1} for December-February:
(a) 75W, (b) 80E.

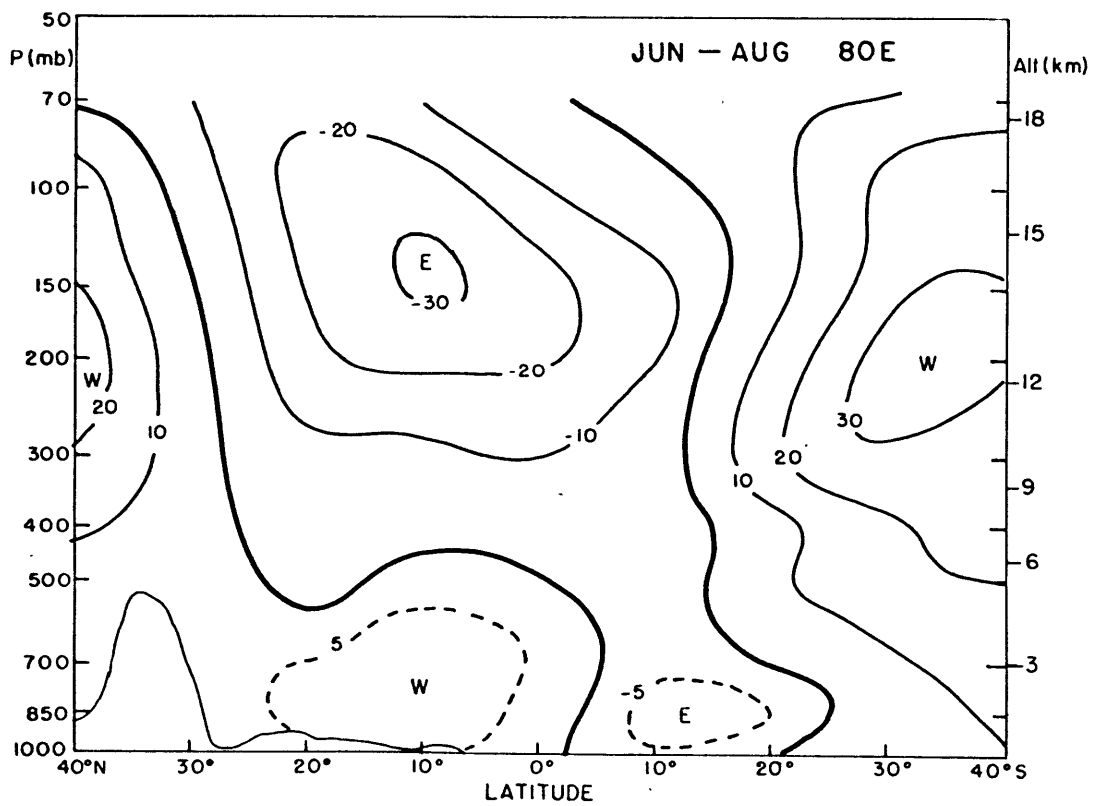
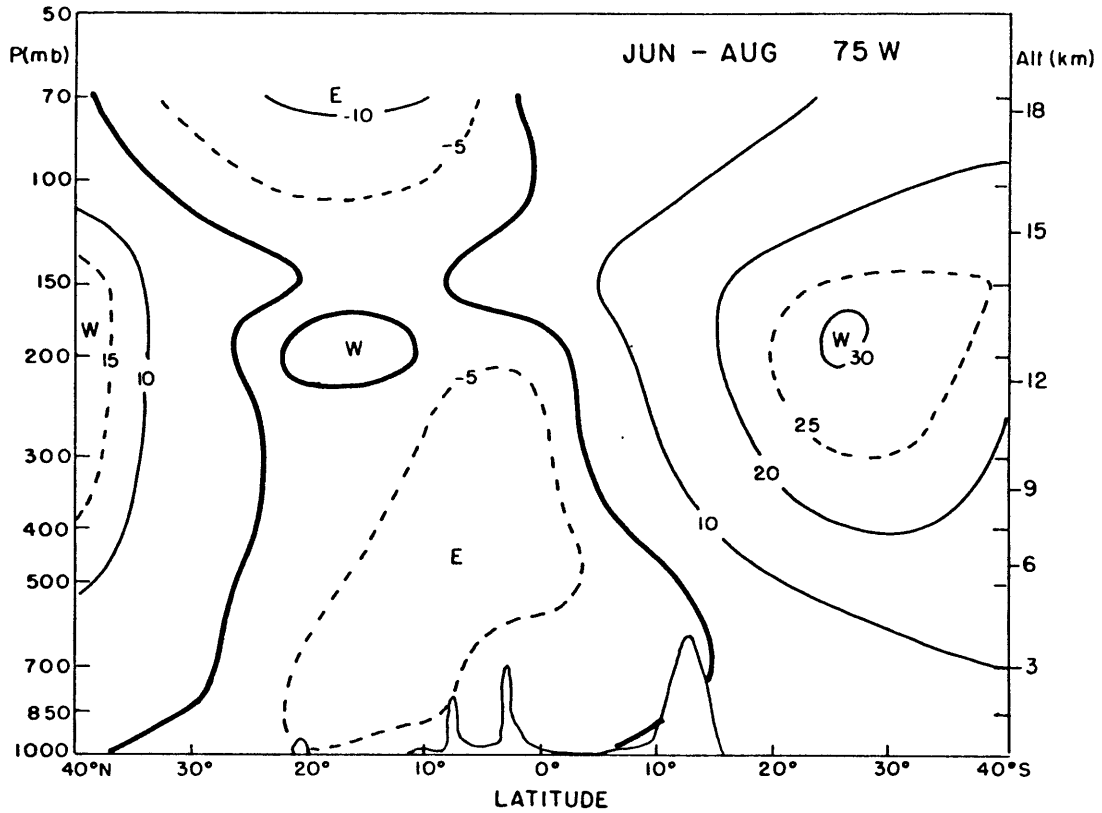


Fig. 4.4: Zonal wind velocity in m sec^{-1} for June-August:
(a) 75W, (b) 80E.

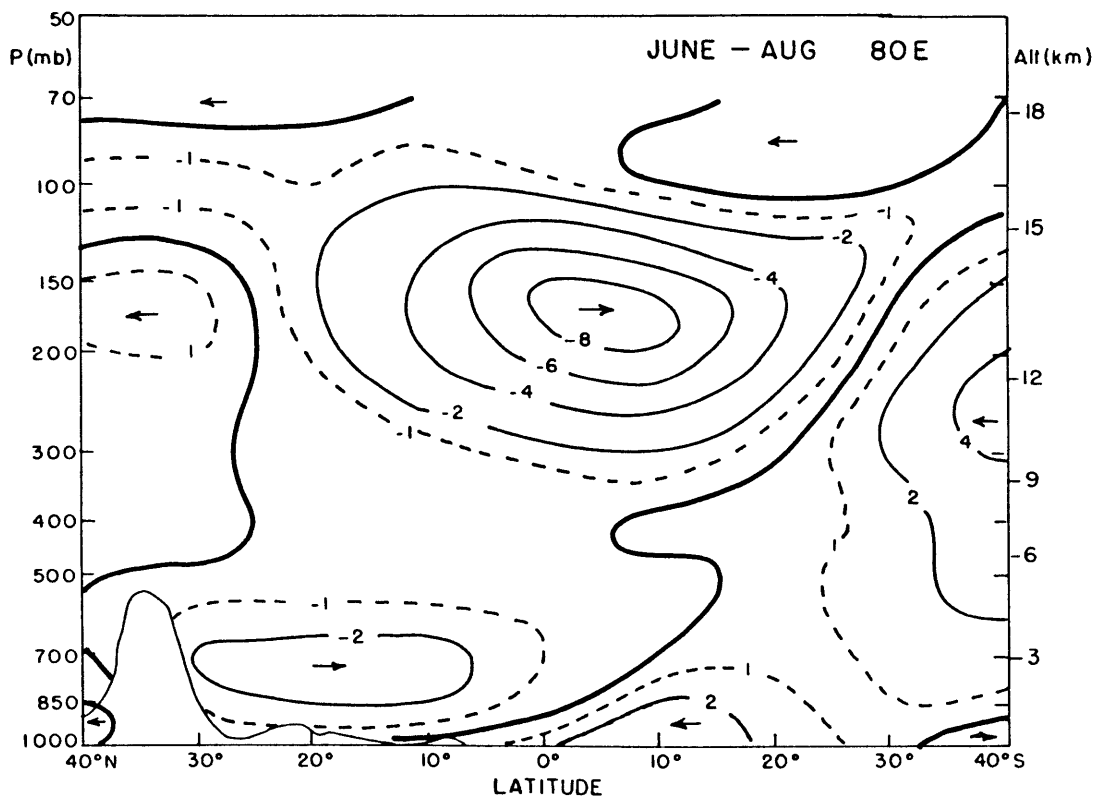
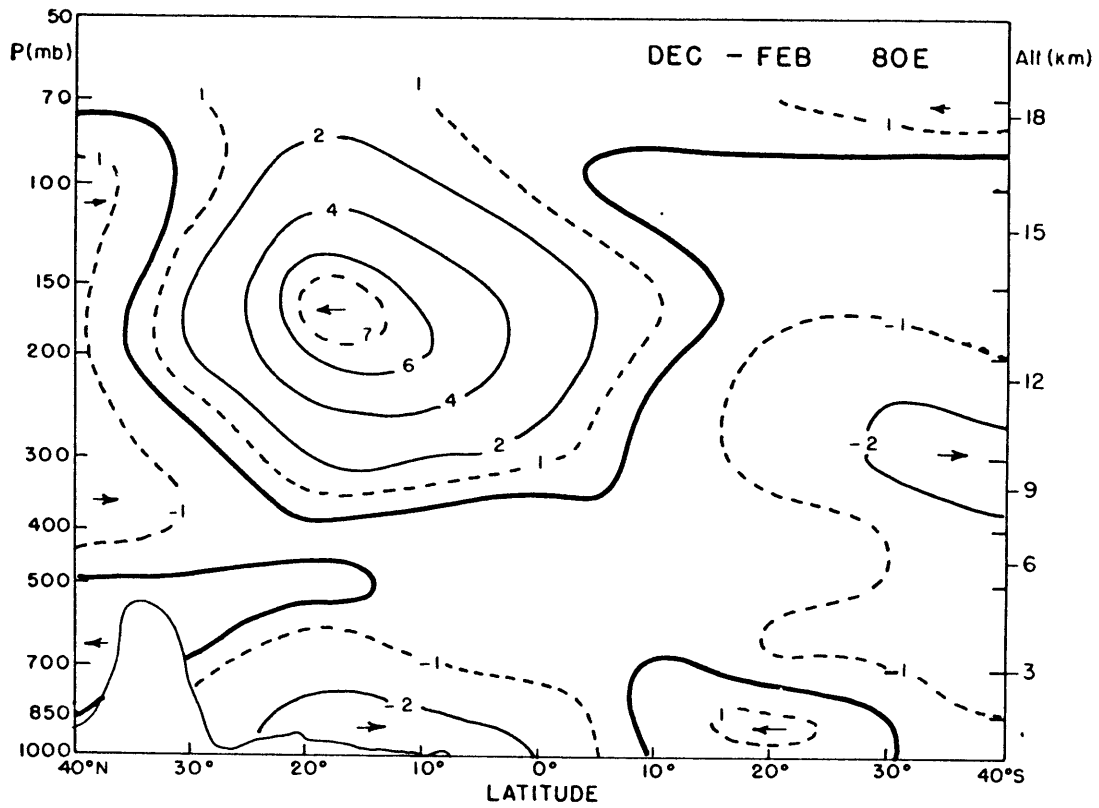


Fig. 4.5: Meridional wind velocity in m sec^{-1} : (a) Dec-Feb 80E, (b) Jun-Aug 80E.

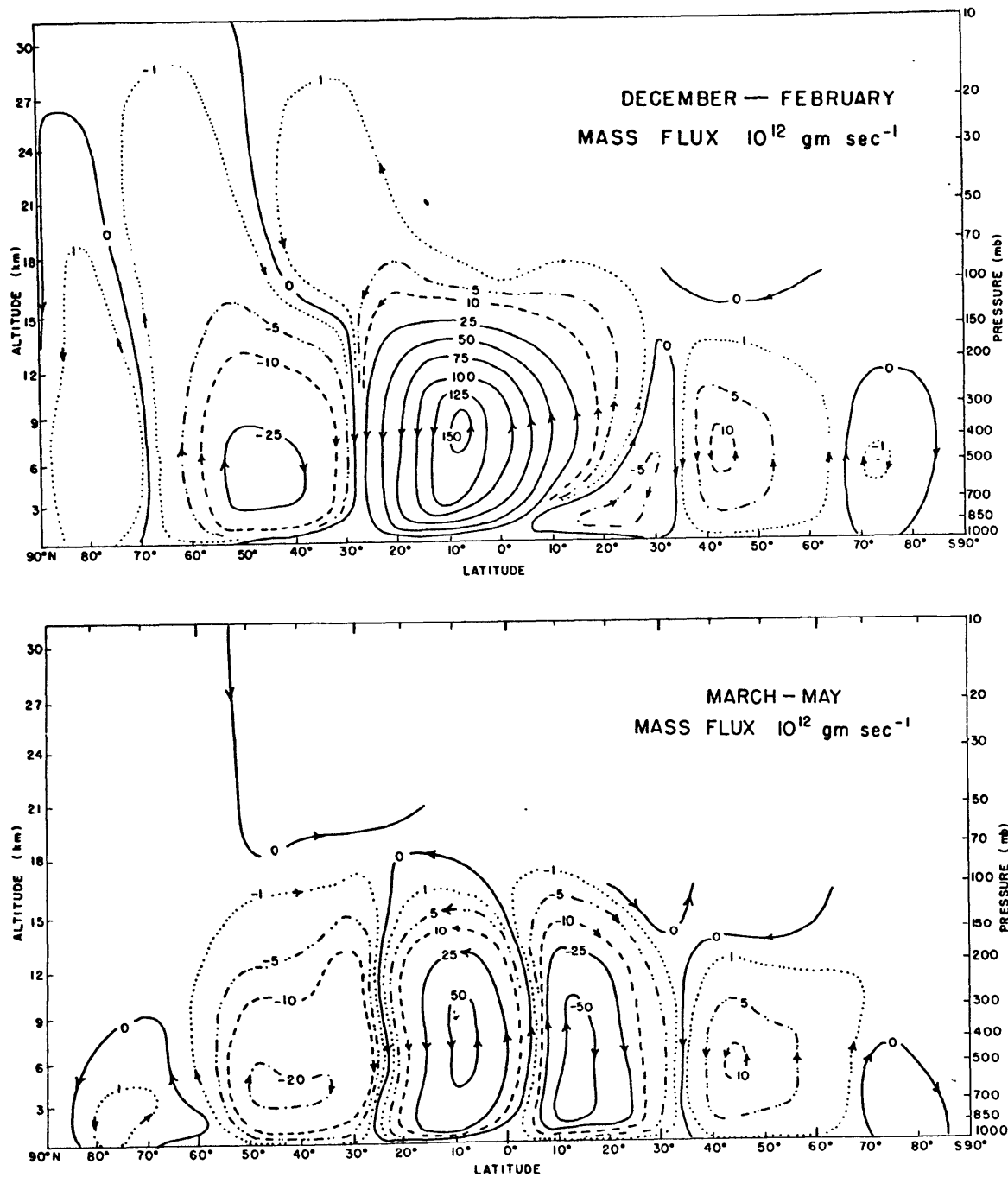


Fig. 4.6: Mass flux: (a) Dec-Feb, (b) Mar-May.

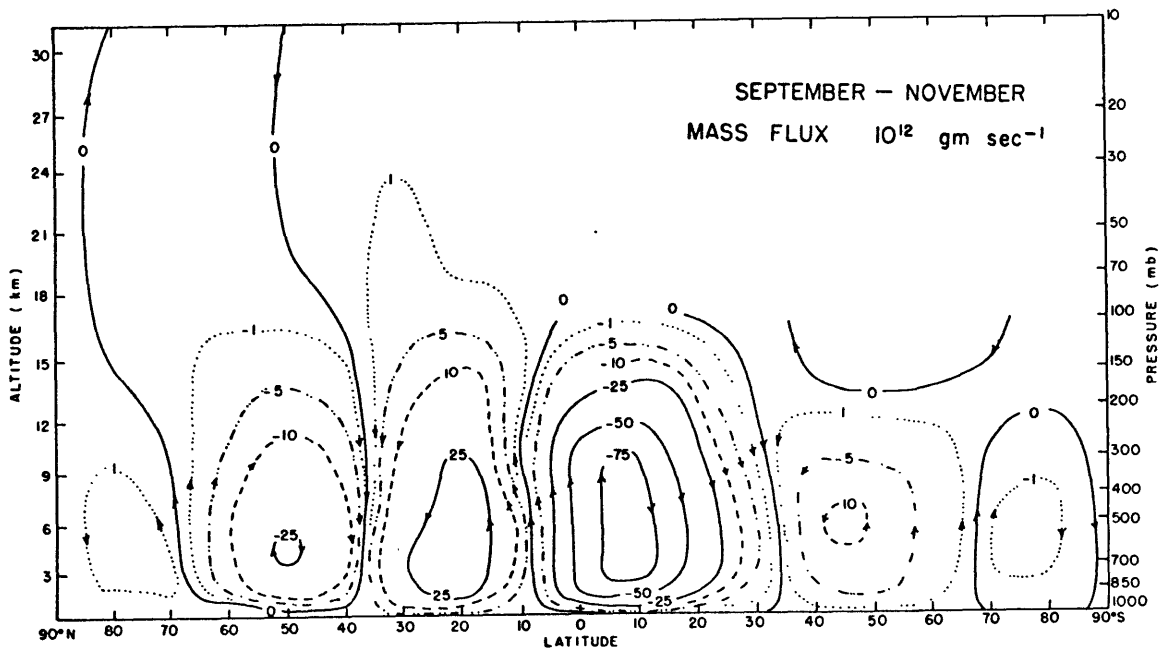
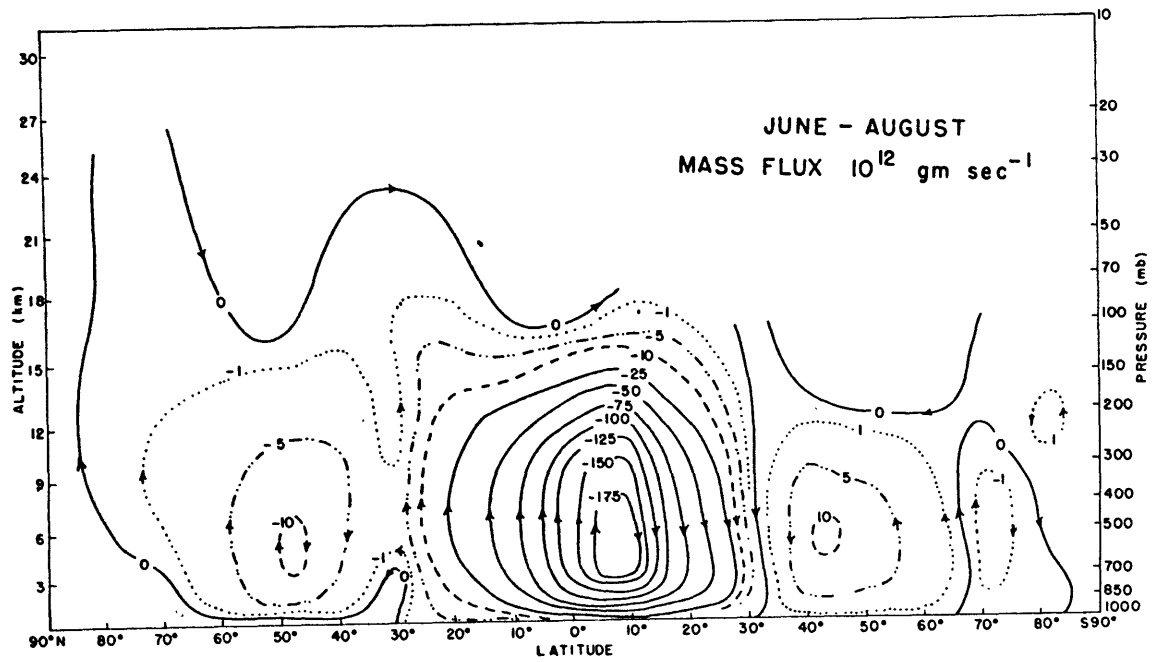


Fig. 4.6 (cont.): Mass flux: (c) Jun-Aug, (d) Sep-Nov.

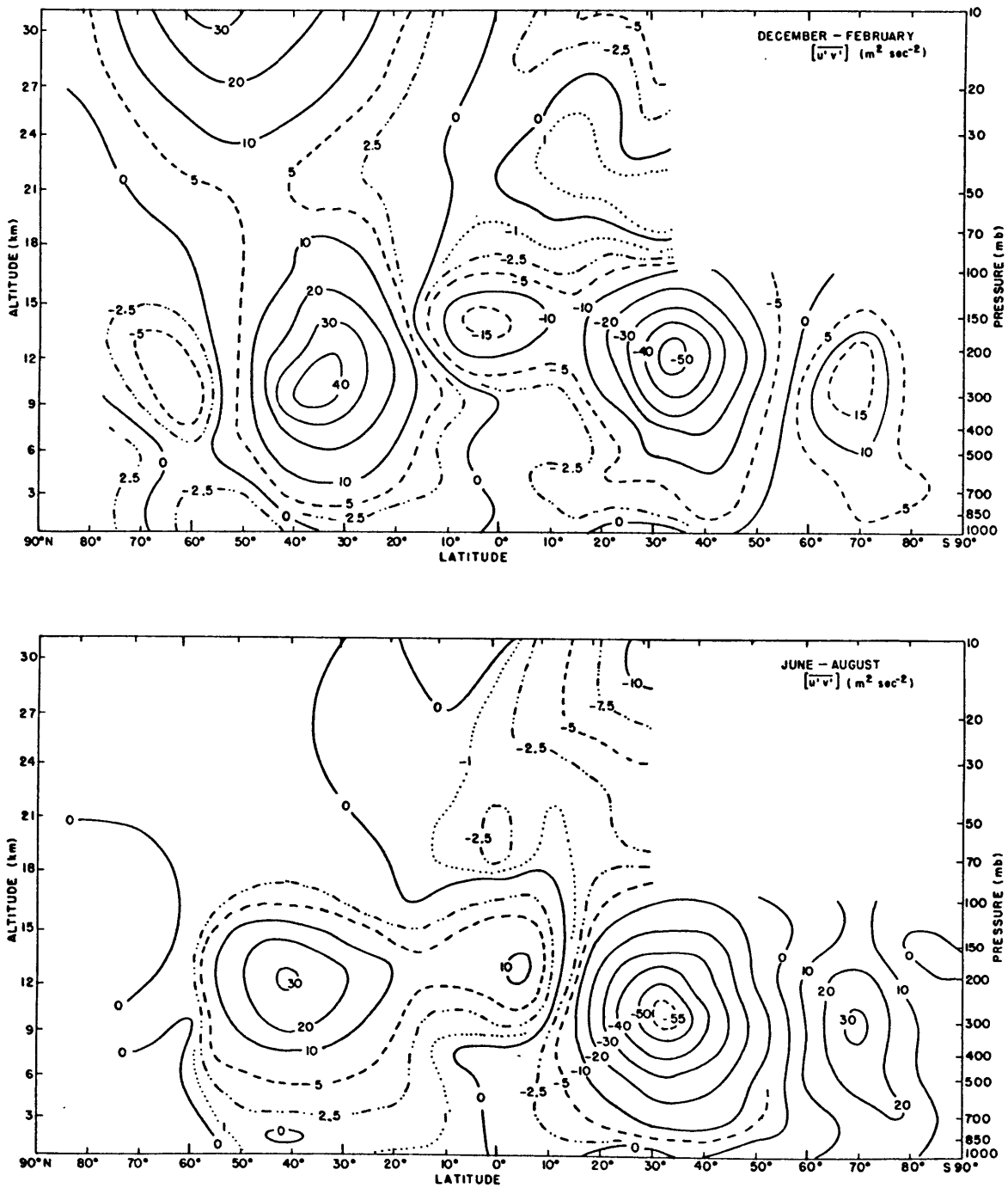


Fig. 4.7: Momentum transport by transient eddies.

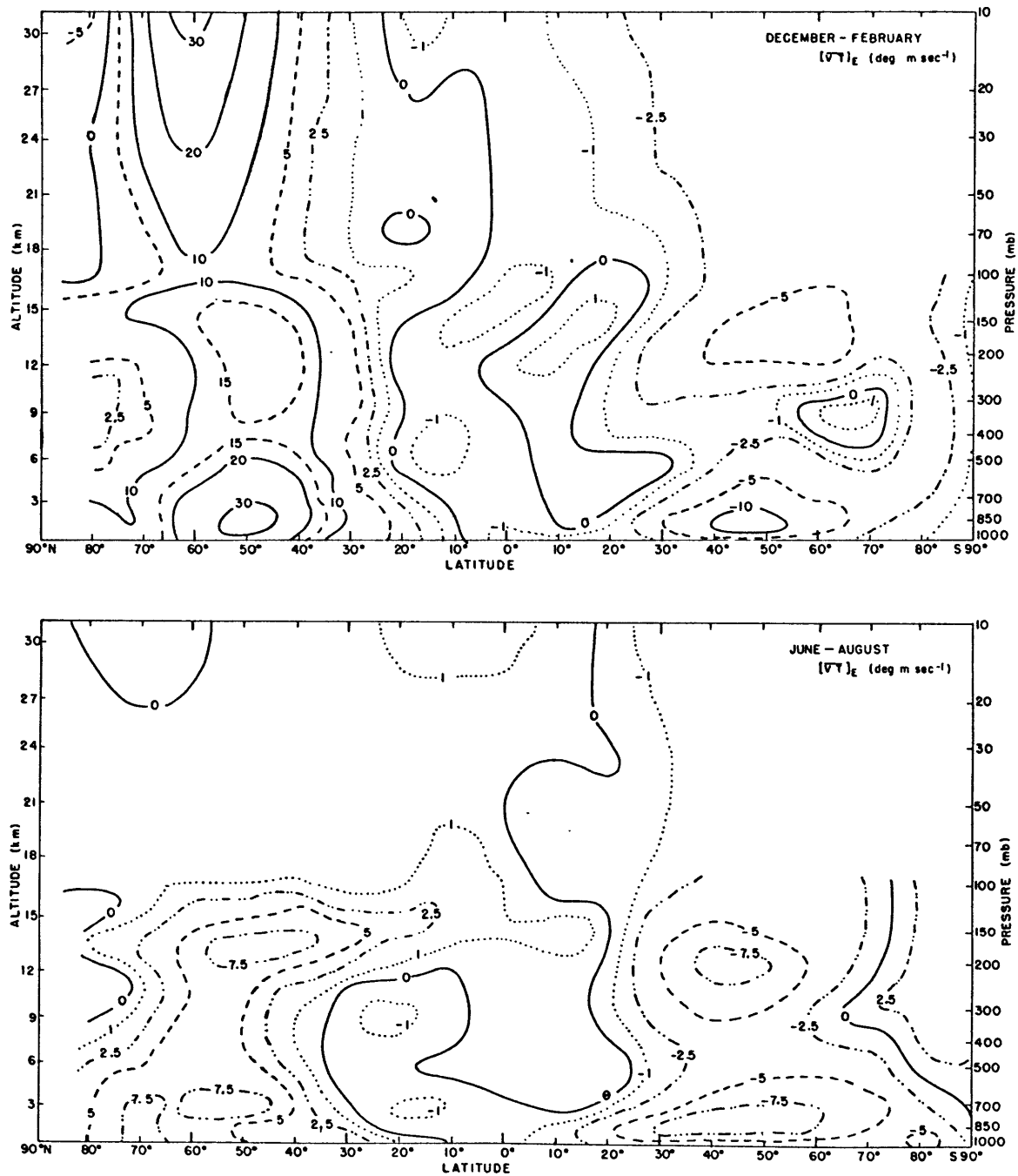


Fig. 4.8: Total eddy transport of sensible heat.

CHAPTER 5

TEMPERATURE CHANGES

One method of examining the atmospheric heat balance is to consider the various factors which control the mean temperature distribution. In a specific region, temperature changes may be due to diabatic heating (or cooling) and to heat transport by atmospheric motions. These factors are related explicitly in the First Law of Thermodynamics, which, when temporally and zonally averaged, is given by Eq. (5.1)

$$\begin{aligned} \frac{\partial [\bar{T}]}{\partial t} = & \frac{[\bar{Q}]}{c_p} + \beta [\bar{\omega}] - (a \cos \phi)^{-1} \frac{\partial}{\partial \phi} [\bar{v}'T' + \bar{v}^* \bar{T}^*] \cos \phi \\ & - \frac{[\bar{v}]}{a} \frac{\partial [\bar{T}]}{\partial \phi} - \frac{\partial}{\partial p} [\bar{\omega}'T' + \bar{\omega}^* \bar{T}^*] \\ & + \frac{R_d}{c_p p} [\bar{\omega}'T' + \bar{\omega}^* \bar{T}^*] + D_H \end{aligned} \quad (5.1)$$

where

$$\beta = -[\bar{T}] \frac{\partial}{\partial p} \ln [\bar{\theta}] = \frac{R_d}{c_p p} [\bar{T}] - \frac{\partial [\bar{T}]}{\partial p}$$

The terms on the right hand side (RHS) of Eq. (5.1) were evaluated from the data presented in Chapters 3 and 4 with the exception of the vertical heat fluxes and the last term which represents the eddy

diffusion. Typical magnitudes of the first three terms on the RHS of Eq. (5.1) were one degree per day, whereas the fourth term was on the order of 10^{-1} degrees per day and was only important in the lower boundary layer. Estimates of the fifth and sixth terms using vertical heat fluxes presented by Manabe and Hunt (1968) for an 18-level general circulation model were also on the order of 10^{-1} degrees per day but the former approached values near one degree per day in the middle latitude upper troposphere. Since typical values of the time derivative are on the order of 10^{-1} degrees per day the seasonal heat balance can be treated as a steady state problem and if contributions by the last term are insignificant the balance is governed, to a first approximation, by diabatic heating (cooling), adiabatic compression (expansion) and meridional eddy convergence (divergence) of sensible heat.

5.1 Diabatic Heat Sources

Meridional cross sections of net diabatic heating are given in Fig. 5.1 for each season. In general they show heating in the tropical troposphere and stratosphere extending to middle latitudes in the stratosphere and cooling elsewhere with the exception of the lower boundary layer where heating predominates at middle latitudes. In the troposphere seasonal changes in the latitudinal distributions of maximum heating near the equator are a direct reflection of the maximum latent heat release which occurs where the rising motion in the Hadley circulation is most intense; the highest values are located

between 500 mb and 400 mb near 5 degrees latitude in the summer hemisphere. The latitudinal extent of net heating at low latitudes decreases from about 35 degrees in the middle troposphere to less than 20 degrees in the upper troposphere and increases again to about 80 degrees in the lower stratosphere. The center of gravity of the net radiational heating in the stratosphere is in the spring and summer hemispheres and extends to the summer pole at 10 mb.

Diabatic cooling takes place throughout most of the middle and high latitude troposphere in both hemispheres because net radiative cooling predominates over latent heat release. Largest cooling rates occur in the middle troposphere during the fall and winter seasons, with maximum values reaching 2.0 deg day^{-1} over the polar cap (recall that net radiative heating rates in the Southern Hemisphere are reflected from the Northern Hemisphere). Table 3.1 shows that the largest values of radiative cooling at middle and high latitudes in the Northern Hemisphere are approximately 0.7 deg day^{-1} more in January and October than in April and July. In middle latitudes the radiative cooling rates in July are more than in April but there is also more latent heat release in July (see Table 3.3). Note that in the Southern Hemisphere near 700 mb and 50S diabatic heating occurs in a small region during December-February and September-November. This is due to a decrease in radiative cooling in southern spring and summer. In addition there is a secondary maximum in precipitation at 50S in southern summer (see Fig. 3.1) which produces more latent heat release. Radiative cooling in the stratosphere reaches maximum

values of 1.2 deg day^{-1} at the upper levels near the pole in fall and winter. In summer at high latitudes the stratosphere approaches radiative equilibrium.

Near the surface seasonal variations in diabatic heating are mainly influenced by changes in the boundary layer heating (BLH). For example, in northern hemisphere middle latitudes maximum values of diabatic heating at low levels are centered further to the north in June-August when the large land masses are relatively hot. Analyses of BLH due to sensible and latent heat, based on ship data taken in the Atlantic region from 30N-25S, are presented by Garstang (1967). They show that the ocean-to-atmosphere exchange in this region is mainly caused by latent heat transport. Another interesting feature is the intense diabatic cooling which occurs near the surface at 50S in December-February. Budyko's maps (1963) of turbulent heat exchange show that during the summer months there is a broad band (approximately 15 degrees latitude in width) of atmosphere-to-ocean flux which extends around the global oceans.

5.2 Adiabatic Subsidence

The second term on the RHS of Eq. (5.1) represents the heating (cooling) due to adiabatic compression (expansion). Since the potential temperature increases with height the stability parameter, β , is always positive and downward motion produces heating, commonly referred to as subsidence heating while upward motion produces cooling. Values of ω , used to compute this term were also used to compute

vertical velocities (see Table 4.4), while values of the stability parameter were computed from zonal mean temperatures given in Table 4.1. Meridional cross sections of adiabatic subsidence are illustrated in Fig. 5.2 for each season. In general tropospheric patterns show seasonal symmetry about the equator with cooling in the tropics and high latitudes associated with ascending air and heating in the subtropics and middle latitudes associated with descending air. Above 100 mb data were only available from 90N-20N and the alternating patterns of cooling and heating are generally polewards of their tropospheric positions. The monthly trend of stratospheric mean meridional circulations has been discussed elsewhere (Vincent, 1968).

In the troposphere cooling due to adiabatic expansion in the rising branch of the Hadley circulation is approximately the same in all seasons and tends to balance the diabatic heating. Maximum values of about 1.0 deg day^{-1} occur near 500 mb at 5S in December-February and March-May and at 5N in the other two periods. Tropospheric heating rates due to adiabatic compression in the descending air show much greater seasonal fluctuations. Maximum values of approximately 1.5 deg day^{-1} occur in the winter hemisphere and are associated with the stronger downward motion in the Ferrel and Hadley cells; in the summer hemisphere values decrease to about 0.2 deg day^{-1} . In both hemispheres the highest heating rates are nearest the equator in the winter and spring seasons and in each season they are closer to the equator in the Southern Hemisphere than for the corresponding season in the Northern Hemisphere. Tropospheric cooling rates in the rising

branch of the Ferrel cell show a marked seasonal variation in the Northern Hemisphere but not in the Southern Hemisphere. Maximum values in the Southern Hemisphere are approximately 0.1 deg day^{-1} in all seasons and are located near 60S. The values are probably too small because of the assumptions used to compute mean meridional circulations (see Chapters 2 and 4). In the Northern Hemisphere maximum cooling of approximately 0.6 deg day^{-1} occurs in winter near 55N when three cells are evident. In spring the highest cooling rates remain near 55N but values have decreased to about 0.4 deg day^{-1} . In summer when vertical motions are weak and only two cells are evident peak values continue to decrease and are located further north. In fall values increase again as the winter pattern is approached.

As noted in Chapter 4 the stratospheric circulations in fall and winter appear to be an extension of the tropospheric circulations and there is a poleward tilt with height in the patterns so that two cells essentially dominate the stratospheric circulation. Miyakoda (1963) and Perry (1967) found a similar two cell structure in the stratosphere for January 1958 and January 1963. During fall and winter cooling rates at low latitudes are approximately one-third of those in the troposphere whereas heating rates at middle latitudes are almost as large as the tropospheric values in December-February and approximately one-half the tropospheric values in September-November. In spring there is subsidence heating in most of the stratosphere south of 65N and peak values reach $0.25 \text{ deg day}^{-1}$ between 30 mb and 20 mb at 55N; in summer values are small. At high

latitudes maximum cooling of about 2.0 deg day^{-1} occurs in winter near 20 mb. This value is approximately three times as large as the corresponding maximum value in the troposphere. In the other seasons, cooling rates are comparable to those in the troposphere.

5.3 Eddy Heat Flux Convergence

The third term on the RHS of Eq. (5.1) represents the heating (cooling) due to the convergence (divergence) of sensible heat transport by transient and standing eddies. Meridional cross sections of the eddy heat flux convergence are presented in Fig. 5.3 for each season. The tropospheric patterns generally show weak convergence near the equator, moderate divergence in the subtropics and middle latitudes and strong convergence at higher latitudes. Above 100 mb data were only available from 90N-30S and Fig. 5.3 generally shows patterns of convergence and divergence at the same latitudes as in the troposphere except in June-August when there is very little heat transport. South of 30S only six-month averages of sensible heat transport by transient eddies were available and spring and fall values were taken as the average, consequently the convergence patterns for these seasons are identical.

In the high latitude troposphere of both hemispheres there is generally a large supply of heat due to eddy heat flux convergence which compensates for radiation cooling and cooling by adiabatic expansion in the ascending branch of the Ferrel cell. Values are somewhat sporadic near the polar regions but suggest that peak heating

occurs at the lower levels. Values in the Northern Hemisphere tend to be larger than those in the Southern Hemisphere but the latter do not include contributions by standing eddies and are based on six-month averages.

5.4 Atmospheric Heat Balance

To summarize the major factors which control the heat balance of the atmosphere a set of curves is presented for each season (Figs. 5.4-5.9) showing meridional distributions of the three terms discussed above at selected pressure levels. The levels chosen were 700, 400, 200, 70 and 20 mb since they generally give the most comprehensive representation of the results.

1. December-February

At 700 mb (Fig. 5.4a) there is a reasonable balance among the terms from 90N-40S except near 75N where the heat flux convergence may have been underestimated and near 35N where there is also too much cooling. In the latter region there is some heating at low levels in the Ferrel cell due to mean meridional flow down the temperature gradient but this amounts to less than 0.1 deg day^{-1} . It should be recognized that latitudes of peak heating and cooling can be estimated only to within about 5 degrees; thus, for example, an approximate balance could be achieved near 35N if peak heating due to subsidence and peak cooling due to heat flux divergence were shifted about 5 degrees polewards and equatorwards, respectively. From 40S-70S the results indicate too much heating and over the south polar

cap they show excessive cooling but as noted previously the patterns at middle and high latitudes in the Southern Hemisphere are not as well known as those over the remainder of the globe. In the Northern Hemisphere the curves show quite clearly the relative importance of the three major terms at 700 mb. At high latitudes diabatic cooling is balanced mainly by the eddy convergence of sensible heat whereas heating (or cooling) due to mean vertical motions is secondary. From 45N-10N there is an approximate balance between heating due to subsidence and cooling due to sensible heat flux divergence, while in the equatorial region diabatic heating is nearly equivalent to cooling by adiabatic expansion.

At 400 mb (Fig. 5.4b) two features are outstanding. First, in the equatorial zone the heat balance is similar to that at 700 mb but peak values are larger reflecting the increased importance of latent heat release. Secondly, polewards of the tropical region there is a tendency for the heat flux convergence and the subsidence terms to oppose each other with heating generally predominating; however, diabatic cooling (mainly radiational cooling) is sufficiently large to produce values of net cooling on the order of one degree per day. Consequently, other factors such as vertical heat transports or small scale diffusion must be important in this region if a heat balance is to be maintained. A cross section of vertical eddy heat fluxes presented by Manabe and Hunt (1968), shows that there is a supply of heat to the upper troposphere and based on their figure a rough calculation of the fifth and sixth terms on the RHS of Eq. (5.1) was per-

formed. Maximum heating of almost 1.0 deg day^{-1} occurred between 500 mb and 300 mb near 35N in the region of strong baroclinic disturbances; estimated heating rates at 400 mb were 0.2, 0.3 and 0.7 deg day^{-1} at 70N, 50N and 30N. Their results indicate that large scale vertical eddy heat transports may be an important heat source in the extratropical middle and upper troposphere.

At 200 mb the meridional distributions of the three terms are similar to those at 400 mb with the major exception that radiational cooling at middle and high latitudes has substantially decreased so that an approximate heat balance is again maintained. Note also that diabatic heating near the equator has significantly decreased because of the reduced role of latent heat release. At 70 mb (Fig. 5.8a) the three terms generally balance except north of 65N where it appears that vertical motions are too large. At high latitudes the heat source is due to eddy heat flux convergence while the heat sink is due to radiation and adiabatic expansion in the rising air; at middle latitudes the heating is due to subsidence while cooling is due to radiation and eddy heat flux divergence; and in the tropics radiational heating balances the cooling by expansion in the ascending motion while the contribution of eddy heat transport is small. At 20 mb (Fig. 5.8b) the patterns are similar to those at 70 mb except the magnitudes of the terms are larger at middle and high latitudes.

In a recent study Murgatroyd (1969) computed mean meridional and vertical velocities and examined the heat balance of the upper troposphere and lower stratosphere. His results for a six month

winter season in the Northern Hemisphere are in agreement with the present results for December-February except for the contribution by the subsidence term in the stratosphere. The major difference appears to be that Murgatroyd's mean meridional cells, although they extend from the troposphere into the stratosphere, do not tilt polewards with height near the tropopause and in the lower stratosphere.

2. March-May

The meridional distributions of the three terms are similar to those in December-February but values have generally decreased especially at middle and high latitudes in the stratosphere. A notable exception to the similarity between seasons is the change in the subtropical tropospheric subsidence distributions which is a direct reflection of changes in the mean meridional circulation patterns. In both seasons, however, the distribution of cooling in the rising branch of the Hadley circulation remains the same. In the stratosphere there is a poleward progression of the patterns between the winter and spring seasons which tends to follow the migration of the mean meridional circulation (Vincent, 1968). At 700 mb and 200 mb (Figs. 5.5a and 5.5c) there is generally a heat balance except over the south polar cap where, as noted previously, the results are not well known. At 400 mb there is a balance at low latitudes but, as in December-February, there is too much cooling in middle and high latitudes. In the Northern Hemisphere where results are more reliable excessive cooling amounts to about 0.5 deg day^{-1} at high latitudes and 1.0 deg day^{-1} in middle latitudes. If the results of Manabe and

Hunt (loc. cit.) are applicable to all seasons, heating due to vertical eddy heat transport is approximately 50% of the apparent surplus cooling and consequently an important factor in maintaining the heat budget of the upper troposphere. In most of the stratospheric region the three terms considered show an approximate heat balance (see Fig. 5.8c, d).

3. June-August

The three terms (see Fig. 5.6) generally show seasonal symmetry with the period December-February. For example, in middle latitudes at 700 mb, peak values of diabatic heating occur at 40 degrees latitude in the winter hemisphere and 55 degrees latitude in the summer hemisphere; however, there is more heating in southern winter and summer than in the corresponding seasons in the Northern Hemisphere. This is due to higher values of latent heat release which reflect the larger precipitation amounts in the middle latitude region of the Southern Hemisphere. In June-August in the descending branch of the Hadley circulation there appears to be too much subsidence heating in the troposphere. Vertical velocities given in Table 4.4 show that maximum values of almost 6.0 mm sec^{-1} are associated with these large heating rates. In contrast, peak values of vertical velocity in the descending branch of the Hadley circulation in northern winter are approximately 4.5 mm sec^{-1} while values in the ascending air are about 4.0 mm sec^{-1} during both periods. At 400 mb the curves again illustrate a cooling imbalance of about 1.0 deg day^{-1} in middle and high latitudes and, as noted previously, there is a need for addi-

tional heat sources in the upper troposphere.

In the southern hemisphere winter the Ferrel cell does not extend above the 200 mb level whereas in the northern hemisphere winter the extension of the cell into the stratosphere is a dominant feature of the circulation. At 200 mb, therefore, the cooling due to adiabatic expansion at high latitudes which was evident in the Northern Hemisphere in Fig. 5.4c is not evident in the Southern Hemisphere in Fig. 5.6c.

A comparison of heating rates, due to eddy heat flux convergence, between northern and southern winters suggests that the computed values at high latitudes in the southern hemisphere troposphere are too small during June-August. If seasonal averages instead of six-month averages were available and the standing eddy contribution was known, values of eddy heat transport and perhaps heat flux convergence would be larger in southern winter. It was noted above that values of each of the three terms in the northern hemisphere stratosphere were extremely small in June-August and no further comments are presented. For convenience the scale of the values in Fig. 5.9a, b has been increased by four.

4. September-November

The meridional distributions of the three terms are similar to those in March-May with two exceptions. First, as noted previously, there is more diabatic cooling (mainly radiational cooling) in the northern hemisphere troposphere during the fall season than during spring. Since southern hemisphere values of radiation are reflected

from northern hemisphere values, diabatic heating curves in the southern hemisphere troposphere also show more cooling in fall than in spring. Secondly, the September–November distributions of subsidence heating in the northern hemisphere troposphere are shifted about 10 degrees to the north of their positions in March–May. The major equatorward migration of the northern hemisphere tropospheric mean meridional circulation patterns apparently takes place between fall and winter as the subsidence curves for December–February and March–May are nearly identical. The three terms generally balance each other in the troposphere except at middle and high latitudes in both hemispheres between 500 mb and 300 mb where there is too much cooling and at middle latitudes in the Southern Hemisphere between 700 mb and 850 mb where there is too much heating. The former occurs during all seasons and reference to the work of Manabe and Hunt (loc. cit.) has already been discussed in detail. In another study Berggren and Nyberg (1967) investigated the vertical eddy heat transport by sensible and latent heat for the region from 90N–30N in October, 1961. Their results showed a total flux upwards through the 700 mb surface which gave an equivalent warming to the middle and upper troposphere ranging from 0.4 deg day^{-1} at 85N to a maximum value of 2.6 deg day^{-1} at 50N. They suggest that heat transports by vertical eddies are at least as large as those by horizontal eddies and perhaps one to three times larger; enough to compensate for the intense radiational cooling above 700 mb by themselves. The general conclusion reached by Berggren and Nyberg is in agreement with Manabe and Hunt and strongly suggests

the need for additional estimates of this term.

The excessive heating at low levels in the middle latitude Southern Hemisphere appears to be due to too much diabatic heating (see Fig. 5.7a) which could result from overestimating the latent heat release or from using reflected radiative heating rates. There is also a heat imbalance at 700 mb in the Northern Hemisphere at middle latitudes which apparently is due to the abrupt changes in the meridional distribution of heat flux convergence. If the curve were smoothed from 60N-30N an approximate heat balance would be achieved.

The stratospheric distributions of heating due to subsidence and eddy heat flux convergence are similar to those in March-May, but the distributions of radiative heating are different. The change is most notable at 20 mb (cp. Figs. 5.8d and 5.9d) where the curves shift about 30 degrees latitude between the two periods; peak heating is near 15N in March-May and 15S in September-November. There appears to be too much cooling in September-November at high latitudes especially from 30-20 mb where imbalances average about 0.6 deg day^{-1} . It is worth noting that maximum decreases in temperature occur in this region during September-November with cooling amounting to approximately 0.2 deg day^{-1} .

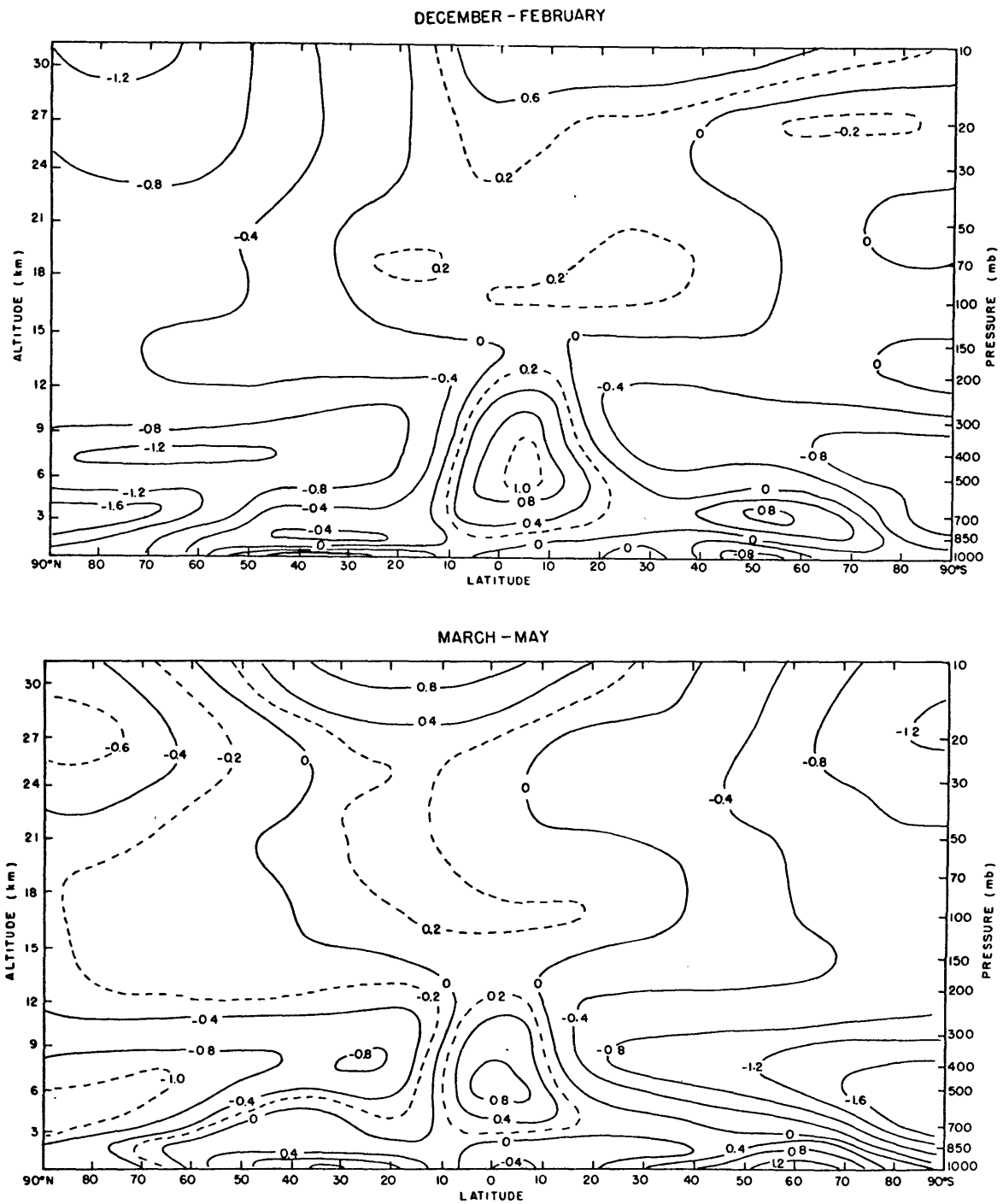


Fig. 5.1a, b: Net diabatic heating in deg day^{-1} . (a) Dec-Feb, (b) Mar-May.

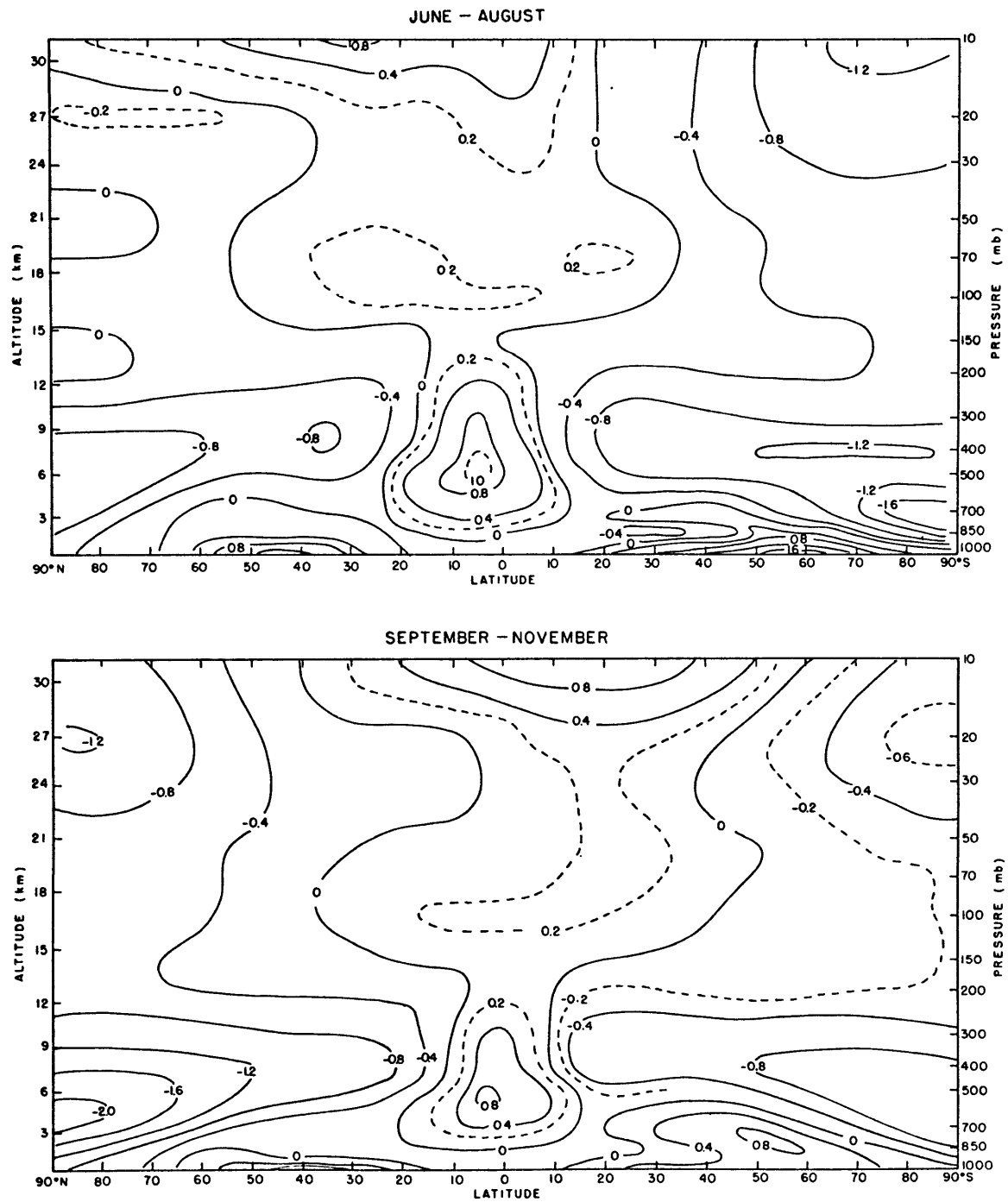


Fig. 5.1c, d: Net diabatic heating in deg day^{-1} . (c) Jun-Aug, (d) Sep-Nov.

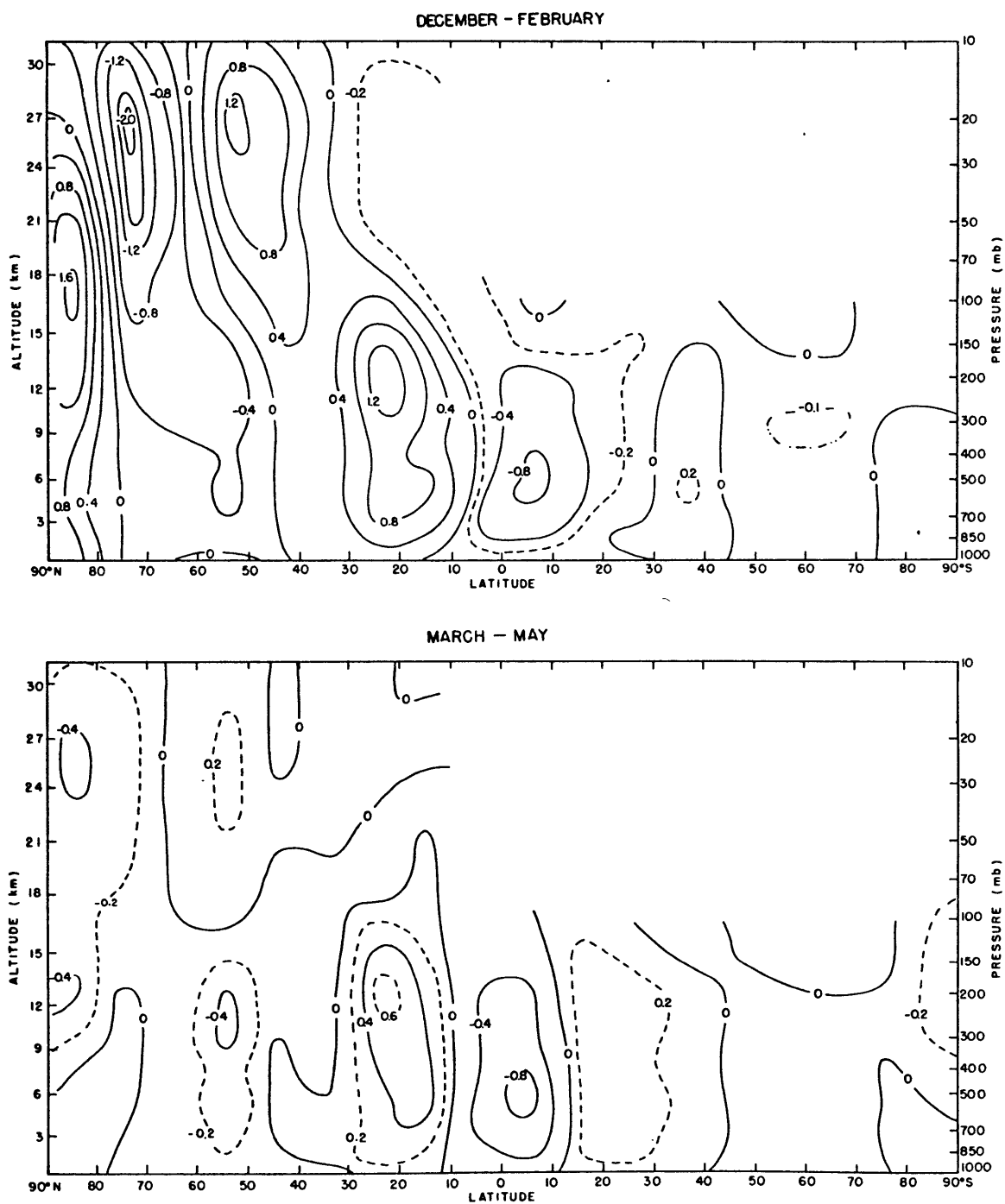


Fig. 5.2a, b: Subsidence heating in deg day^{-1} . (a) Dec-Feb, (b) Mar-May.

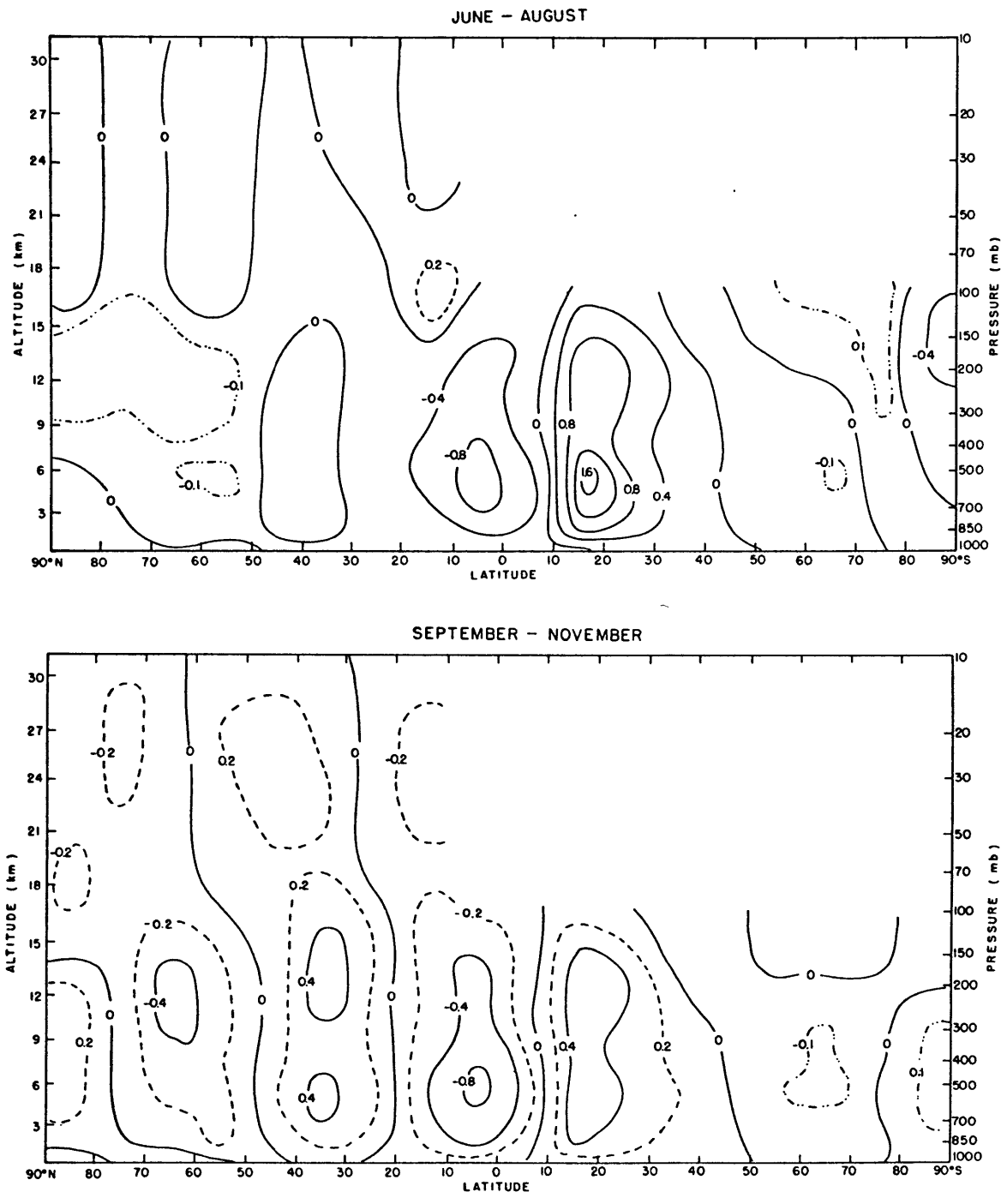


Fig. 5.2c, d: Subsidence heating in deg day⁻¹. (c) Jun-Aug, (d) Sep-Nov.

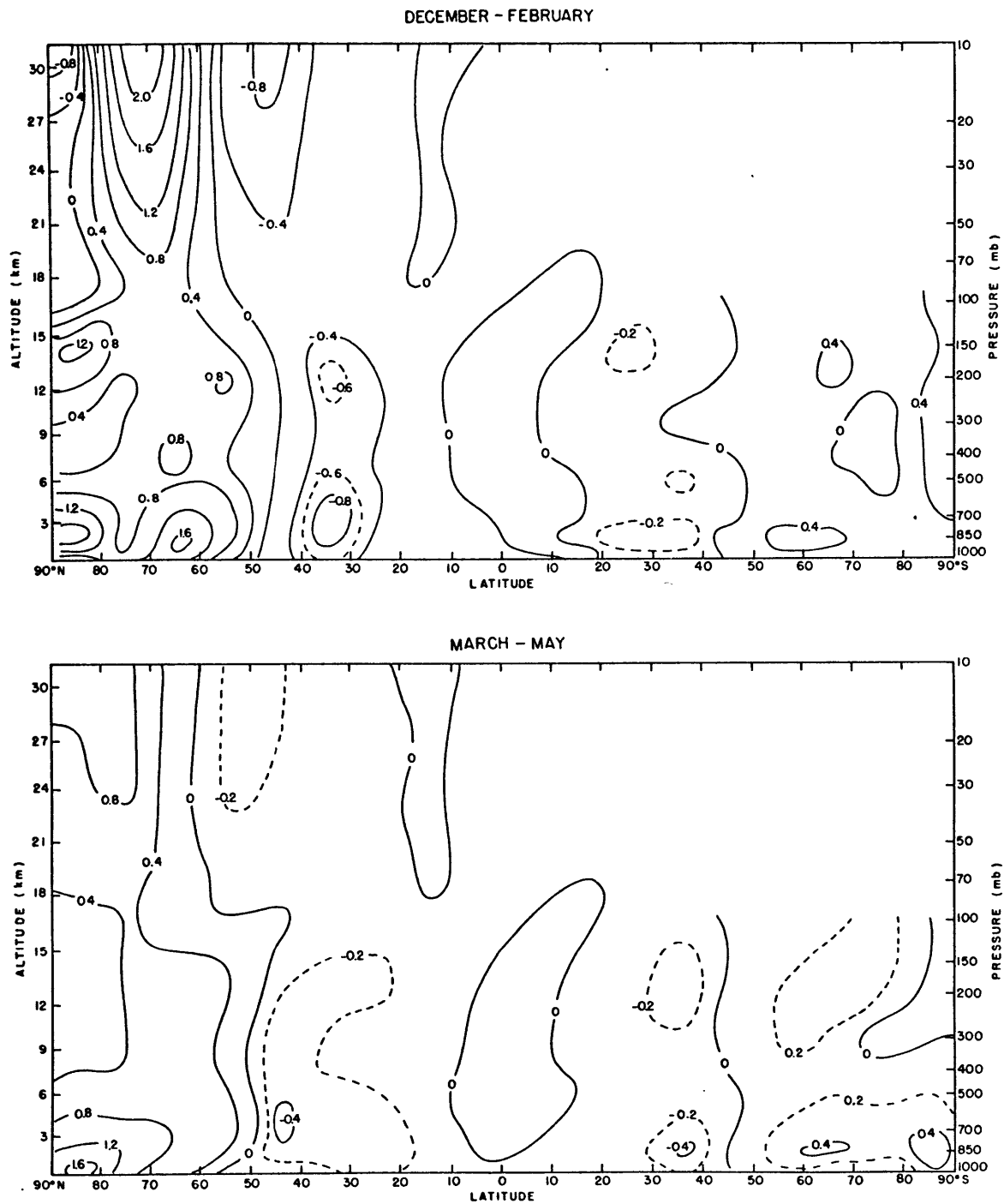


Fig. 5.3a, b: Convergence of sensible heat flux in deg day^{-1} .
 (a) Dec-Feb, (b) Mar-May.

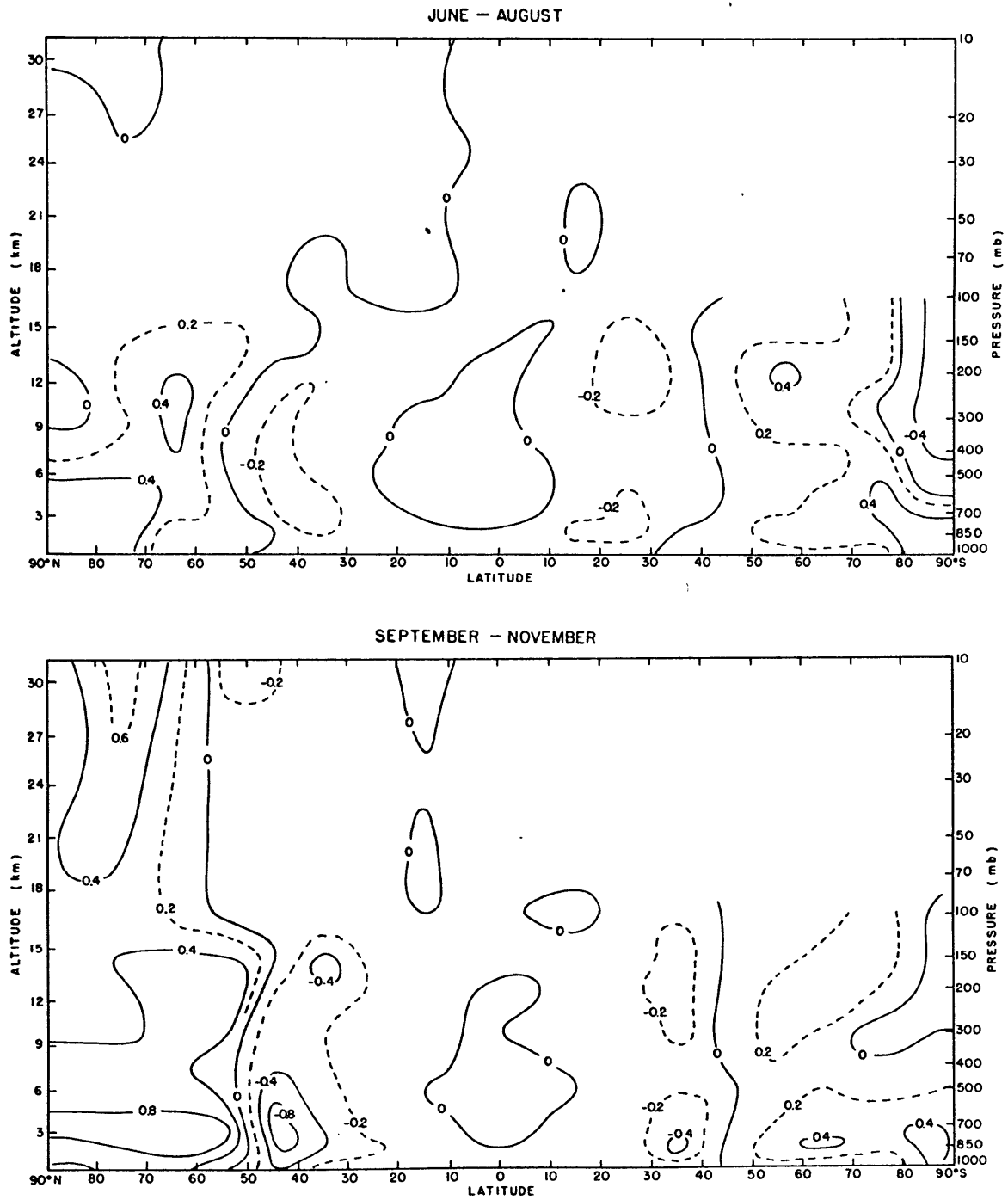


Fig. 5.3c, d: Convergence of sensible heat flux in deg day^{-1} :
 (c) Jun-Aug, (d) Sep-Nov.

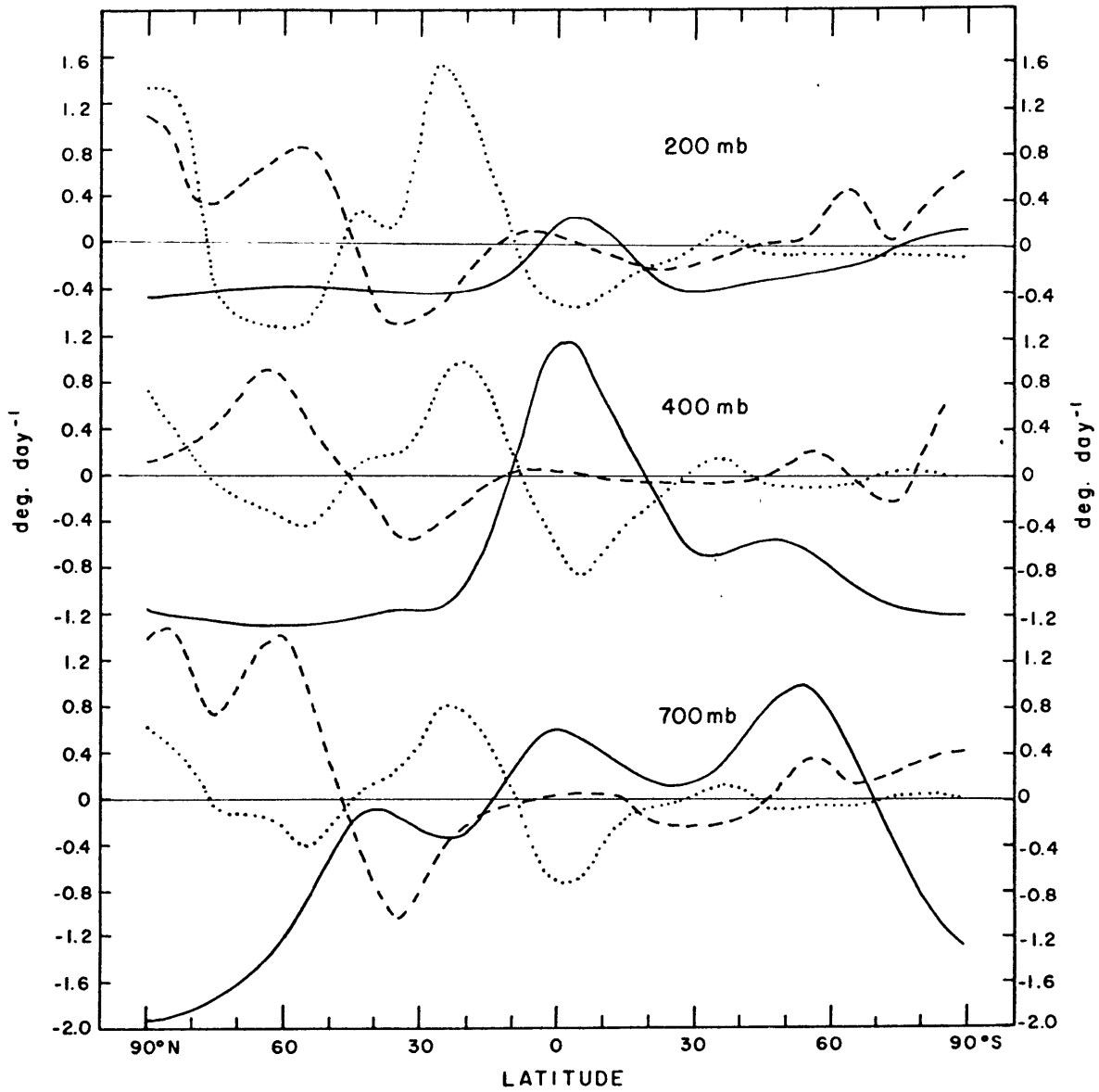


Fig. 5.4: Heat balance components for December-February: (a) 700 mb, (b) 400 mb, (c) 200 mb; solid line is diabatic heating, dashed line is heat flux convergence, dotted line is subsidence heating.

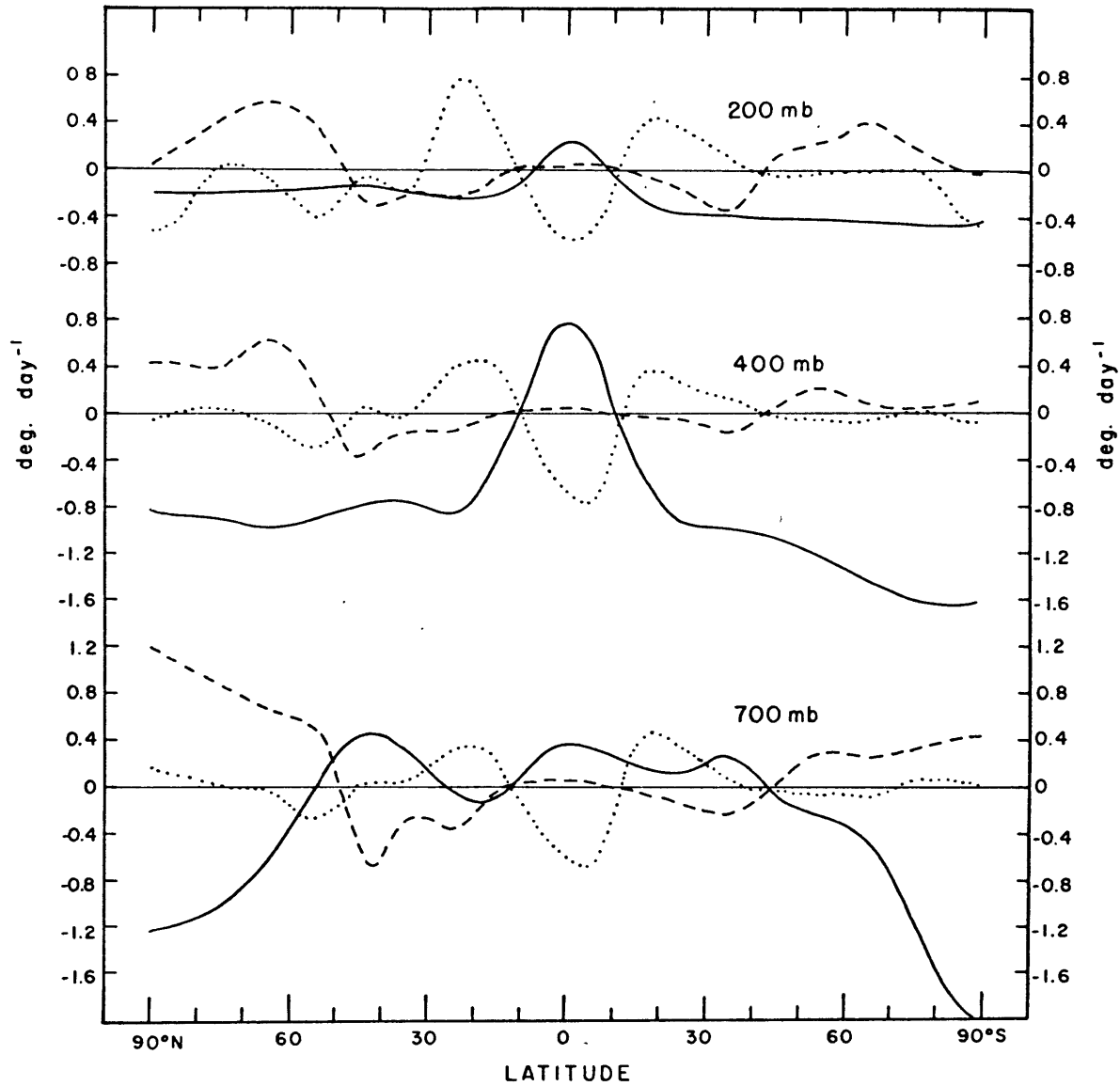


Fig. 5.5: Heat balance components for March-May: (a) 700 mb, (b) 400 mb, (c) 200 mb; solid line is diabatic heating, dashed line is heat flux convergence, dotted line is subsidence heating.

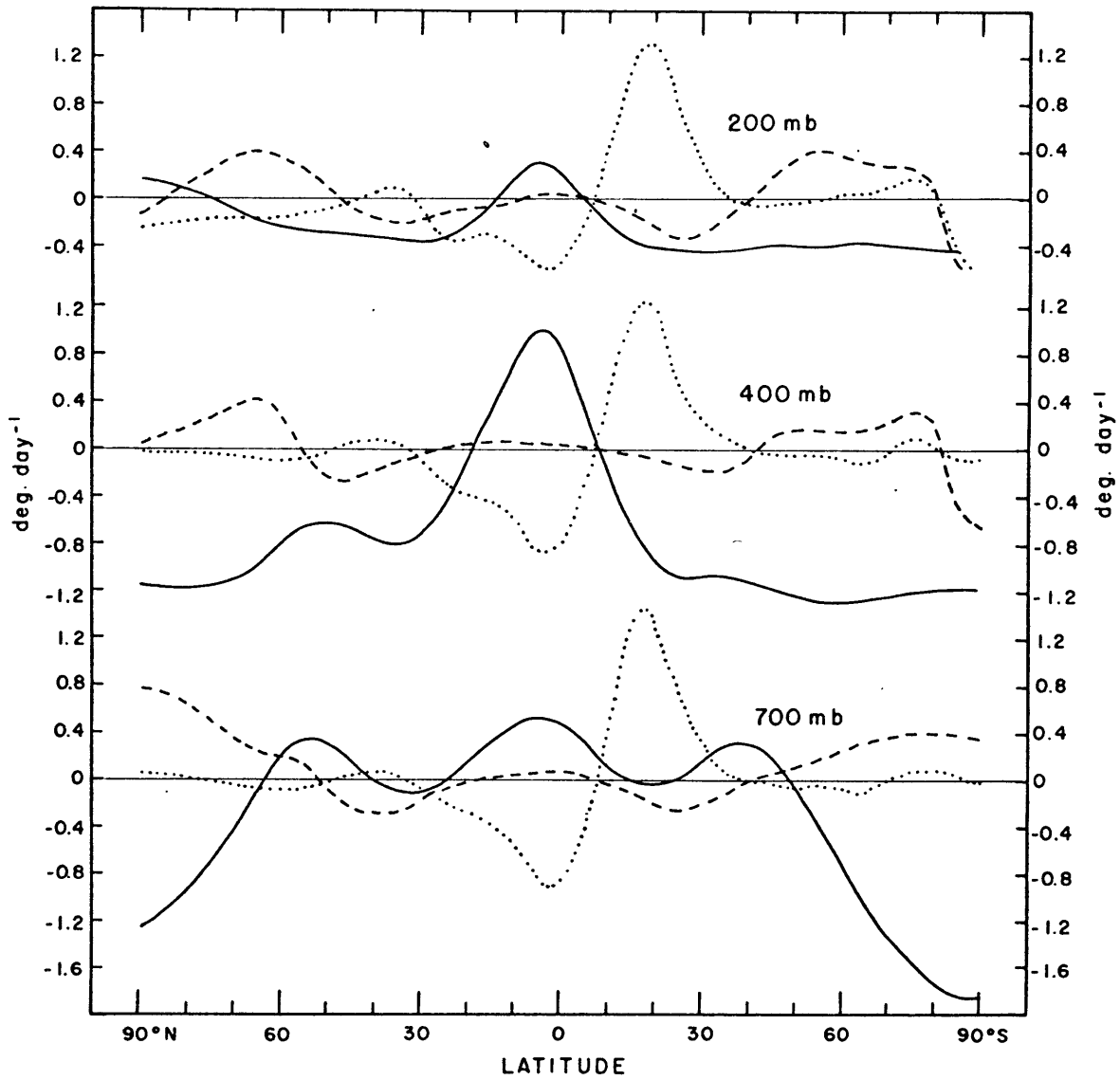


Fig. 5.6: Heat balance components for June-August: (a) 700 mb, (b) 400 mb, (c) 200 mb; solid line is diabatic heating, dashed line is heat flux convergence, dotted line is subsidence heating.

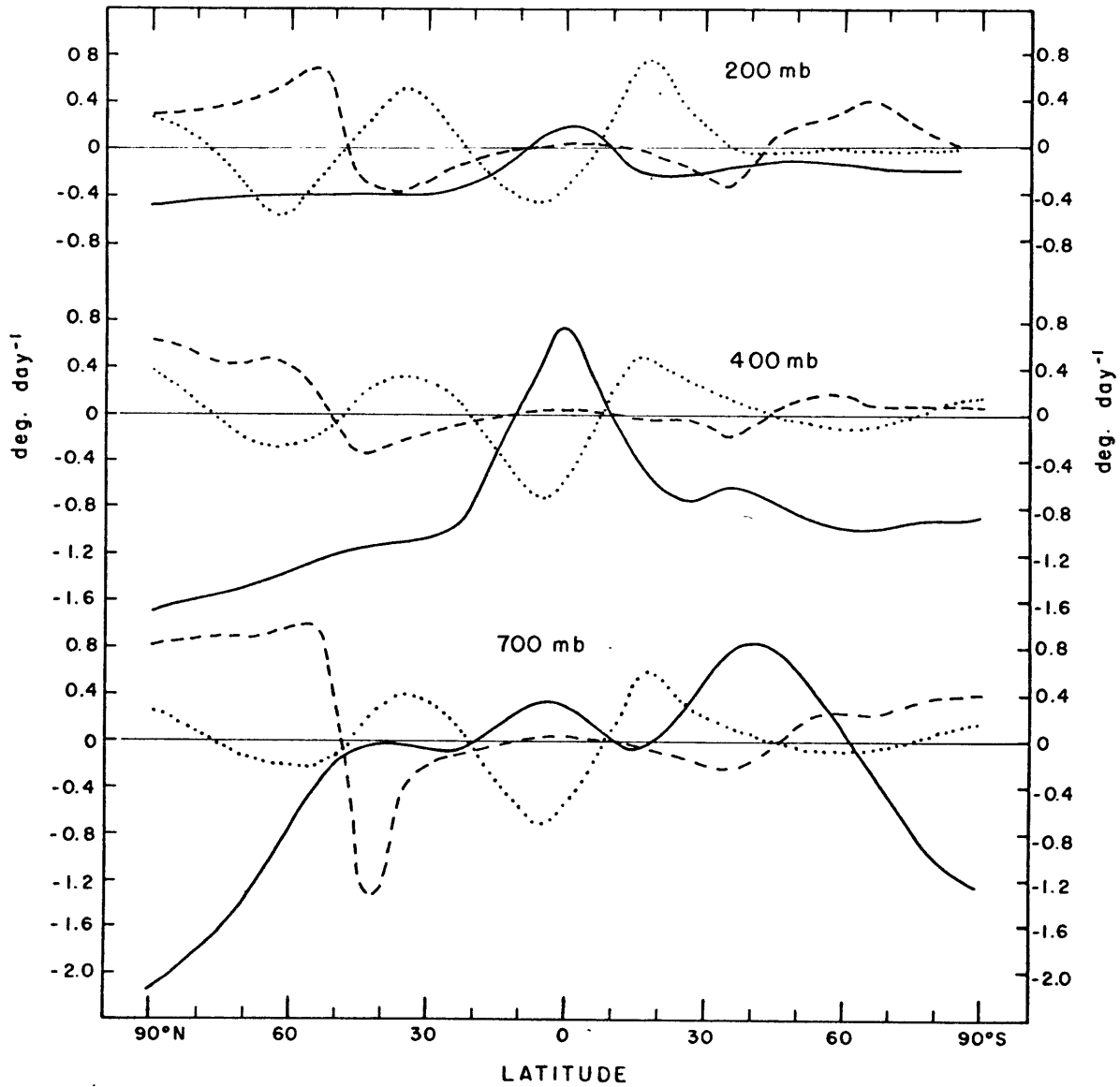


Fig. 5.7: Heat balance components for September–November: (a) 700 mb, (b) 400 mb, (c) 200 mb; solid line is diabatic heating, dashed line is heat flux convergence, dotted line is subsidence heating.

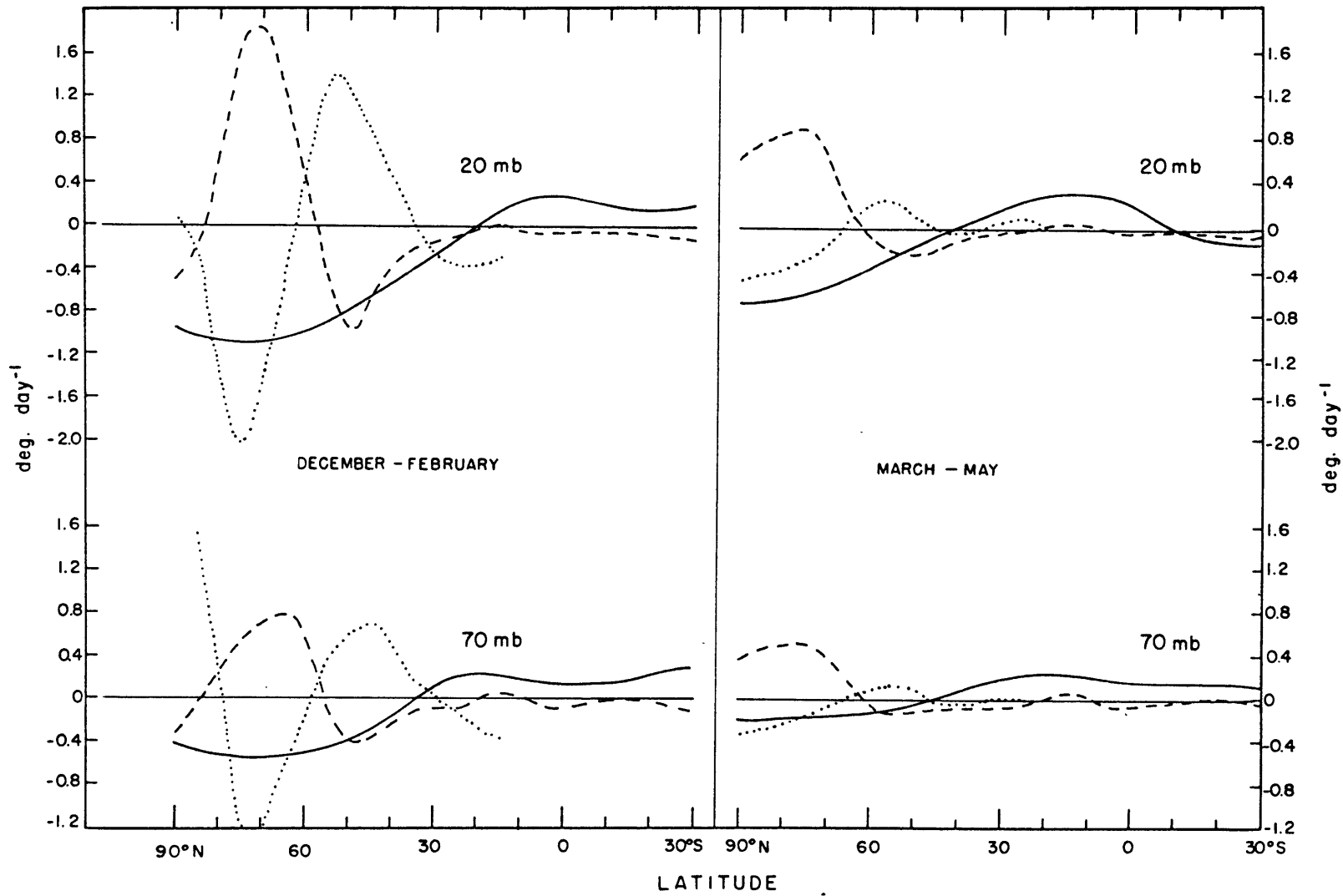


Fig. 5.8: Heat balance components for: (a) Dec-Feb 70 mb, (b) Dec-Feb 20 mb, (c) Mar-May 70 mb, (d) Mar-May 20 mb.

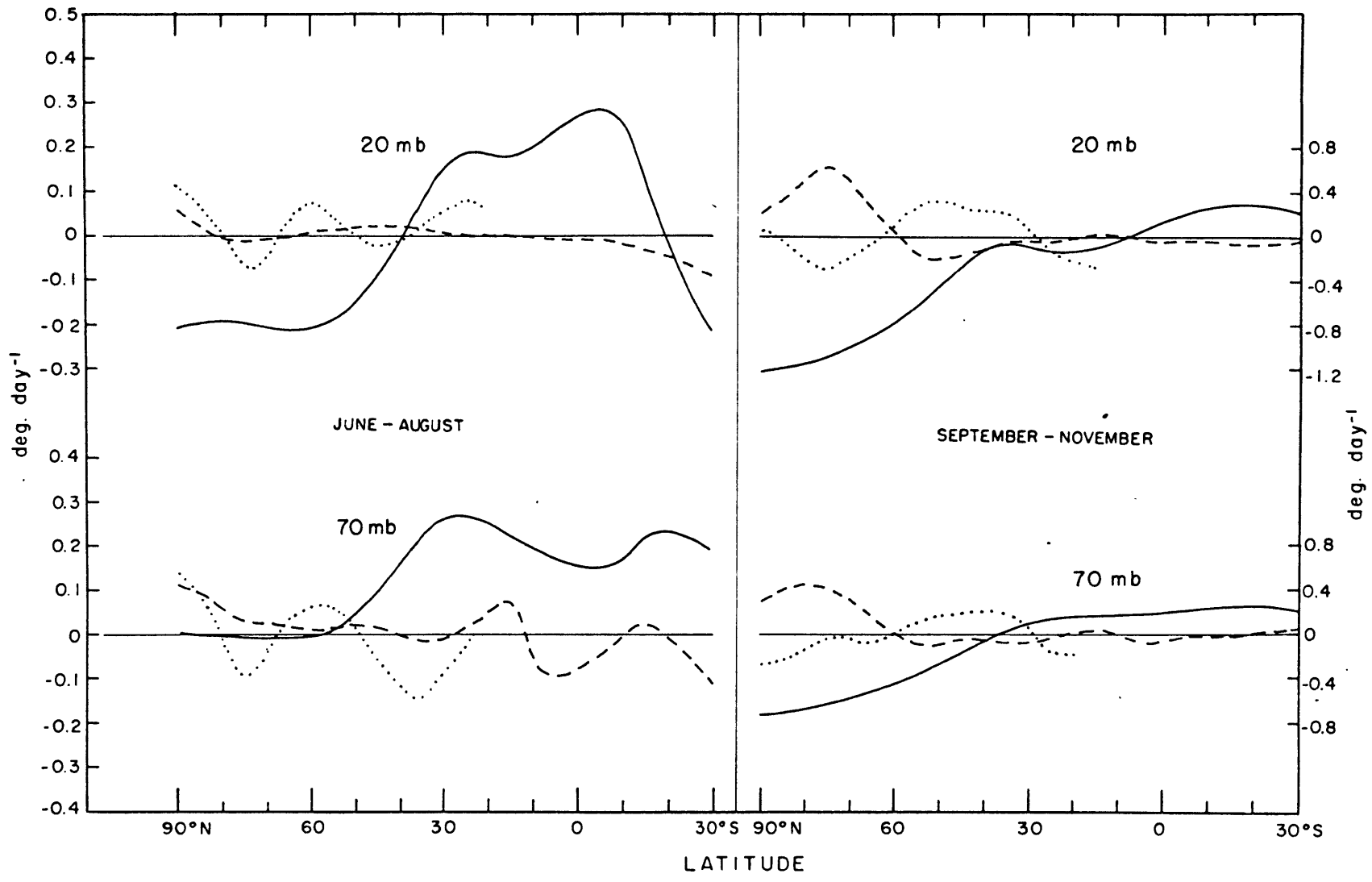


Fig. 5.9: Heat balance components for: (a) Jun-Aug 70 mb, (b) Jun-Aug 20 mb, (c) Sep-Nov 70 mb, (d) Sep-Nov 20 mb.

CHAPTER 6

ATMOSPHERIC ENERGY BUDGET

The sun is the ultimate source of energy in the earth-atmosphere system; its rays create internal energy as they heat the atmosphere and underlying surfaces. Air motions due to differential heating and the earth's rotation are the source of kinetic energy; frictional dissipation is continually removing atmospheric kinetic energy. A fundamental question in studies of the atmospheric energy balance is, "How does the energy from the sun get converted into kinetic energy to replenish frictional losses?" In this chapter seasonal changes in the atmospheric energy budget are discussed and attention is given to this question.

6.1 Available Potential Energy

In a column of air from the surface to the top of the atmosphere much of the incoming solar radiation reaches the surface and heats the land and oceans. Vertical currents are set up and heat exchange takes place between the earth and atmosphere. There is also a heat exchange due to phase changes in water such as evaporation and condensation. In addition the presence of clouds affects the net radiative heating. Each of these factors contributes to diabatic heating (see Chapters 3 and 5) which is responsible for generating internal energy. For a dry hydrostatic atmosphere the internal energy in a vertical column is proportional to the potential energy and an increase (decrease) in one

form of energy is accompanied by an increase (decrease) in the other form of energy. Thus, it appears that internal energy and potential energy should be considered as a single form of energy. This concept was originally introduced by Margules (1903) who investigated the energetics of local storms. He called the sum of the two energy forms total potential energy (TPE). Margules also introduced the concept of available potential energy but called it available kinetic energy. Lorenz (1955a, b; 1967), subsequently expanded these concepts to include the general circulation of the atmosphere and formulated the equations for the availability of energy on a global basis. He defines the available potential energy as the difference between the TPE of the atmosphere and the TPE of the reference state. The reference state is achieved when the isentropic and isobaric surfaces are parallel to the ground. Lorenz suggests that frictional heating probably raises the TPE of the existing state as much as it raises the TPE of the reference state. Therefore, only nonfrictional heating is an important source of available potential energy. The reversible adiabatic processes which convert TPE into kinetic energy do not alter the TPE of the reference state, consequently they can account for a conversion of available potential energy to kinetic energy. The sink of kinetic energy is frictional dissipation. Over the long run as much available potential energy must be generated by nonfrictional heating as is converted into kinetic energy or kinetic energy dissipated by friction. Thus, the atmospheric energy cycle consists of a generation of available potential energy by nonfrictional heating, a conversion

of available potential energy to kinetic energy by adiabatic processes and a dissipation of kinetic energy by friction. This concept has been adopted in the present investigation.

6.2 General Equations for Energy Balance

Following Lorenz (1967), the available potential energy for the atmosphere is given by

$$A = (1+\kappa)^{-1} c_p g p_0^{-\kappa} \int_S \int_0^\infty (p^{1+\kappa} - p_r^{1+\kappa}) d\theta dS \quad (6.1)$$

The time rate of change of available potential energy is

$$\frac{\partial A}{\partial t} = \int QN dm + \int \omega \alpha dm \quad (6.2)$$

where the integral is over the mass of the atmosphere.

For a dry hydrostatic atmosphere, neglecting topography these are the exact equations for available potential energy. In Eq. (6.2) the first integral on the RHS represents the generation of available potential energy while the second integral represents the conversion of available potential energy to kinetic energy. The quantity N , which equals $1 - (P_r/p)^\kappa$ where P_r is the reference pressure, has been called the efficiency factor by Lorenz (1955b, 1967) and Dutton and Johnson (1967) and specifies where on an isentropic surface heating (cooling) creates (destroys) available potential energy most efficiently.

Lorenz (1955b) gives a detailed discussion of N and computes the generation of available potential energy for a simple model using only net radiative heating rates. Our results and those of Dutton and Johnson (loc. cit.) suggest that generation by latent heat release is equally as important. Lorenz (1967) gives a hypothetical cross section of N which is similar to the cross sections presented herein for December-February and June-August (see Fig. 6.1).

The present values of the efficiency factor were derived using seasonally-averaged values of $[\bar{T}]$ to compute $[\bar{\theta}]$ as a function of pressure and subsequently to compute the mean reference pressure $[\bar{P}_r]$ as a function of potential temperature. In the exact expression the reference pressure is the value of pressure on an isentropic surface and is therefore a function of longitude as well as latitude, pressure and time.

Dutton and Johnson (loc. cit.) present cross sections of N along longitude 75W for January, April, July and October, 1958 but their results are in a θ -coordinate system and the efficiency factor has been multiplied by $\partial z / \partial \theta$. Since the gradient is positive everywhere in the atmosphere the signs of their results for January and July can be compared with those in Fig. 6.1. There is good agreement between the patterns during both periods; note particularly that in December-February values near the polar tropopause are the same in both hemispheres whereas in June-August values are 2-3 times larger in the Southern Hemisphere.

The generation of available potential energy depends on the tem-

perature distribution as well as diabatic heating. For example, if the isothermal surfaces were everywhere parallel to the isobaric surfaces there would be no energy generation, nor would generation occur if the various diabatic heat sources described in Chapter 3 cancelled each other. The generation of available potential energy depends on the correlation between temperature and diabatic heating and, in particular, the intensity of the energy cycle depends on the temperature distribution. The seasonal distributions of temperature and the factors which govern them have already been discussed in detail in Chapters 4 and 5. Lorenz (1955a) developed the following approximate expressions for available potential energy

$$A \approx \frac{c_p}{2} \int \Gamma_d (\Gamma_d - \tilde{\Gamma})^{-1} \tilde{T}^{-1} T''^2 dm \quad (6.3)$$

$$\frac{\partial A}{\partial t} \approx \int \Gamma_d (\Gamma_d - \tilde{\Gamma})^{-1} \tilde{T}^{-1} Q'' T'' dm + \int \omega \alpha dm \quad (6.4)$$

which are generally more useful in diagnostic computations than Eqs. (6.1 and 6.2) because most data are available at constant pressure rather than at constant potential temperature. Note that the first integral on the RHS of Eq. (6.4), which represents the generation of available potential energy, explicitly depends on a spatial correlation between diabatic heating and temperature.

The kinetic energy of the atmosphere can be defined as

$$K = \int \frac{\mathbf{V}_p \cdot \mathbf{V}_p}{2} dm \quad (6.5)$$

and the time rate of change of kinetic energy as

$$\frac{\partial K}{\partial t} = - \int \omega \alpha \, dm + \int V_p \cdot \mathbb{F}_p \, dm \quad (6.6)$$

In Eq. (6.6) the first integral on the RHS represents the conversion of available potential energy into kinetic energy and the second integral represents the loss of kinetic energy due to frictional dissipation. A direct assessment of the dissipation of kinetic energy is extremely difficult because of the limited knowledge about friction. Values are usually based on the term $\mathbb{W}_p \cdot \nabla_p \phi$ in Eq. (6.11) which is a measure of the work done on the air as it flows down the pressure gradient. This term is commonly referred to as cross-isobar flow. Numerous investigations have helped to provide a better understanding of the distribution and time variability of kinetic energy dissipation; particularly notable are the recent theories concerning the importance of frictional dissipation above the atmospheric boundary layer, mainly near the upper level jet, and the apparent diurnal variation in the free atmosphere.

A colleague, Major D. Ferruzza, presents a detailed discussion of kinetic energy dissipation (Newell et al., 1970b) and his table of frictional losses has been reproduced in Table 6.1. Note that an average estimate for the rate of frictional dissipation is about 5000 ergs $\text{cm}^{-2} \text{sec}^{-1}$. Kung (1969) suggests that the intensity of the general circulation is greater than previously assumed (Oort, 1964) and cites his own results as well as those of Dutton and Johnson (1967),

Table 6.1: Frictional Dissipation Estimates by Various Investigators
(ergs cm⁻² sec⁻¹)

	<u>Total</u>		<u>"Boundary" Layer</u>			<u>400-150 mb</u>	
	<u>Value</u>	<u>Thickness</u>	<u>Value</u>	<u>Thickness</u>	<u>% of total</u>	<u>Value</u>	<u>% of total</u>
Brunt (1926)	5000	0-10 km	3000	0-1 km	60%	---	---
Smith (1955)	8500	1000-100 mb	----	-----	---	---	---
Jensen (1961)	4284	1000-50 mb	3358	1000-925 mb	79%	521	12%
Holopainen (1963)	10400	Sfc-200 mb	4200	Sfc-900 mb	40%	3600+360	(35+10) %
Oort (1964)†	2300	1000-100 mb	----	-----	---	---	---
Kung (1966a)	6380	Sfc-75 mb	1870	*	29%	---	---
Kung (1966b)	7180	Sfc-50 mb	1732	Sfc-900 mb	24%	1561	22%
Kung (1967)†	4120	Sfc-50 mb	1573	Sfc-900 mb	38%	551	13%
Kung (1969)†	5584	Sfc-50 mb	2027	Sfc-868 mb	36%	940	17%
Ellsaesser (1969)	4634	1000-0 mb	1529	1000-900 mb	33%	1680	36%
Trout and Panofsky (1969)	----	-----	----	-----	---	1320 ^x	---

* computed from "surface" winds

† mean annual values

x 25000-40000 feet

Ellsaesser (1969) and Trout and Panofsky (1969) as evidence. He states that dissipation rates are too low because of underestimates in the free atmosphere.

Seasonal and diurnal variations of energy dissipation have been computed and discussed by Kung (1967, 1969). His results show that dissipation rates are about 50% greater in winter than in summer while spring and fall values are near the annual mean. When he combined six months of data together for 0000 GMT and 1200 GMT there was no apparent diurnal variation in the winter period (November-April) except possibly above 400 mb where negative dissipation occurred at some levels at 1200 GMT. In the summer period, however, there was a definite tendency for larger dissipation rates at 0000 GMT; between 300 mb and 70 mb negative dissipation occurred at 1200 GMT.

It should be noted that frictional dissipation is basically a small scale phenomenon and that methods of investigating it have been based mainly on large scale considerations. Moreover, in observational studies the smaller scale features often go undetected. In view of this and the wide range of results by various investigators it appears that accurate estimates of the intensity of the large scale general circulation based on frictional dissipation rates need further refinements.

6.3 Treatment of Restricted Regions

Although available potential energy is defined only for the entire atmosphere, it is possible to treat the contribution of a limited

region of mass m_j to the available potential energy of the entire atmosphere. Using the exact equations P. J. Smith (1969) has shown that

$$A_j = \frac{c_p}{g} \int_S \int_{p_1}^{p_2} \frac{p^x - p_r^x}{p^x} T dp dS \quad (6.7)$$

If p_1 and p_2 are taken to be constant, the time rate of change of A_j is found to be

$$\begin{aligned} \frac{\partial A_j}{\partial t} = & \int_{m_j} QN dm + \int_{m_j} \omega \alpha dm \\ & - c_p \int_{m_j} \nabla_p \cdot (N V_p T) dm - c_p \int_{m_j} \frac{\partial}{\partial p} (N \omega T) dm \end{aligned} \quad (6.8)$$

Likewise if the kinetic energy of the limited region is defined to be

$$K_j = \int_{m_j} \frac{V_p \cdot V_p}{2} dm \quad (6.9)$$

then the time rate of change of K_j is

$$\begin{aligned} \frac{\partial K_j}{\partial t} = & \int_{m_j} V_p \cdot F_p dm - \int_{m_j} V_p \cdot \nabla_p \phi dm \\ & - \int_{m_j} \nabla_p \cdot \left(\frac{V_p \cdot V_p}{2} V_p \right) dm - \int_{m_j} \frac{\partial}{\partial p} \left(\frac{V_p \cdot V_p}{2} \omega \right) dm \end{aligned} \quad (6.10)$$

For the entire atmosphere the conversion from available potential energy into kinetic energy involves the integral of $\omega\alpha$ over the mass of the atmosphere; however, for a limited region the following relationship holds:

$$\int_{m_j} \omega\alpha dm - \int_{m_j} \nabla_p \cdot \nabla_p \phi dm = \int_{m_j} \nabla_p \cdot \nabla_p \phi dm - \int_{m_j} \frac{\partial}{\partial p} \omega \phi dm \quad (6.11)$$

If the boundary terms are identically zero the conversion of available potential energy to kinetic energy in the limited region will be given by the integral of $\omega\alpha$ over the mass of the region. When the boundary terms are not zero an increase in the kinetic energy in the region may result from boundary flux of energy rather than a direct conversion of available potential energy. Similar treatments of limited regions using the approximate expressions in Eqs. (6.3) and (6.4) have been derived by various researchers including Oort (1964) and Muench (1965).

6.4 Zonal and Eddy Forms of Energy

Because of the observed zonal symmetry of the motion and temperature fields in the atmosphere, a plausible resolution of the approximate expression involving available potential energy (Eq. 6.3) is to replace the mass and motion fields by the amounts associated with the zonal average and the amounts associated with the eddies. Also, to reduce the computational requirements for diagnostic studies over

long time periods, the fields of mass and motion are averaged over time before space. Under such a resolution the zonal available potential energy (AZ) and the eddy available potential energy (AE) become

$$AZ = \frac{c_p}{2} \int \gamma [\bar{T}]''^2 dm \quad (6.12)$$

$$AE = \frac{c_p}{2} \int \gamma [\bar{T}^{*2}] dm \quad (6.13)$$

where

$$\gamma = - \left(\frac{[\bar{\theta}]}{[\bar{T}]} \right)^2 \frac{R_d}{c_p(p_2 - p_1)} \int_{p_1}^{p_2} \frac{[\bar{T}]}{[\bar{\theta}]} \frac{1}{p} \left(\frac{\partial [\tilde{\theta}]}{\partial p} \right)^{-1} dp \quad (6.14)$$

Here the integral is over the entire mass of the atmosphere. Likewise the zonal kinetic energy and the eddy kinetic energy are

$$KZ = \frac{1}{2} \int ([\bar{u}]^2 + [\bar{v}]^2) dm \quad (6.15)$$

$$KE = \frac{1}{2} \int [\bar{u}^{*2} + \bar{v}^{*2}] dm \quad (6.16)$$

The energy budget equations for each type of energy have the form:

$$\frac{\partial}{\partial t} AZ = GZ - CZ - CA \quad (6.17)$$

$$\frac{\partial}{\partial t} AE = GE - CE + CA \quad (6.18)$$

$$\frac{\partial}{\partial t} KZ = CZ + CK - DZ \quad (6.19)$$

$$\frac{\partial}{\partial t} KE = CE - CK - DE \quad (6.20)$$

where

$$GZ = c_p \int \gamma [\bar{Q}]'' [\bar{T}]'' dm \quad (6.21)$$

$$GE = c_p \int \gamma [\bar{Q}^* \bar{T}^*] dm \quad (6.22)$$

$$CE = - \int [\bar{\omega}' \bar{\alpha}' + \bar{\omega}^* \bar{\alpha}^*] dm \quad (6.23)$$

$$CZ = - \int [\bar{\omega}]'' [\bar{\alpha}]'' dm = \int f [\bar{u}_g] [\bar{v}] dm \quad (6.24)$$

$$\begin{aligned}
CK = & \int [\bar{u}'v' + \bar{u}^*\bar{v}^*] \frac{\cos \phi}{a} \frac{\partial}{\partial \phi} \left(\frac{[\bar{u}]}{\cos \phi} \right) dm \\
& + \int [\bar{u}'\omega' + \bar{u}^*\bar{\omega}^*] \frac{\partial [\bar{u}]}{\partial p} dm \quad (6.25)
\end{aligned}$$

$$\begin{aligned}
CA = & -c_p \int \gamma [\bar{v}'T' + \bar{v}^*\bar{T}^*] \frac{1}{a} \frac{\partial [\bar{T}]}{\partial \phi} dm \\
& - c_p \int \gamma \left(\frac{[\bar{T}]}{[\bar{\theta}]} \right) [\bar{\omega}'T' + \bar{\omega}^*\bar{T}^*] \frac{\partial [\bar{\theta}]}{\partial p} dm \quad (6.26)
\end{aligned}$$

$$DZ = - \int ([\bar{u}][\bar{F}_\lambda] + [\bar{v}][\bar{F}_\phi]) dm \quad (6.27)$$

$$DE = - \int [\bar{u}'F'_\lambda + \bar{v}'F'_\phi + \bar{u}^*\bar{F}_\lambda^* + \bar{v}^*\bar{F}_\phi^*] dm \quad (6.28)$$

The picture of the energetics of the atmosphere becomes more complicated as now there are conversions between the eddy and zonal forms of both available potential energy and kinetic energy. It is very difficult to say a priori which way many of the conversion processes proceed and it is necessary to turn to atmospheric observations in order to assess the energetics for the zonal and eddy forms of energy. Other resolutions of the approximate equations for available potential

energy have been developed and a summary of three possible resolutions is given by Oort (1964).

6.5 Global Energy Budget

The data described in Chapters 2 and 3 were used in Eqs. (6.12-6.16, 6.21-6.26) to compute approximate values of the contents, generations and conversions in the atmospheric energy budget. As noted previously all of the quantities were not available on a global basis. Unfortunately, covariance terms which included "vertical velocity" (ω) were not known; hence, the conversion CE, for example, was not calculated. In addition the contributions of time fluctuations to GE, AE and KE were not known and no attempt was made to compute values of the dissipation terms, DZ and DE. The results are shown in the form of energy box diagrams (see Figs. 6.12-6.18) as a function of three-month seasons for several different regions whose boundaries are defined by latitude and pressure.

Global values are given in Fig. 6.12. AZ is 7-8 times larger than KZ in all seasons. In addition the zonal forms of energy appear to be much larger than the corresponding eddy forms but, as noted above, time variations were not included in computing eddy forms of energy. Thus, AE and KE have undoubtedly been underestimated. For example, values of AE were based on longitudinal deviations from seasonal averages (\bar{T}^2) instead of daily averages ($\overline{T^2}$). KE estimates were only available from 90N-30S and also will be too small. A cross section of the integrand of AZ is presented

for December-February in Fig. 6.2. Similar cross sections were analyzed for the other periods. Maximum values of almost 7×10^7 ergs g^{-1} were located over the summer pole in the lower stratosphere and near the winter pole in the troposphere. In March-May and September-November maximum values of $2-4 \times 10^7$ ergs g^{-1} occurred at high latitudes in both hemispheres. In low and middle latitudes values were comparatively small except near the equatorial tropopause (100 mb level) where they were $1-2 \times 10^7$ ergs g^{-1} during all seasons. Cross sections of the integrand of AE showed maximum values in December-February near the surface between 55N and 65N which approached 4×10^7 ergs g^{-1} . In the Southern Hemisphere values were much smaller than those in the Northern Hemisphere reflecting a stronger zonal symmetry in the temperature field of the former region. Cross sections of the integrand of KE were only available from the North Pole to 30S and the largest values (6×10^5 ergs g^{-1}) occurred in the vicinity of the northern hemisphere winter jet stream. Cross sections of the integrand of KZ reflected the zonal wind component, which is given in Table 4.2 for all seasons. Maximum values of nearly 6×10^6 ergs g^{-1} were associated with the northern hemisphere winter jet stream. This region also showed the greatest seasonal variations with values decreasing to almost 1×10^6 ergs g^{-1} by June-August. In the Southern Hemisphere two specific regions showed large values of KZ, one associated with the middle latitude upper tropospheric jet and the other associated with the higher latitude stratospheric jet which was evident in all periods except December-February. The latter, of

course, only showed large values at 100 mb, as this was the uppermost level considered on a global scale. In the vicinity of the tropospheric jet, KZ varied seasonally only from $2.8-4.3 \times 10^6$ ergs g^{-1} which was considerably smaller than the corresponding variations in the Northern Hemisphere; however, at 100 mb near 55S seasonal values ranged from $1.1-4.1 \times 10^6$ ergs g^{-1} with the low value occurring in December-February when the stratospheric jet was not evident.

The generation of zonal available potential energy, GZ, was computed by two methods: one based on an approximation to the exact expression for the integrand of the first term on the RHS of Eq. (6.2) and the other using Eq. (6.21). In the first method the adopted integral for GZ was

$$GZ = \int [\bar{Q}] [\bar{N}] dm \quad (6.29)$$

Cross sections of the integrand of GZ computed by each method are given in Figs. 6.3 and 6.4 for December-February and June-August. In general the features of the patterns by each method are similar except, (1) there is usually more destruction above 150 mb when the efficiency factor is not included and (2) the large generation rates over polar regions of both hemispheres are at a higher altitude and central values in the rising branch of the Hadley circulation are smaller when the efficiency factor is included. The patterns by each method of computation for the other two seasons are represented approximately by the average of those in December-February and June-August.

Values of GZ by both methods are given in the upper right hand corner of each energy diagram with the top value being that obtained from Eq. (6.29). Note that in all seasons the use of the efficiency factor has resulted in larger values. Dutton and Johnson (1967) give a critical evaluation of diagnostic studies of the atmospheric energy budget and note the dangers of using the approximate expression in Eq. (6.21) instead of the exact expression based on the efficiency factor. Their average annual value of GZ using N is approximately 285×10^{20} ergs sec⁻¹ for the global atmosphere which is about two times larger than the seasonal values presented in Fig. 6.12. It is difficult to determine what factors are responsible for this difference in generation rates. Perhaps the use of different coordinate systems, data sources and methods of computation are the reason; however, it is believed that Dutton and Johnson's partitioning of Lettau's (1954) diabatic heating components into two free atmosphere layers and a lower boundary layer is the major problem. For example, their distribution gave 44%, 41% and 15% of the total GZ produced by net radiation, latent heat release and boundary layer heating. In the present investigation the relative roles of these heat sources are considerably different. Generation rates based on Eq. (6.29) are given in Table 6.2. Note that the annual mean (average of the seasonal values) of GZ shows that radiative processes tend to destroy AZ whereas latent heat liberation is the primary source of AZ. These results agree with the opinion stressed by Peixoto (1965) and suggest a change of perspective from the classical viewpoint that a radiative

imbalance between low and high latitudes is the direct primary driving force for the general circulation. The results also show that boundary layer heating makes a significant contribution to GZ. The same general trend was found when the values of $[\bar{Q}]$ in the integrand of Eq. (6.21) were divided into components.

Table 6.2: Distribution of Global GZ Produced by Net Radiation, Latent Heat Release and Boundary Layer Heating (10^{20} ergs sec^{-1})

	<u>Components</u>			<u>TOTAL</u>	<u>Percentage of Total</u>		
	<u>RAD</u>	<u>LH</u>	<u>BLH</u>		<u>RAD</u>	<u>LH</u>	<u>BLH</u>
Dec-Feb	22.5	86.8	35.9	145.2	15	60	25
Mar-May	14.6	88.4	38.9	141.9	10	63	27
Jun-Aug	-47.6	121.0	55.3	128.7	-37	94	43
Sep-Nov	-19.0	99.5	41.4	121.9	-16	82	34
Ann Mean	- 7.4	98.9	42.9	134.4	- 7	75	32

Because the complete exact expression for GZ could not be calculated it is difficult to infer which of the approximations, Eq. (6.21) or Eq. (6.29), gives the more precise values. Both have been presented in the energy box diagrams but the discussion hereafter will be based on the generation rates computed using Eq. (6.29).

If we assume that seasonal changes, small scale diffusion and the upward flux of AZ through the 100 mb level are small compared to the conversion from AZ to AE, then there is a large imbalance in the AZ box in all seasons. That is, much more AZ is generated than is required for conversions to AE and KZ. The apparent surplus, based on GZ calculations using N, ranges from 60-100 x 10^{20} ergs sec^{-1} with an

average annual value of about 80×10^{20} ergs sec^{-1} . The results of Wiin-Nielsen (1967) for the Northern Hemisphere during the period February 1963-January 1964 indicate that AZ decreased about 8×10^{20} ergs sec^{-1} during March-May and increased about 6×10^{20} ergs sec^{-1} in September-November, whereas the values in winter and summer showed little change; consequently, seasonal changes alone can not account for the surplus produced in AZ. The energy flux of AZ upwards through 100 mb, by the boundary term in Eq. (6.9), has been estimated by my colleague, Captain T.G. Dopplick, to be 0.05×10^{20} ergs sec^{-1} for the region 90N-20N in January 1964 (Newell et al., 1970b). Clearly, this effect is not too important unless the value magnifies considerably in other months and regions. It also seems unlikely that small scale diffusion could consume an appreciable amount but our knowledge of this quantity is very limited. Thus it would appear that we are left with an unexplained surplus of AZ. In Chapter 5 it was suggested that vertical eddy heat transport might be an important source in maintaining the heat balance of the upper troposphere at middle and high latitudes. Rough estimates of the vertical heat flux term in Eq. (6.26) were computed for December-February and June-August using heat fluxes from Manabe and Hunt (1968) in conjunction with the present temperature data; the contributions were found to be negligible. Hence, for the present, the apparent surplus in AZ remains an unresolved problem. Further comments are given later.

The energy box diagrams show that the global conversion CA is always from AZ to AE and that it is largest in December-February

being about 2.5 times greater than in June-August. Bear in mind again that the use of six-month averages for meridional heat fluxes between 30S and 90S tends to decrease the global value of CA in June-August. In March-May and September-November, the values of CA are approximately the same and are between those of the other two seasons. Cross sections of the integrand of CA for December-February and June-August are given in Fig. 6.5. There is reasonable symmetry in the patterns for the respective winter and summer seasons in each hemisphere.

The conversion, CZ, was based on the expression $f[\bar{u}][\bar{v}]$ in Eq. (6.24) rather than $[\bar{\omega}][\bar{\alpha}]$ since the latter requires $[\bar{\omega}] = 0$ on each pressure surface which is probably incorrect in regions of limited volume. Our discussion later is concerned with restricted regions, thus for consistency the former expression was selected. Note that the expression involves the product of the mean meridional flow and the gradient of geopotential, such that a positive value increases CZ in Eq. (6.24). Therefore, if the mean flow is down the gradient of geopotential there is a conversion from AZ to KZ. In the actual computations of CZ the observed zonal wind component was substituted for the geostrophic wind and the singularity in $[\bar{u}_g]$ at the equator was avoided. The method by which the values of $[\bar{v}]$ were obtained is described in Chapter 2.

The seasonal values of CZ in the energy box diagrams are small compared to CA and CK and are strongly influenced by the Hadley circulation. In December-February and June-August when the tropical

circulation mainly consists of a strong and extensive winter hemisphere Hadley cell (see Fig. 4.6), the conversion is from AZ to KZ. In March-May and September-November the Hadley cells (one in each hemisphere) are less extensive and considerably weaker and CZ is from KZ to AZ (although it is near zero in the latter period), illustrating the increased role of the middle latitude indirect (Ferrel) cells. Cross sections of the integrand of CZ are given in Fig. 6.6 for December-February and June-August. In both periods the largest conversions from AZ to KZ occur in the winter hemisphere on the middle latitude side of the poleward branch of the main Hadley cell where \bar{v} is positive and the zonal wind is westerly. In June-August there is also a conversion from AZ to KZ in the summer hemisphere in the equatorward branch of the Hadley cells. The tropical data of geopotential which were used in the atmospheric energy transport calculations given by Kidson et al. (1969) show the largest values in the upper troposphere near 5S in December-February and near 25N in June-August. Thus, the conversions from AZ to KZ in the upper branches of the Hadley circulations are brought about by air motions down the gradient of geopotential. It is encouraging that two independent analyses, using $[\bar{u}]$ and $[\bar{\phi}]$, give the same result, since one is based on direct wind observations and the other is dependent on temperature. In both periods there are conversions from KZ to AZ in the middle latitude upper tropospheric regions of both hemispheres which are related to the Ferrel cells.

The conversion CK was computed from Eq. (6.25) but the vertical

momentum fluxes were not included; in addition, from 30S-90S only the transient eddy momentum fluxes were available for the first term. The energy box diagrams show that the conversion is from KE to KZ in all seasons and that the seasonal changes in CK are small compared to those for the other conversions. Furthermore it appears that the values of CK due to transient eddy momentum fluxes (given below and to the left of the total CK value) are responsible for most of the conversion. Cross sections of the integrand of CK are given in Fig. 6.7 for December-February and June-August. The most noticeable feature in the CK patterns is the seasonal symmetry, that is, winter in one hemisphere is almost a mirror image of winter in the other hemisphere and likewise for summer. Another interesting feature is the conversion from KZ to KE in the upper tropical troposphere in both seasons with maximum values occurring near 5 degrees latitude in the winter hemisphere. This arises because there are westerlies at middle latitudes in both hemispheres and tropical easterlies with maximum values located near 5 degrees latitude in the summer hemisphere, in conjunction with momentum fluxes from the winter to the summer hemisphere which have maximum values near 5 degrees in the winter hemisphere. Consequently, in the upper tropical troposphere, between about 15 degrees in the winter hemisphere and 5 degrees in the summer hemisphere, the eddies act in the classical sense and tend to reduce the kinetic energy of the zonal flow by transferring momentum down the gradient. A smaller less extensive region of KZ→KE is evident during the other two seasons.

On a global basis, KZ always gains through the combined processes of CZ and CK. CK builds up KZ in all seasons and CZ builds up KZ in December-February and June-August. Only in March-May is there an appreciable loss of KZ through CZ and in this period the conversion from KE to KZ overcompensates. A net balance in KZ is maintained by a continuous dissipation at the earth's surface, in the lower boundary layer and in the free atmosphere. Table 6.3 summarizes the effects of CZ and CK on KZ.

Table 6.3: Global Conversions to KZ (10^{20} ergs sec⁻¹)

	<u>C(AZ→KZ)</u>	<u>C(KE→KZ)</u>	<u>Sum</u>
Dec-Feb	4.0	14.8	18.8
Mar-May	-4.7	15.8	11.1
Jun-Aug	5.9	11.5	17.4
Sep-Nov	-0.1	16.9	16.8

KZ can only be lost by dissipation and by a boundary flux through 100 mb. The latter has been estimated by Captain T. Dopplick as 0.6×10^{20} ergs sec⁻¹ for the region 90N-20N in January 1964 (Newell et al., 1970b). Thus, it appears that most of the zonal kinetic energy must be lost through frictional dissipation. Estimates of frictional dissipation of total kinetic energy derived by several investigators were already noted (see Table 6.1). Since none of the studies was on a global scale a direct comparison is not possible. Extending a typical estimate of $5000 \text{ ergs cm}^{-2} \text{ sec}^{-1}$ to the globe gives a total dissipation of 250×10^{20} ergs sec⁻¹, while the estimate here is

about 15×10^{20} ergs sec^{-1} for the dissipation of KZ. Hence if total dissipation rates have not been overestimated it appears that most of the frictional losses occur as KE dissipation.

An estimate of the KE dissipation was obtained using values of the conversion from AE to KE (CE) presented by Jensen (1961) for the Northern Hemisphere for the months January and April. Combining results for the two months gave a value of CE of about $4000 \text{ ergs cm}^{-2} \text{ sec}^{-1}$, which when extended to the globe is 200×10^{20} ergs sec^{-1} . Since the value of CK is about 15×10^{20} ergs sec^{-1} , an estimate of the dissipation of KE is approximately 185×10^{20} ergs sec^{-1} which is much larger than the present estimate for the dissipation of KZ. Further estimates of CE are required in order to show more explicitly the relative roles of KE and KZ dissipation.

6.6 Northern Hemisphere vs Southern Hemisphere

The energy box diagrams for the Northern and Southern Hemispheres are given in Figs. 6.13 and 6.14. Seasonal values of GZ and AZ infer a phase lag of less than 90 days and their ratio yields a time response of about 15-20 days for each season. The largest values of both GZ and AZ occur in the winter hemisphere while the smallest values occur in June-August in the Northern Hemisphere. The latter may be due to warmer underlying land surfaces which tend to reduce temperature differences. The results of KZ show the same tendencies as GZ and AZ, suggesting a rather rapid response by conversion processes.

As for the globe, the values of GZ in each hemisphere were

partitioned according to diabatic heating components. The results based on Eq. (6.29) appear in Table 6.4.

Table 6.4: Distribution of GZ by Components (10^{20} ergs sec⁻¹)

	<u>Northern Hemisphere</u>				<u>Southern Hemisphere</u>			
	<u>RAD</u>	<u>LH</u>	<u>BLH</u>	<u>TOTAL</u>	<u>RAD</u>	<u>LH</u>	<u>BLH</u>	<u>TOTAL</u>
Dec-Feb	48.5	30.1	22.8	101.4	-25.9	56.6	13.1	43.8
Mar-May	- 2.6	41.9	21.4	60.7	17.2	46.5	17.5	81.2
Jun-Aug	-89.2	90.7	29.7	31.2	41.6	30.8	25.6	98.0
Sep-Nov	-21.0	62.4	23.5	64.9	2.1	37.1	17.9	57.1

Note the following features: (1) in the winter (summer) hemisphere radiative processes produce (destroy) AZ, (2) latent heat release and boundary layer heating produce AZ in all seasons, (3) seasonal variations are most pronounced in the radiative heating component while boundary layer heating is relatively stable.

In the Northern Hemisphere, as noted in Chapter 4, Katayama's maps (1967) were used to compute values of net diabatic heating which were combined with the present values of temperature in Eq. (6.22) to yield values of GE. The results (see Fig. 6.13) show that GE is much larger in January and indicate that it is small compared to GZ but recall that GE may have been underestimated. A cross section of the integrand of GE is given in Fig. 6.8 for January. Note that maximum generation occurs in the lower troposphere at high latitudes where values exceed $5 \text{ ergs g}^{-1} \text{ sec}^{-1}$.

The conversion CA is always from AZ to AE in both hemispheres as for the global region. The largest value occurs in northern winter.

For comparison we have included the northern hemisphere values of CA computed when the total eddy heat fluxes provided by Drs. A. H. Oort and E. M. Rasmusson were combined with our temperature data. Their heat fluxes produce values of CA that are approximately 70% of those adopted which were based in part on the total heat fluxes provided by Prof. A. Wiin-Nielsen. Seasonal variations of CA in the Southern Hemisphere are much less than those in the Northern Hemisphere but seasonal values for the standing eddies of the meridional heat flux were not available from 30S-90S. Annual values of $[\overline{v'T}']$ and $[\overline{v^*T^*}]$ in this region given by Robinson (1968) show that standing eddies are comparatively small. Note that, except for March-May in the Southern Hemisphere, the seasonal trend of CA is the same as AZ, again suggesting an immediate response.

The conversion CZ is from AZ to KZ in the Southern Hemisphere during all seasons except summer, while in the Northern Hemisphere it alternates with season being from AZ to KZ in winter and summer. The outstanding feature is the importance of the winter hemisphere Hadley circulation in converting AZ to KZ. The conversion CK is always from KE to KZ and shows very little seasonal variation in either hemisphere. Momentum transports by transient eddies give the most important contribution to the integral of CK in the Northern Hemisphere and may do likewise in the Southern Hemisphere although standing eddies are not yet available from 30S-90S. Note that the minimum value of CK occurs during northern summer as for GZ, AZ, KZ, and CA.

Values of the net conversions from AZ to AE and KZ are given in Table 6.5.

Table 6.5: Conversions from AZ by CA, CZ (10^{20} ergs sec $^{-1}$)

	<u>Northern Hemisphere</u>	<u>Southern Hemisphere</u>
Dec-Feb	75.4	9.7
Mar-May	28.3	15.0
Jun-Aug	6.3	31.8
Sep-Nov	30.0	24.4

Values of the boundary flux of AZ across the equator were found to be small compared to CA, a typical magnitude being about 2×10^{20} ergs sec $^{-1}$. In Table 6.5 the seasonal trend of total conversions from AZ is similar in both hemispheres. Monthly changes in AZ for the Northern Hemisphere, as given by Wiin-Nielsen (1967), are in phase with the tabular values. The southern hemisphere winter value of 31.8×10^{20} ergs sec $^{-1}$ is undoubtedly an underestimate since CA would be larger if three-month rather than six-month averages of $[\overline{v'T}']$ had been available. A discussion of the net conversions to KZ by CZ and CK is delayed until the next section.

To summarize the hemispheric energetics the present results for the annual energy budget of the Northern Hemisphere are compared with those deduced by Oort (1964) and Dutton and Johnson (1967) in Fig. 6.9. The present results are found to be more in agreement with those of Oort. It should be emphasized that in Dutton and Johnson's work GZ, CK and CZ are the only transformations based on observational data; the remaining ones are based entirely on Kung's (1966) total dissipation rate and balance requirements. In the present work, all transformations were computed from observed data. Oort's results are also

partly based on balance requirements. It appears that the value of CA may have been underestimated in the present investigation; if this value were increased so that GZ equalled the sum of CA and CZ, then the diagram could also be completed from balance requirements.

Some facts should be emphasized about the treatment of limited regions. By original definition global estimates of the parameters \bar{N} and γ represent the only correct values, therefore, integrals evaluated from data in restricted regions can not be directly compared. As an example the values of \bar{N} at 500 mb, computed separately from northern hemisphere, southern hemisphere and global data, are given in Table 6.6 for December-February. Note the large differences in the winter hemisphere.

Table 6.6: $[\bar{N}]$ in units of 10^{-2} at 500 mb in December-February
(global vs northern and southern hemisphere distributions)

	<u>85N</u>	<u>75N</u>	<u>65N</u>	<u>55N</u>	<u>45N</u>	<u>35N</u>	<u>25N</u>	<u>15N</u>	<u>5N</u>
Global	-13.2	-15.7	-13.0	-12.6	-13.0	- 6.0	1.0	5.3	6.3
N. Hem.	- 9.3	-11.6	- 8.7	- 8.5	- 9.0	- 2.3	4.1	8.0	8.9
	<u>5S</u>	<u>15S</u>	<u>25S</u>	<u>35S</u>	<u>45S</u>	<u>55S</u>	<u>65S</u>	<u>75S</u>	<u>85S</u>
Global	6.4	6.3	4.6	0.4	- 5.3	-11.5	-13.3	-14.5	-13.9
S. Hem.	6.3	6.2	4.5	0.4	- 5.2	-10.9	-12.3	-13.4	-12.9

A more serious problem can occur when data on less than a global scale is used to derive the average value of a variable on a pressure surface which is subsequently used to compute deviations such as $[\tilde{T}]$. For example, AZ would be much less in the tropics if $[\tilde{T}]$ was based solely on tropical temperatures rather than on global temperatures.

Further evidence of this is given in the next section.

6.7 Tropics vs Higher Latitudes

The tropical atmosphere is defined here as the region between 30N and 30S. The values of GZ in the tropics (see Fig. 6.15) are much less when the efficiency factor is used because the isentropic surfaces are nearly parallel to the isobaric surfaces. Recall that $[\bar{N}]$ is extremely small in the tropics even though $[\bar{Q}]$ is relatively large. Table 6.7 shows the partitioning of GZ in the tropics according to diabatic heating components.

Table 6.7: Distribution of GZ by Components (10^{20} ergs sec⁻¹)

	Tropics (30N-30S)			<u>TOTAL</u>
	<u>RAD</u>	<u>LH</u>	<u>BLH</u>	
Dec-Feb	-132.0	132.0	29.0	29.0
Mar-May	-135.0	123.0	24.8	12.8
Jun-Aug	-128.0	122.0	26.1	20.1
Sep-Nov	-139.0	120.0	26.2	7.2

Radiation destroys AZ at a high rate while latent heat release counterbalances by producing AZ. Although small by comparison, the production of AZ by boundary layer heating is essentially responsible for positive values of GZ. Note that seasonal variations in each of the components is small.

The data used to derive the values given in Fig. 6.15 are essentially the same as those used in Kidson et al. (1969) for the region 24N-24S; when the results of the previous study were extrapolated to

the region 30N-30S they were very similar except that AZ was considerably smaller. This is because $\overline{[\tilde{T}]}$ was based solely on tropical temperature data in the earlier study.

The conversions act in the same directions in all periods and are largest in December-February. CK values are nearly comparable to those for the globe because the large up-gradient regions equatorwards of the tropospheric jet streams are included. Note that mean meridional circulations dominate the conversions in December-February and June-August when there is a strong Hadley cell centered in the winter hemisphere. In all seasons CZ acts to produce kinetic energy as suggested by Palmen et al. (1958).

The energy budgets of tropical and extratropical regions in the Northern Hemisphere are presented in Fig. 6.16 (90N-30N) and Fig. 6.17 (30N-0). In three seasons GZ at higher latitudes is much greater than it is in the tropics, however, in summer values are comparable in the two regions. This is due in part to seasonal shifts in the patterns of $\overline{[\tilde{N}]}$ and $\overline{[\tilde{Q}]}$ and to reduced diabatic cooling at high latitudes, but is mainly due to substantial decreases (increases) in the magnitudes of negative (positive) values of $\overline{[\tilde{N}]}$ at high (middle) latitudes.

Table 6.8 shows the effects of each of the heating components on GZ.

Table 6.8: Distribution of GZ by Components (10^{20} ergs sec⁻¹)

	90N-30N				30N-0			
	<u>RAD</u>	<u>LH</u>	<u>BLH</u>	<u>TOTAL</u>	<u>RAD</u>	<u>LH</u>	<u>BLH</u>	<u>TOTAL</u>
Dec-Feb	107.0	-21.8	5.8	91.0	-58.2	52.0	17.0	10.8
Mar-May	62.5	-14.8	6.1	53.8	-65.2	56.7	15.2	6.7
Jun-Aug	-10.6	10.8	16.3	16.5	-78.6	79.9	13.3	14.6
Sep-Nov	58.6	- 6.2	8.5	60.9	-79.7	68.5	14.9	3.7

Note that seasonal changes are relatively small among the components at 30N-0. In the extratropical region radiative effects are the main cause of large seasonal variations in GZ. Radiative processes act to produce AZ except in summer when they destroy it at a slow rate. As noted above the latter is caused by reduced values of cooling in conjunction with positive values for the efficiency factor at middle latitudes and negative values at high latitudes.

The reversal of CK between December-May and June-November in the region 90N-30N is due to the inclusion of the large positive CK region just south of the jet in the latter period (see Fig. 6.7). Again note the dominance of the Hadley cell in the CZ conversion in the tropical region, especially in winter. From 90N-30N, however, the Ferrel cell acts to convert KZ to AZ in all seasons; the value is also largest in winter. Keshava Murty (1968) has calculated the quantity $\bar{u} \bar{v}$ from 50E to 100E for the latitude belt 30N-0 for the month of July. He integrates the result over the whole latitude belt and obtains a value of 3×10^{20} ergs sec⁻¹ for the conversion of AZ to KZ. This compares with the present value of 3.1×10^{20} ergs sec⁻¹ for June-August (see Table 6.9), but for his vertical distribution of CZ he has 60% contributed by the upper troposphere and 40% by the lower troposphere, whereas the present study suggests a large conversion from AZ to KZ in the upper troposphere and a small conversion from KZ to AZ in the lower troposphere.

When the values in Fig. 6.17 are subtracted from those in Fig. 6.15 the results for the region 0-30S are obtained. These results

when compared with those in Fig. 6.17 show a surplus of AZ in the summer hemisphere and deficit in the winter hemisphere whereas a near balance exists in the other two periods. This suggests the possibility of a transport of AZ across the equator from the summer to the winter hemisphere.

Table 6.9 offers a convenient summary of the conversions to KZ by CK and CZ for the limited regions discussed in this chapter.

Table 6.9: Conversions to KZ (10^{20} ergs sec⁻¹)

	90N-30N		30N-0		90N-0	0-90S
	MEAN	EDDY	MEAN	EDDY	NET	NET
	CZ	CK	CZ	CK		
Dec-Feb	-12.1	-2.6	18.0	8.0	11.3	7.5
Mar-May	- 8.1	-0.5	3.3	6.1	0.8	10.3
Jun-Aug	- 2.5	2.7	3.1	1.8	5.1	12.4
Sep-Nov	- 5.2	3.4	3.0	4.4	5.6	11.2

In March-November, there is apparently a need for more dissipation in the Southern Hemisphere than in the Northern Hemisphere unless there is a flux of energy from the Southern Hemisphere into the Northern Hemisphere. In northern winter this argument is the same. The lateral flux of energy across the equator is difficult to assess. In March-May the resultant values for conversions to KZ are relatively small in the Northern Hemisphere which is partly due to an extensive Ferrel cell existing over most of the region north of 25N. In contrast the southern edge of the Ferrel cell in September-November is near 37N, which reduces the value of KZ→AZ. The same arguments can

be applied to northern hemisphere tropical and extratropical regions. That is, in the tropics there is either a need for dissipation of KZ or an energy transport to higher latitudes. The latter appears to be a necessity in any case as there is a deficit in conversions to KZ in all seasons except summer and it is known that KZ is being dissipated. In a discussion of KZ transformations for January 1963 for the tropospheric region 90N-20N, Brown (1967) noted that CK was from KZ to KE which was opposite to other Januarys. Of course, in the particular region studied, CK is probably close to zero in winter (see Table 6.9), but a more important result of Brown's investigation was that the production of KZ due to boundary terms was sufficient to overcome the loss which had occurred through conversion to KE.

6.8 Extratropical Troposphere vs Stratosphere

Most of the data required to investigate the energetics of the region 100-10 mb were available between 90N and 30N; consequently, between these latitudes, the analysis of the energy budget was extended to 10 mb (see Fig. 6.18).

When values in Figs. 6.16 and 6.18 are compared it is seen that most of the quantities show their greatest differences in December-February. The increase of KZ in December-February when the upper region is included is due to the strong zonal winds associated with the polar night jet. Note that values of the conversion CA decrease in all seasons except December-February when the upper region is included. Counter-gradient heat fluxes in the stratosphere convert AE to AZ in

three seasons but in December-February the temperature gradient is reversed in the stratosphere and there is a strong poleward heat flux into the colder polar region. A cross section of the integrand of CA for December-February from 90N-30S, 1000-10 mb is given in Fig. 6.10.

For the extratropical region the conversion CK in December-February is from KE to KZ in the 100-10 mb region and from KZ to KE in the 1000-100 mb region. It is rather remarkable that the upper region which contains less than 1/10 of the total mass can convert kinetic energy at nearly one-half the rate of the lower region. The reversal in the upper region is due to a poleward flux of momentum which is against the zonal wind gradient between 65N and 30N. Note that in the upper region the conversion from KE to KZ is equally as strong by the standing eddy component of momentum flux. Fig. 6.11 shows a cross section of CK from 90N-30S, 1000-10 mb for December-February.

In winter the values for the conversion from KZ to AZ are large in the stratosphere as well as in the troposphere, due mainly to the presence of an indirect (Ferrel) cell (see Fig. 4.6) which forces colder air upwards at high latitudes and warmer air downwards at middle latitudes. Stratospheric energetics based on some of the same data have been discussed in detail elsewhere (Richards, 1967; Newell and Richards, 1969; Newell et al., 1970b).

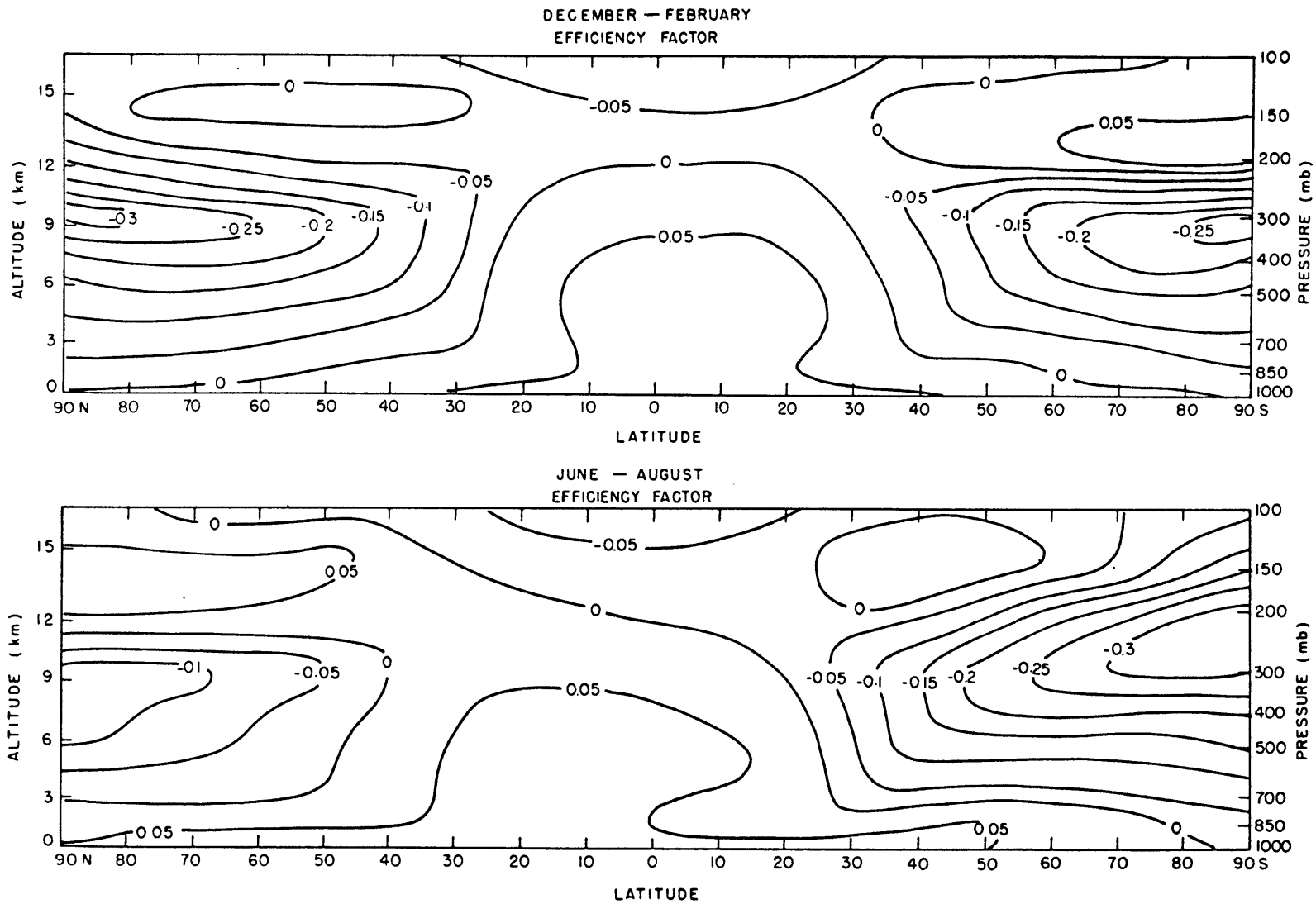


Fig. 6.1: Efficiency factor \bar{N}

DECEMBER - FEBRUARY
AZ (10^7 ergs gm^{-1})

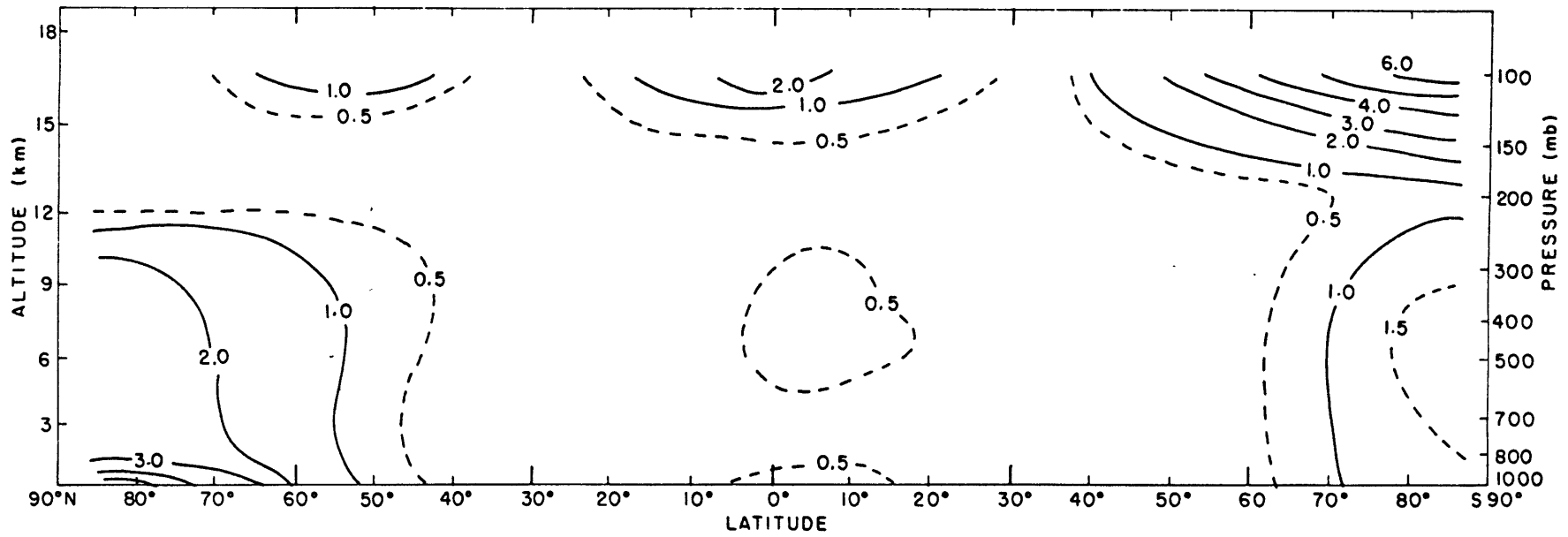


Fig. 6.2: Integrand of the energy content AZ

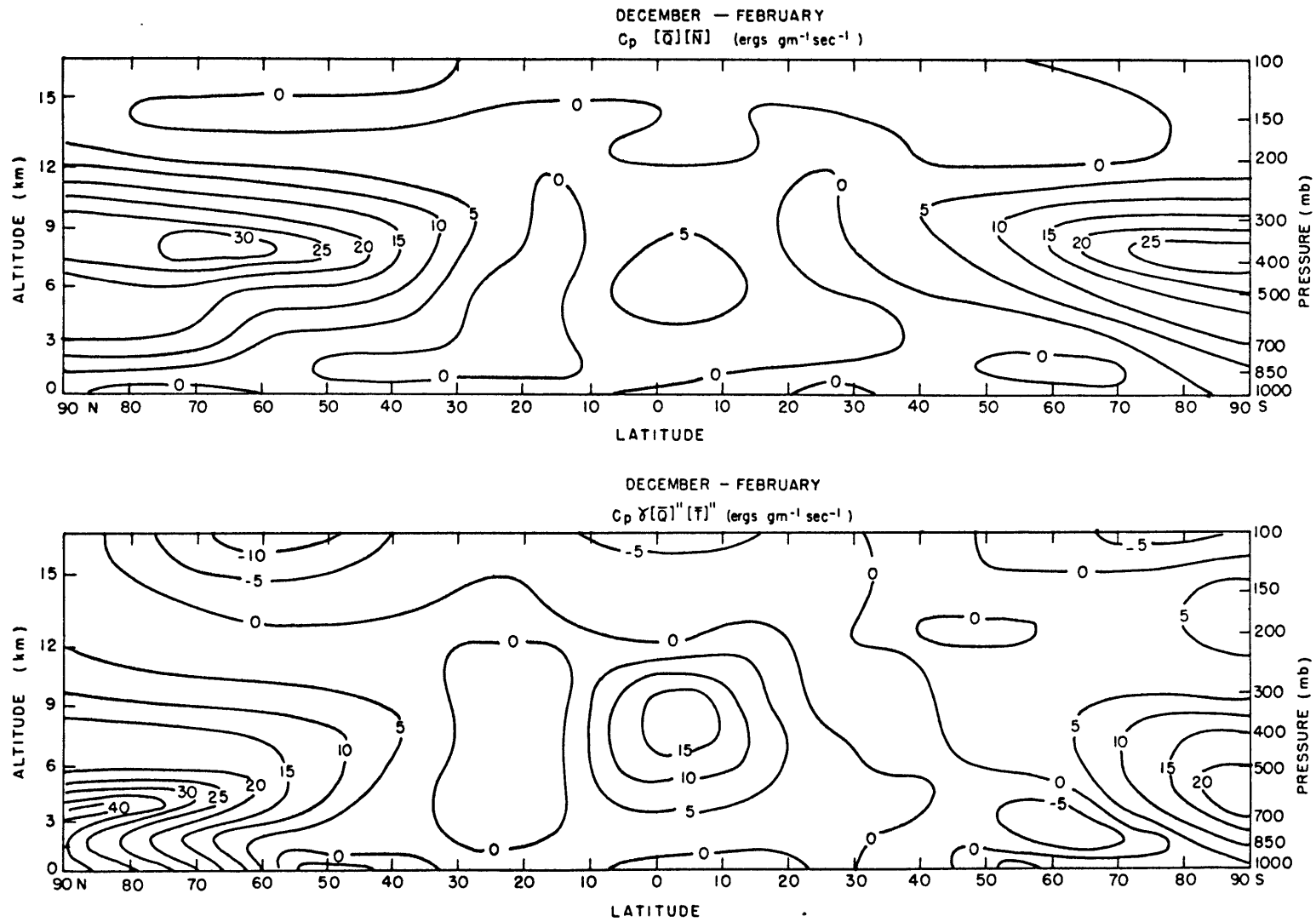


Fig. 6.3: Integrand of the energy generation, GZ, by two methods for December-February

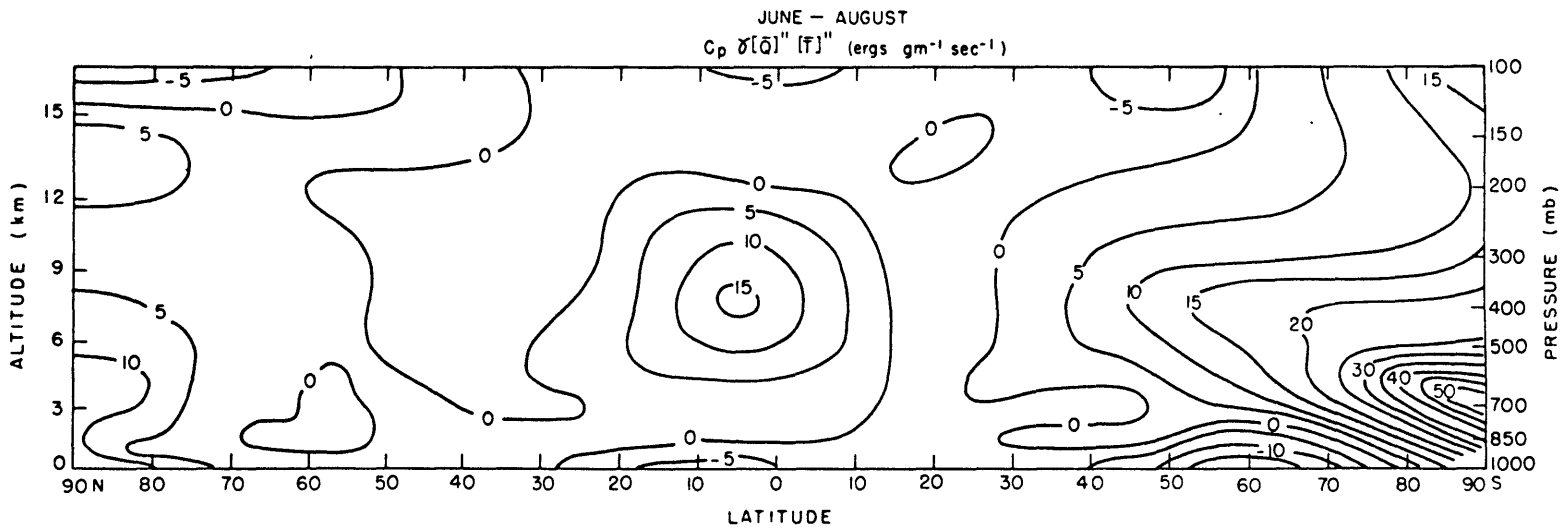
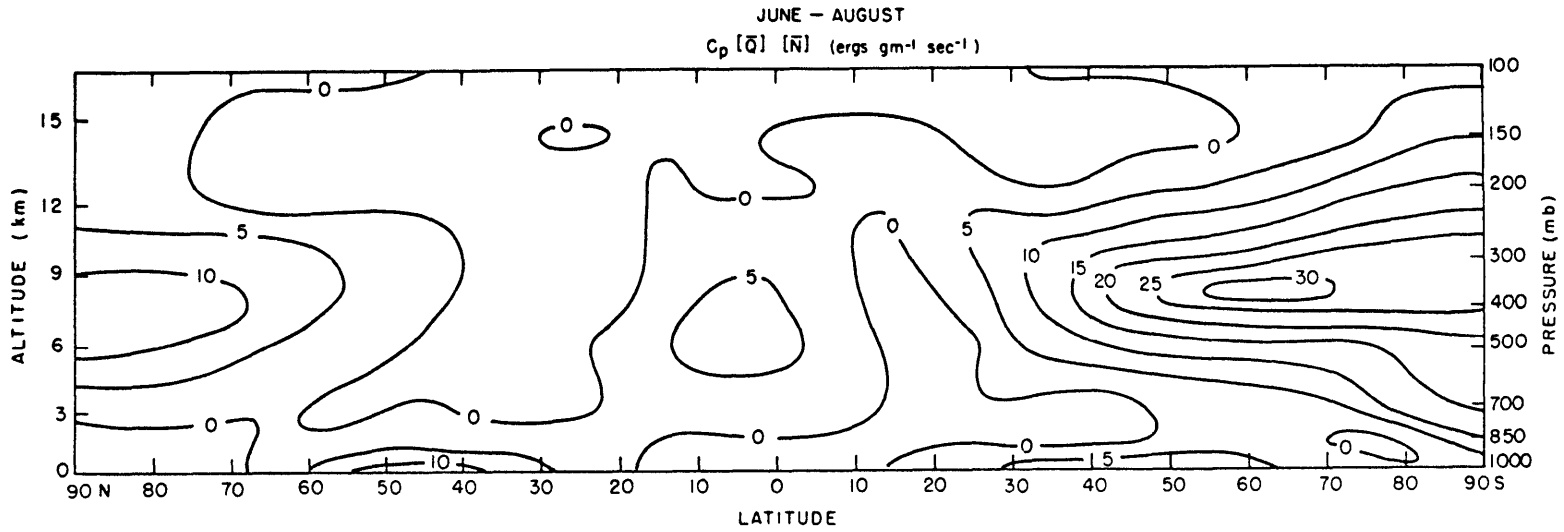


Fig. 6.4: Integrand of the energy generation, GZ, by two methods for June-August

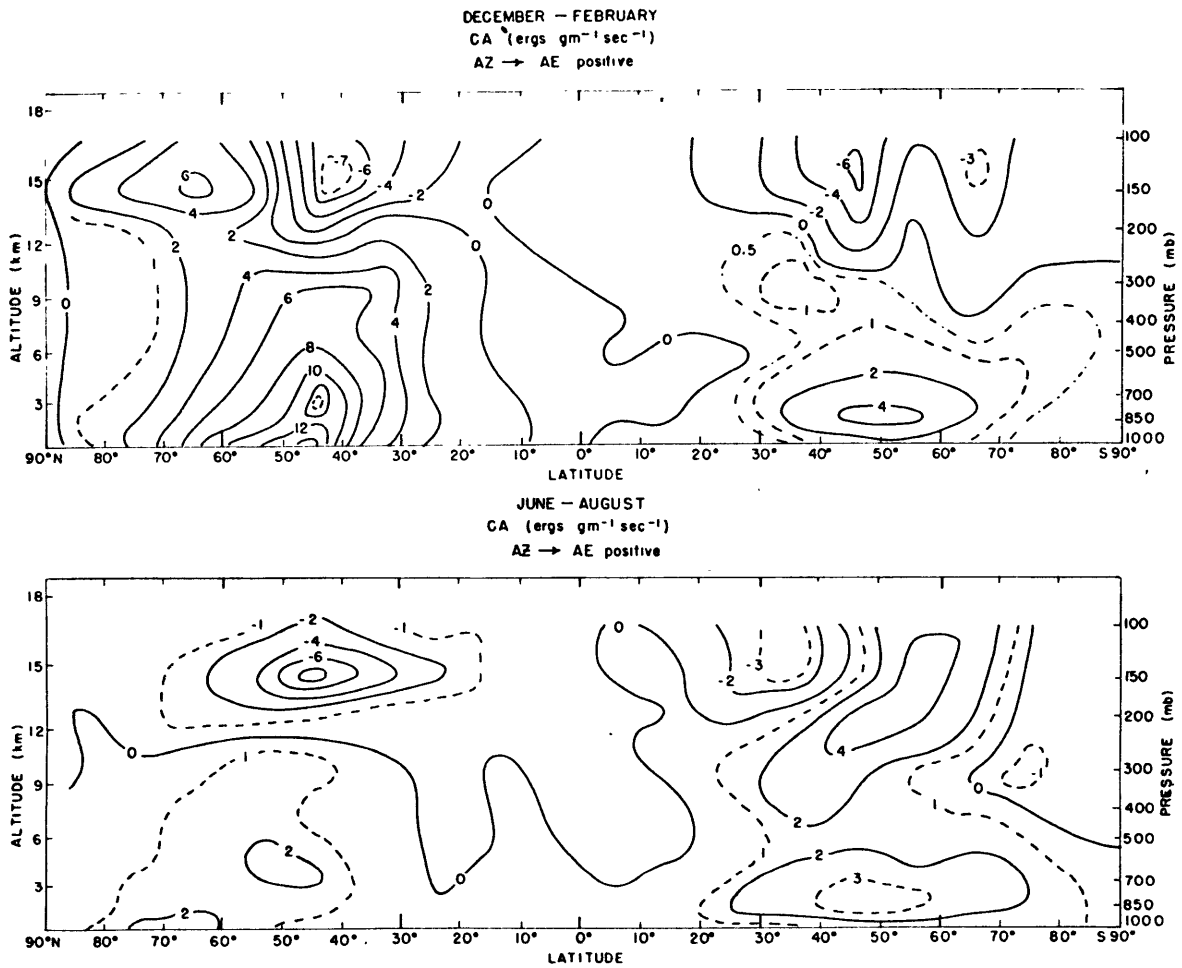


Fig. 6.5: Integrand of the energy conversion CA

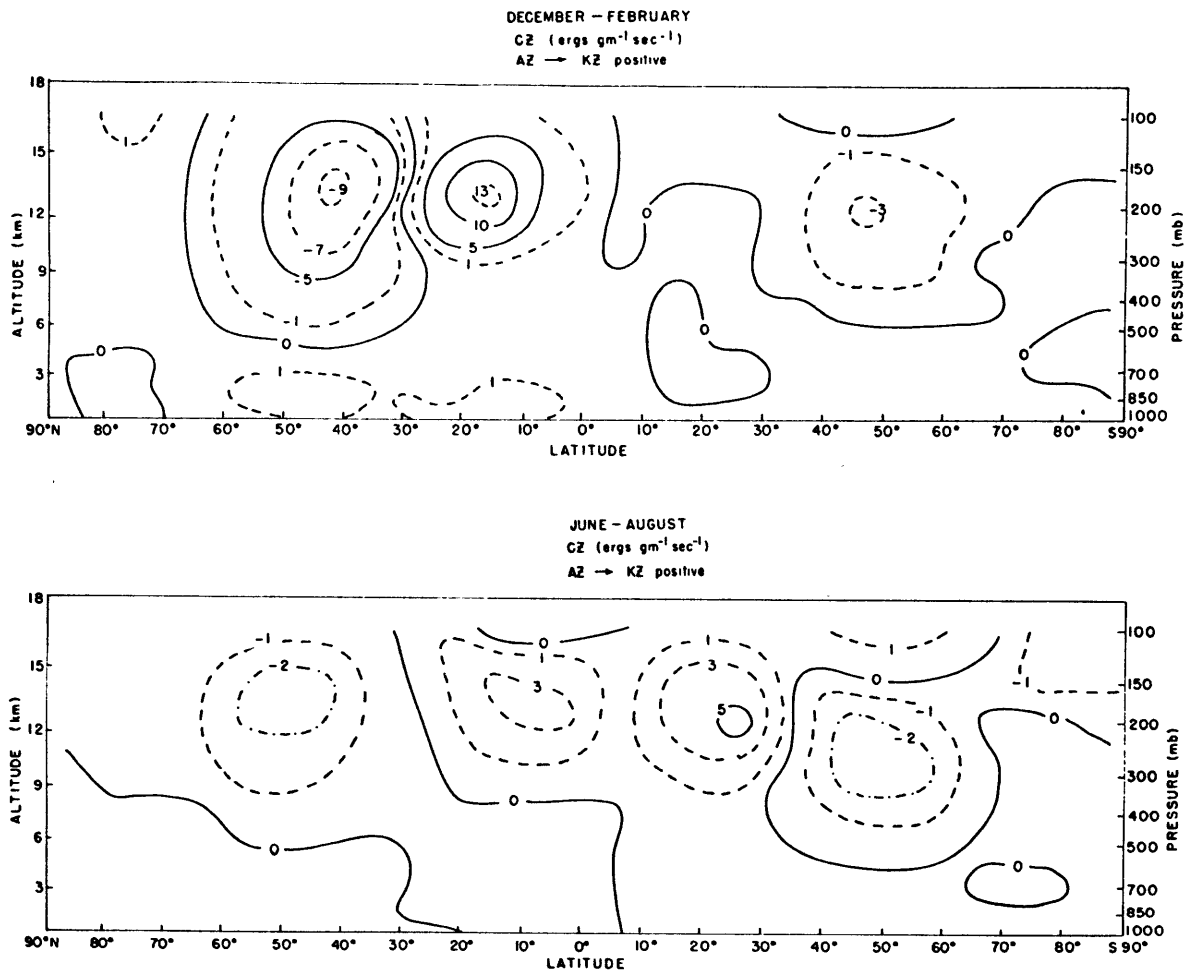


Fig. 6.6: Integrand of the energy conversion CZ

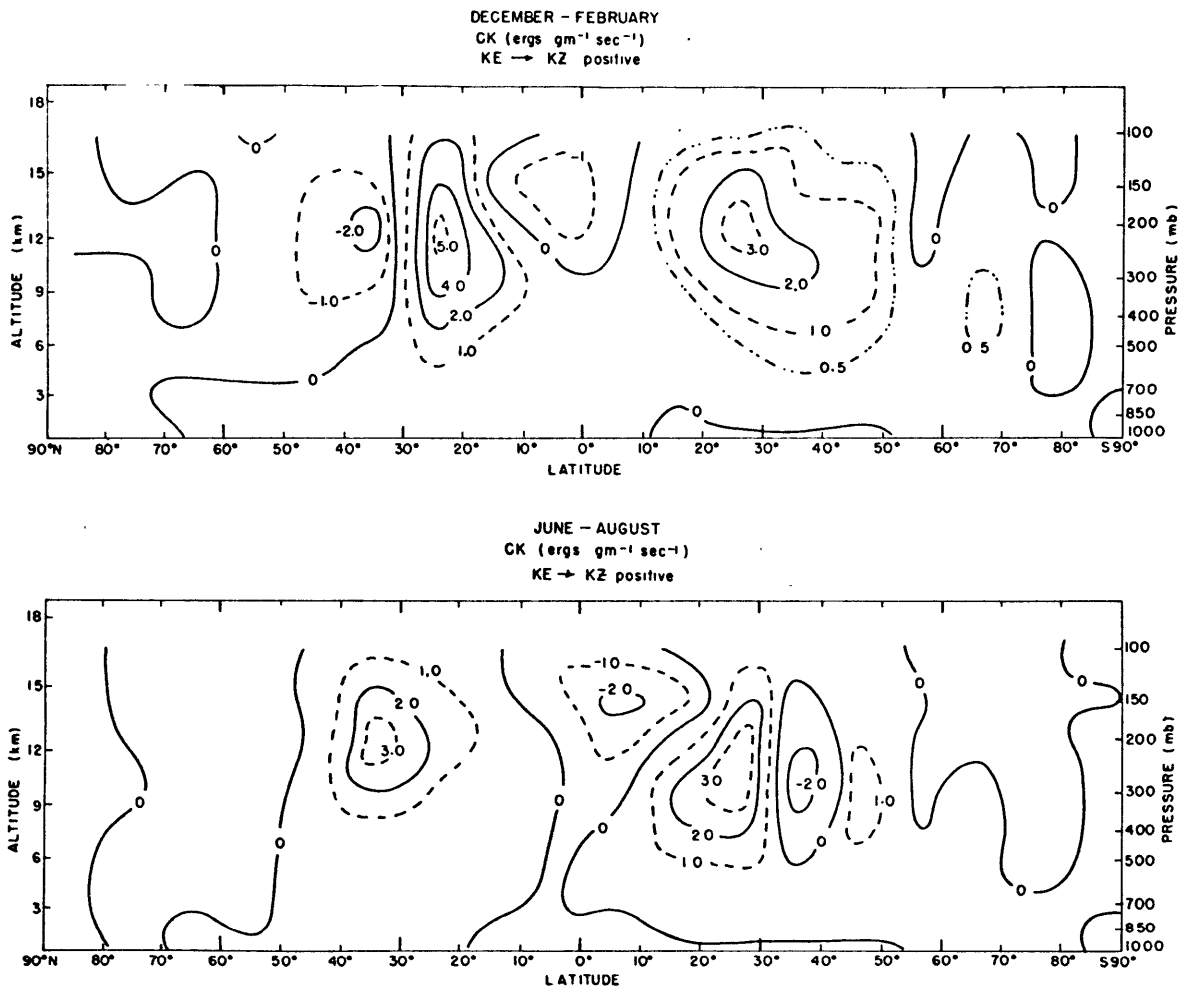


Fig. 6.7: Integrand of the energy conversion CK

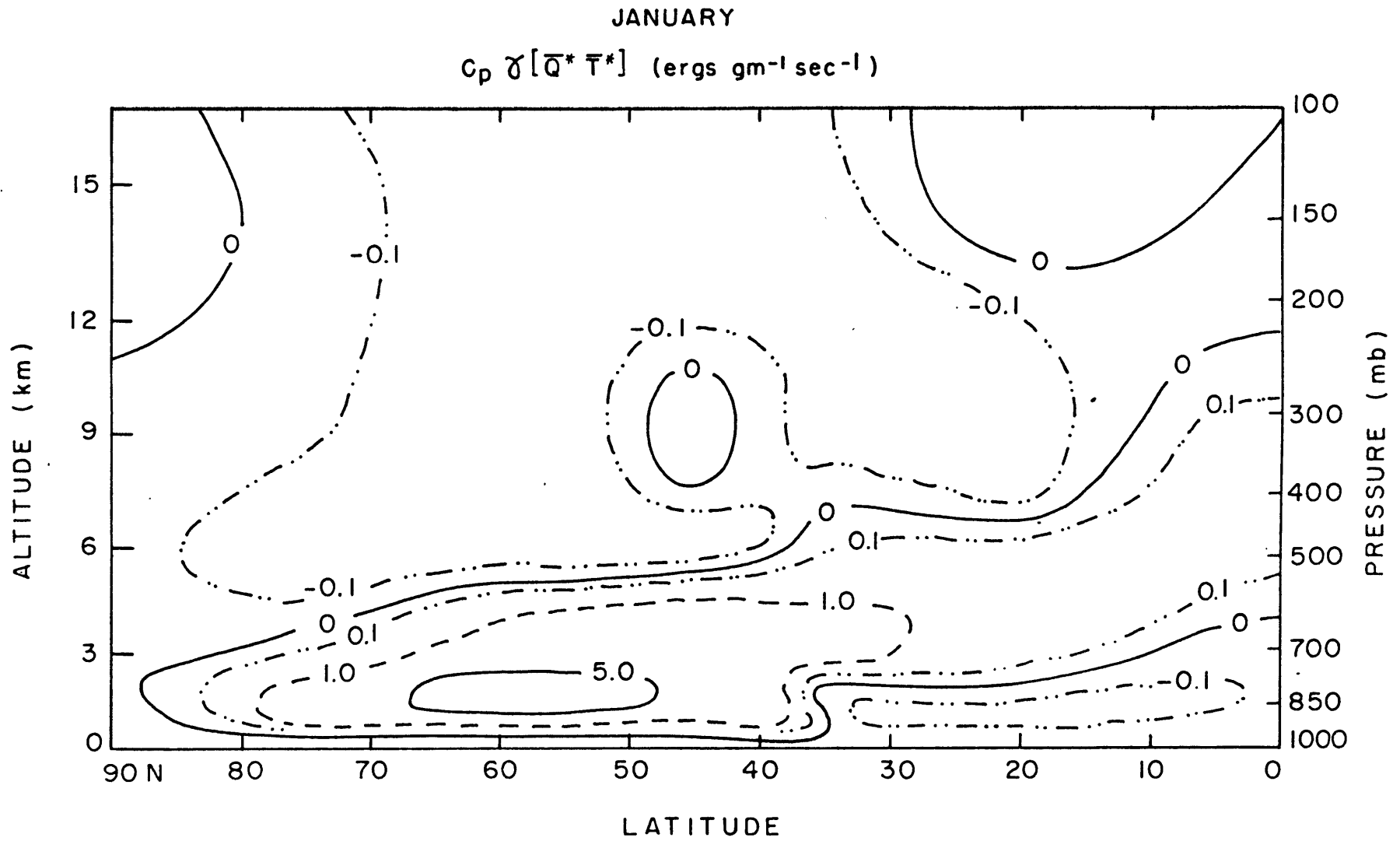
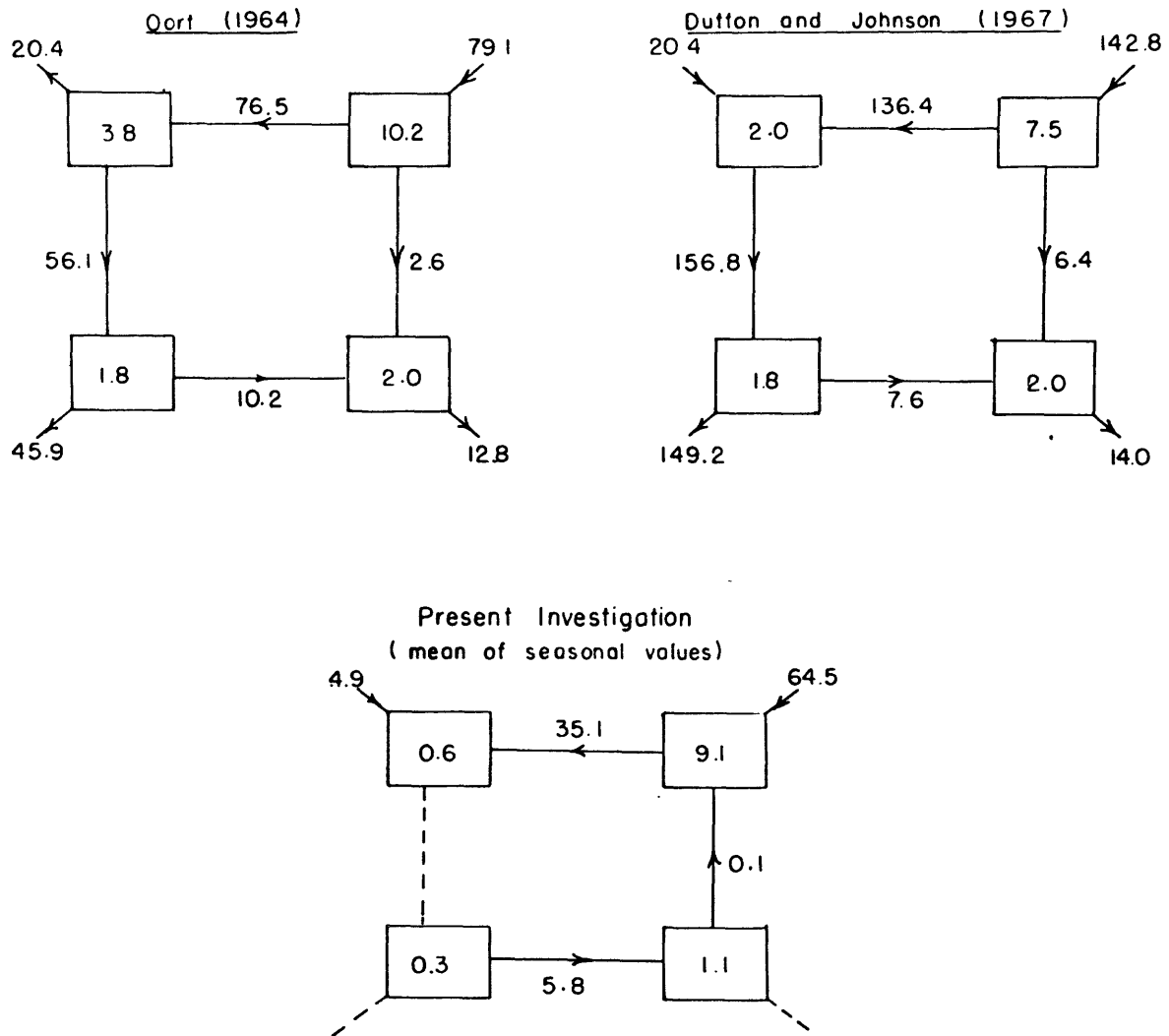


Fig. 6.8: Integrand of the energy generation GE

ENERGY BUDGET
NORTHERN HEMISPHERE ANNUAL MEANS



CONTENTS 10^{27} ergs
CONVERSIONS 10^{20} ergs sec⁻¹

Fig. 6.9: Energy budget for the Northern Hemisphere

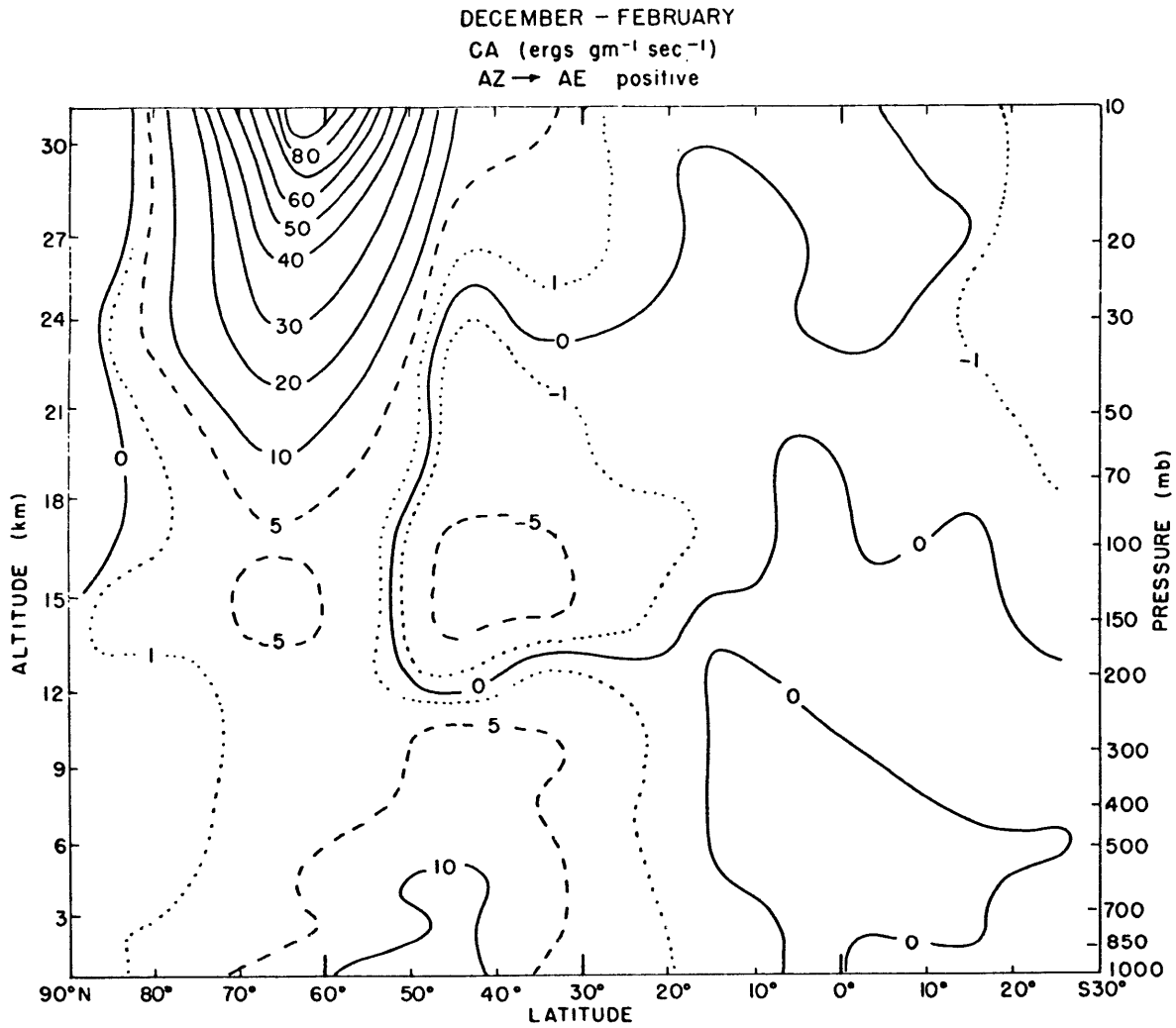


Fig. 6.10: Integrand of the energy conversion CA

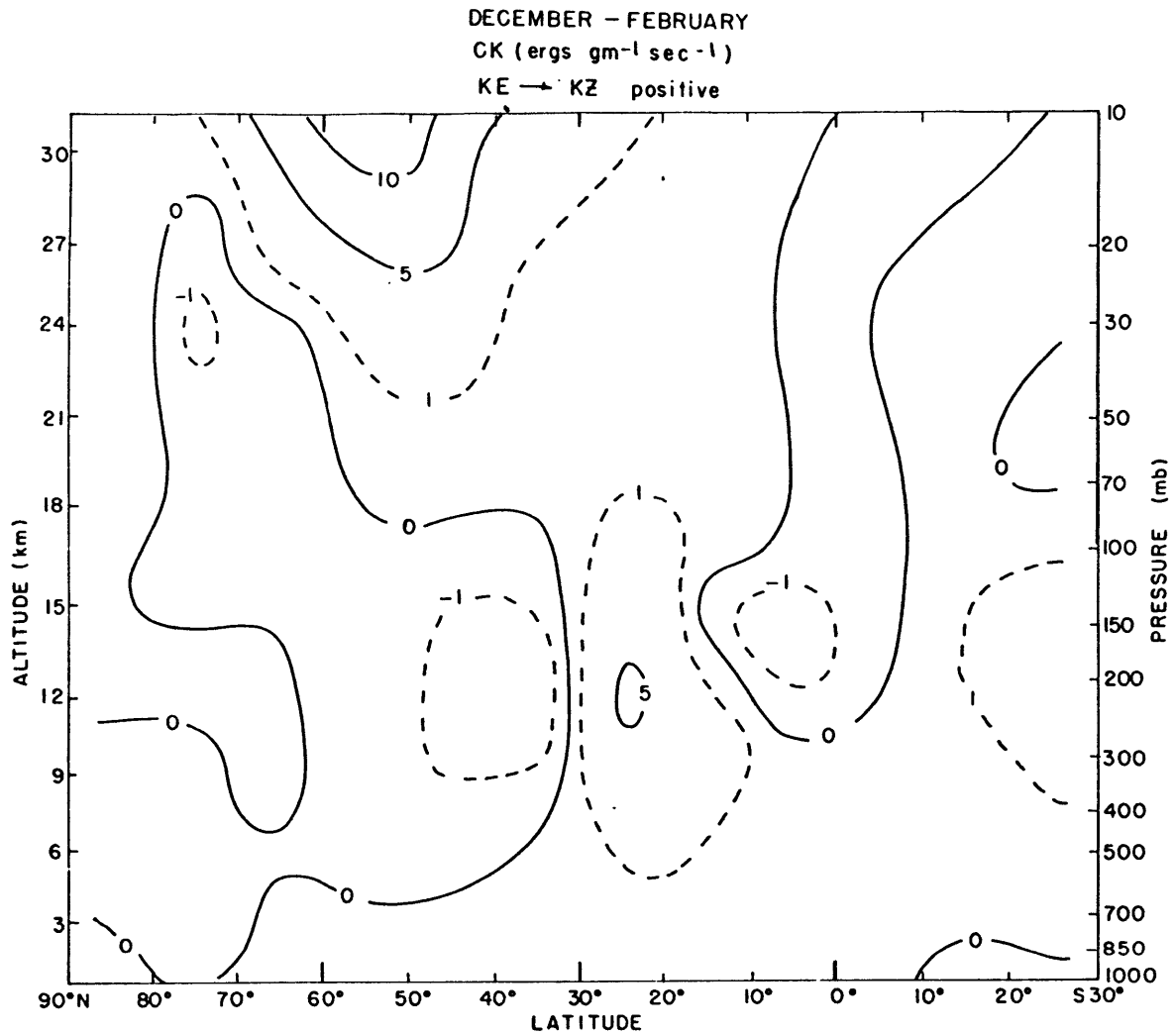
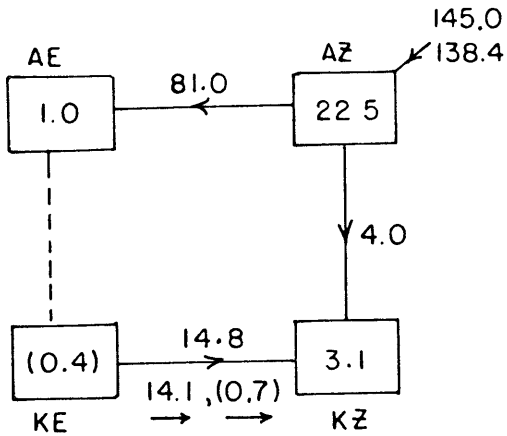


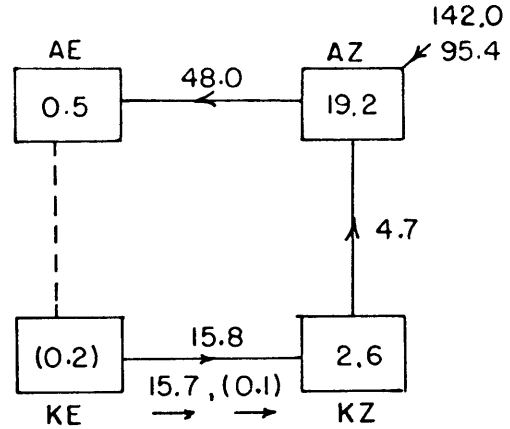
Fig. 6.11: Integrand of the energy conversion CK

ENERGY BUDGET 90°N - 90°S , 1000 - 100mb

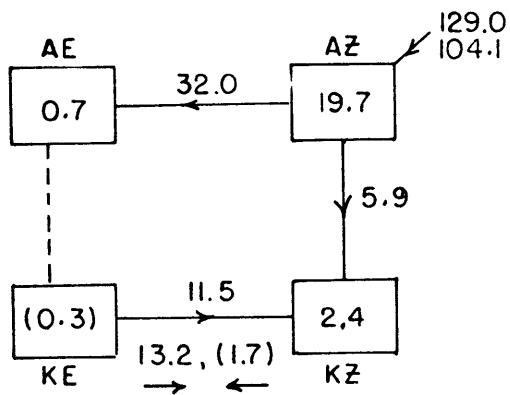
DEC - FEB



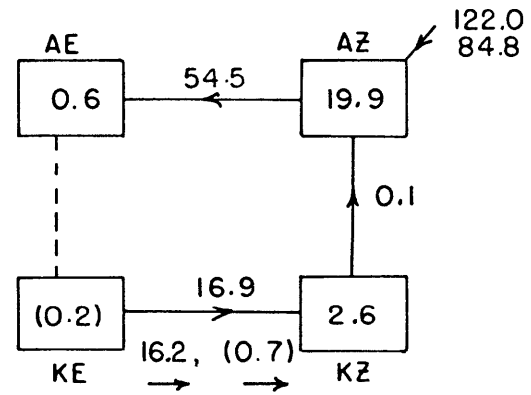
MARCH - MAY



JUNE - AUGUST



SEPT. - NOV.



CONTENTS ergs $\times 10^{27}$
 CONVERSIONS ergs $\text{sec}^{-1} \times 10^{20}$
 () available 90°N - 30°S only

Fig. 6.12: Global energy budget

ENERGY BUDGET
90° N - 0, 1000 - 100 mb

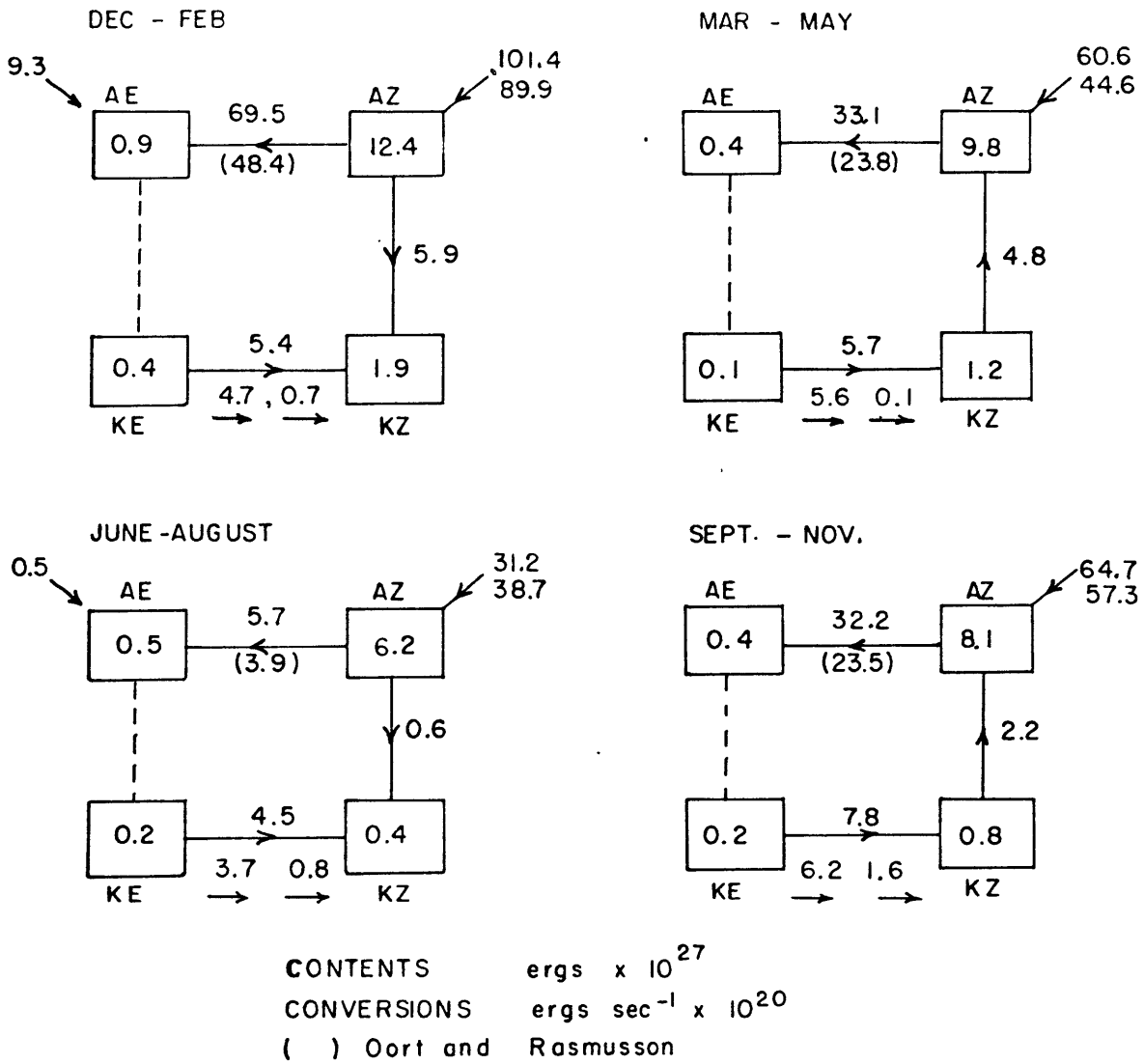
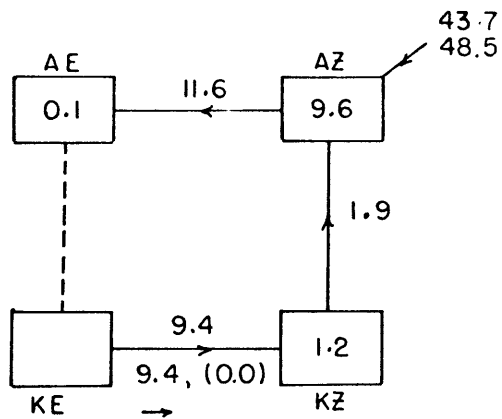


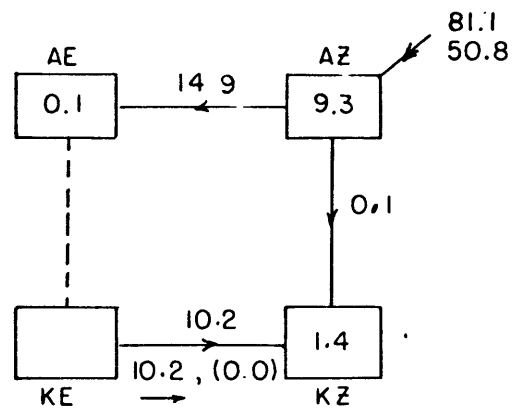
Fig. 6.13: Energy budget for Northern Hemisphere

ENERGY BUDGET
 $0^{\circ} - 90^{\circ}\text{S}$, 1000-100mb

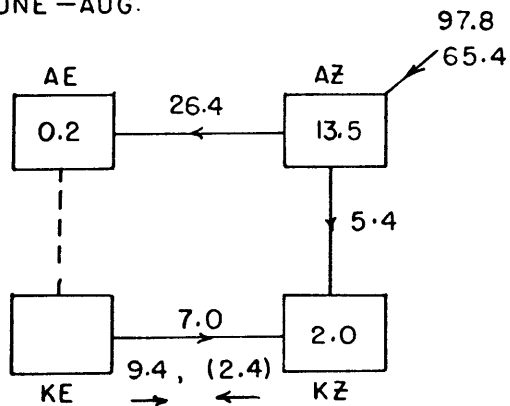
DEC - FEB



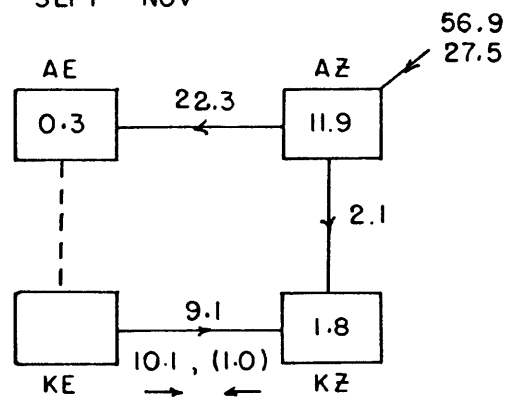
MARCH - MAY



JUNE - AUG.



SEPT - NOV

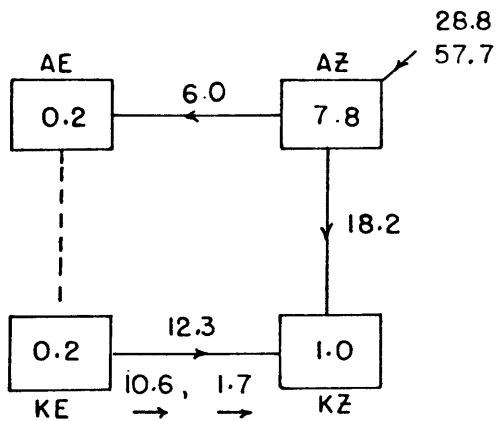


CONTENTS ergs $\times 10^{27}$
 CONVERSIONS ergs $\text{sec}^{-1} \times 10^{20}$
 () [$\bar{u}^* \bar{v}^*$] $0^{\circ} - 30^{\circ}\text{S}$ only

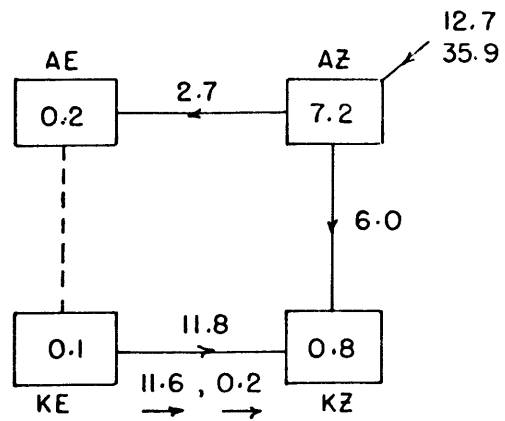
Fig. 6.14: Energy budget for Southern Hemisphere

ENERGY BUDGET
30°N - 30°S , 1000 - 100 mb

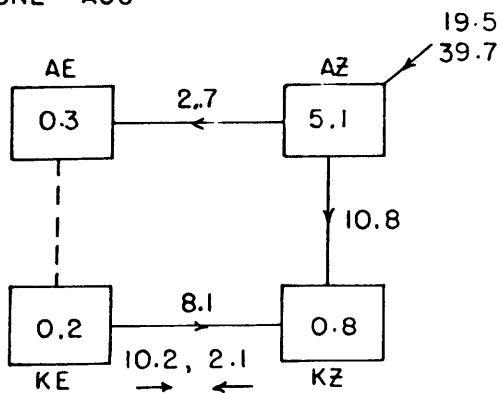
DEC - FEB



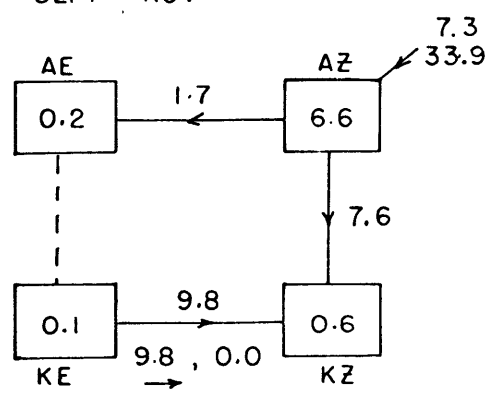
MARCH - MAY



JUNE - AUG



SEPT - NOV



CONTENTS ergs x 10²⁷
 CONVERSIONS ergs sec⁻¹ x 10²⁰

Fig. 6.15: Energy budget for tropics

ENERGY BUDGET
90° N - 30° N, 1000 - 100 mb

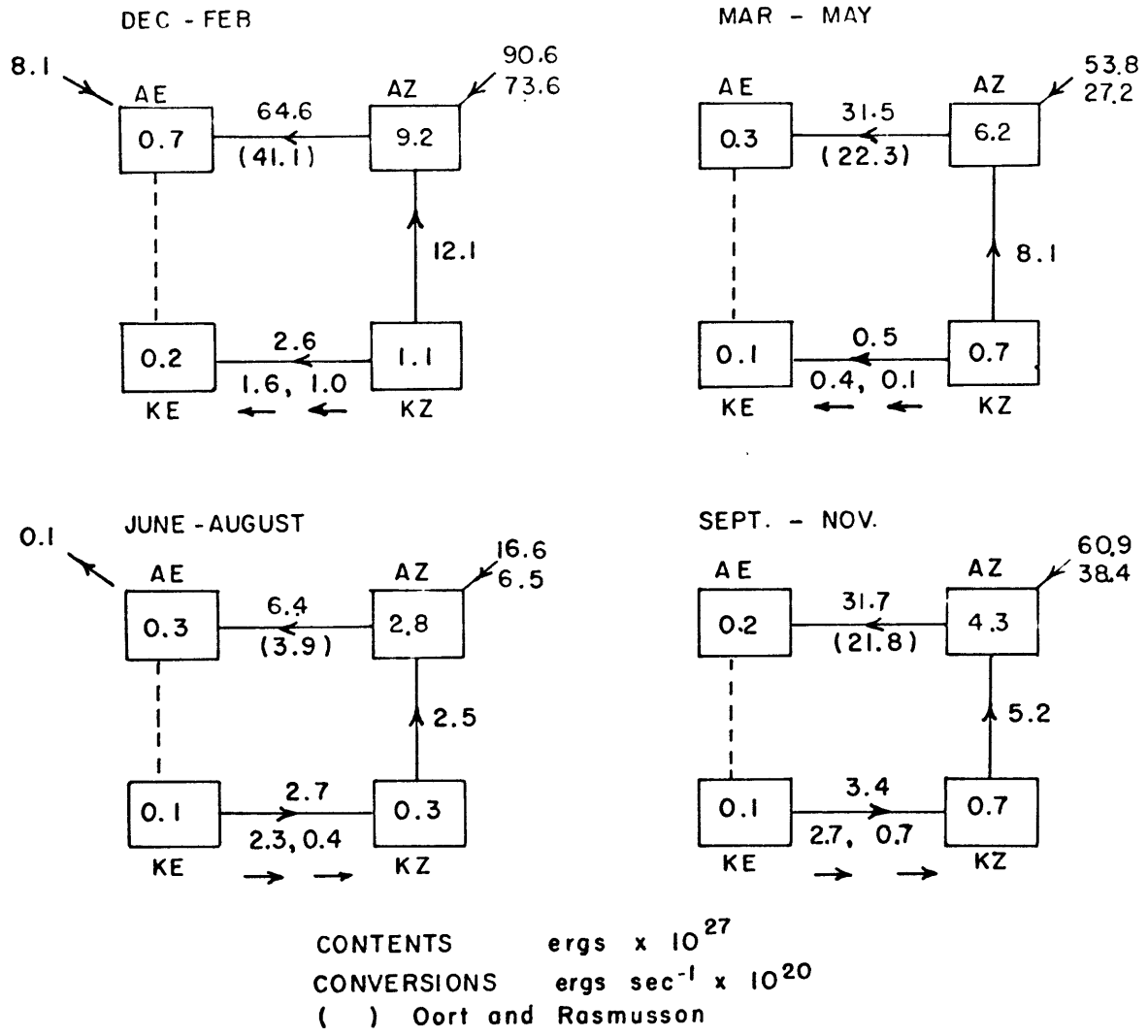


Fig. 6.16: Energy budget for extratropical troposphere in Northern Hemisphere

ENERGY BUDGET
30°N - 0 1000 - 100 mb

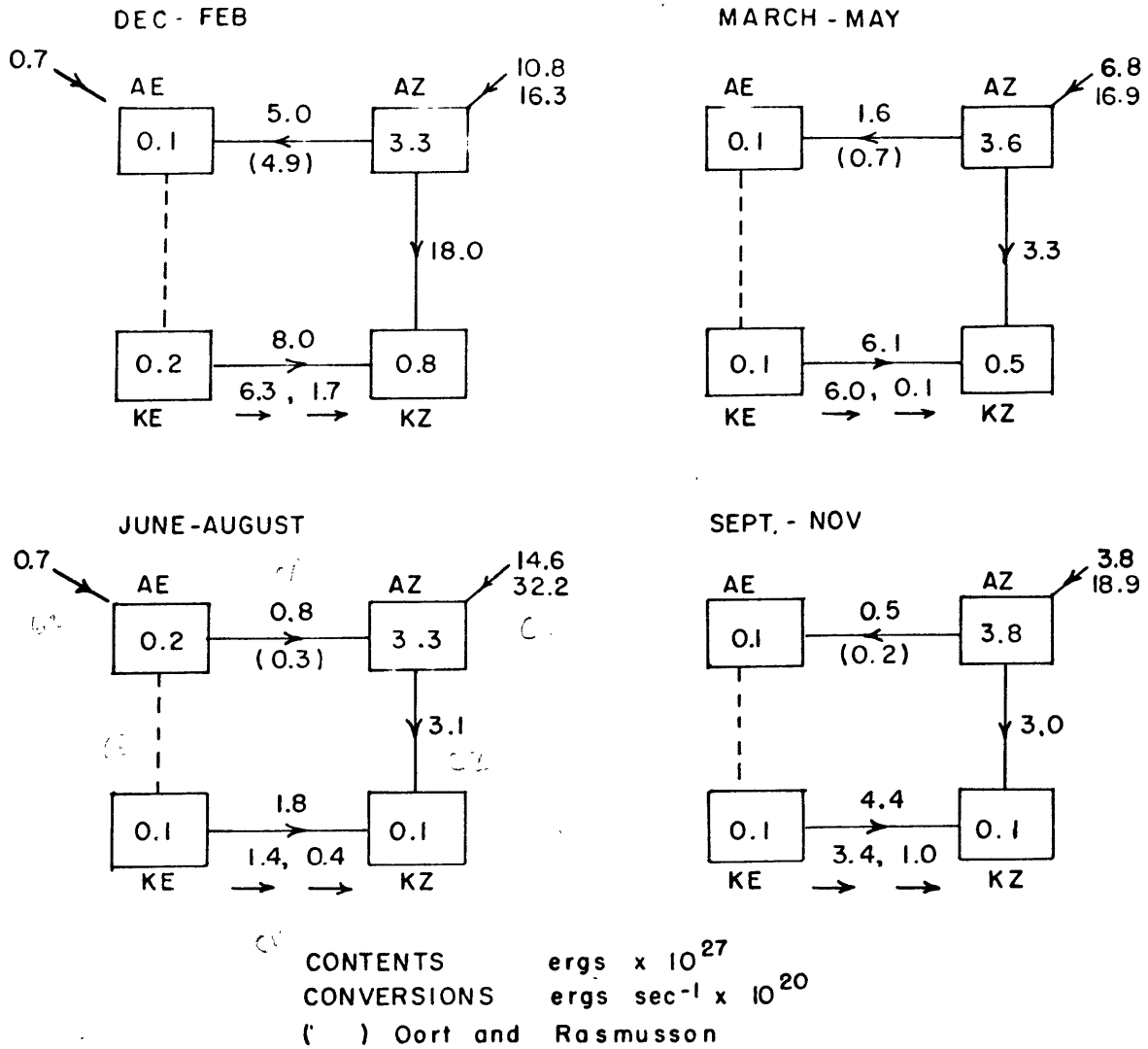


Fig. 6.17: Energy budget for tropical troposphere in Northern Hemisphere

ENERGY BUDGET
90°N - 30°N , 1000 - 10mb

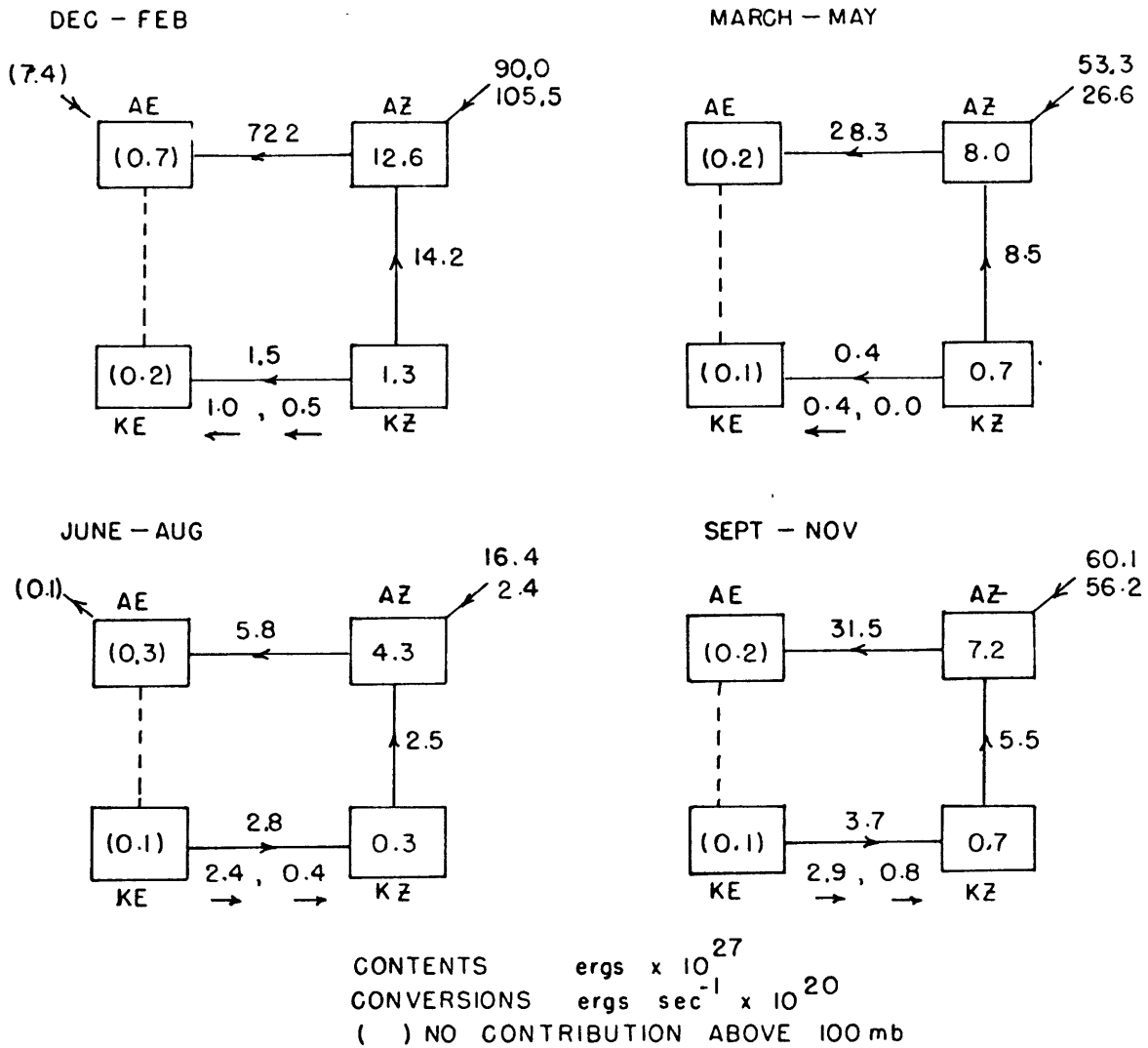


Fig. 6.18: Energy budget for extratropical troposphere and stratosphere in Northern Hemisphere

CHAPTER 7

CONCLUDING REMARKS AND UNRESOLVED PROBLEMS

The major purpose of this investigation has been to obtain a better understanding of the global energy budget. The main question put forth was, "How does the energy from the sun get converted into kinetic energy to replenish frictional losses?". In an attempt to obtain the most comprehensive answer to this question the study was subdivided in the time and space domains; seasonal changes in the energy balance were considered and results for restricted regions, grouped according to latitude, were computed.

Considerable insight into the first part of the question was obtained by computing the fraction of AZ generated by each diabatic heating component. For the globe seasonal changes of each component showed a well established trend; values over the long run indicated that radiative processes have a slight tendency to destroy AZ, while latent heat release and boundary layer heating are sources of AZ. Latent heat release was found to be more than twice as effective as boundary layer heating in producing AZ. When restricted regions were considered, the tropical results showed a strong destruction of AZ by radiative heating but an equally strong production by latent heat release. Although boundary layer heating was comparatively small it was essentially responsible for positive values of GZ in the tropics. In extratropical regions (only northern hemisphere results were computed) radiation produced AZ in all seasons except summer. The other

components were relatively small and the net value of GZ was approximately the same as that given by radiative heating alone, again with the exception of summer. The results show the importance of latent heat liberation in maintaining the intensity of the global atmospheric general circulation.

With the possible exception of CK the energy conversions for the globe showed marked seasonal variations. CA was from AZ to AE in all seasons and was largest in winter. In the Northern Hemisphere almost all of the conversion from AZ to AE took place north of 30N. Tropical values were extremely small and, in summer, the conversion reversed and was from AE to AZ. Values of CZ showed the dominance of the Hadley circulation in the tropics and the Ferrel circulation in middle latitudes. On a global basis CZ was from AZ to KZ in December-February and June-August, mainly due to the strong influence of the Hadley circulation in the winter hemisphere. The eddy momentum transport was generally polewards in both hemispheres, consequently, CK was from KE to KZ in the tropical regions where transfer was against the zonal wind gradient, and from KZ to KE polewards of the jet. Values of CK for the globe were from KE to KZ and appeared to be mostly due to transient eddies.

To summarize, it appears that the sun not only acts directly through radiation, but indirectly through latent heat release and boundary layer heating, to produce the required available potential energy for conversion to kinetic energy. This conversion is primarily due to eddy processes which are strongest in middle latitudes during

winter. Most of the AZ is converted to AE by downgradient heat transfer and subsequently to KE by large scale baroclinic waves. Mean motions, although of secondary importance, are a significant factor in seasonal changes in the energy budget, particularly at low latitudes in the winter hemisphere where the Hadley circulation converts AZ to KZ. There is also a conversion from KE to KZ. Frictional losses appear to occur mainly through dissipation of KE; KZ dissipation is secondary.

When viewed collectively the results are encouraging. The mean annual generation of available potential energy (GZ + GE) for the globe is about 150×10^{20} ergs sec^{-1} if time fluctuations in GE are comparatively small; an estimate of the kinetic energy dissipation (DZ + DE), based on CE (Jensen, 1961), CK and CZ is about 200×10^{20} ergs sec^{-1} . Jensen's value for CE, when extended to the globe, is 200×10^{20} ergs sec^{-1} ; this is probably an overestimate since his results were derived for the region 80N - 20N which for the most part is characterized by strong baroclinic disturbances, notably absent at low latitudes. The only other estimate of CE, based on observations, appears to be that by Miyakoda et al. (1969) for two weeks in January, 1964. Integrating their results gives an approximate value of $2500 \text{ ergs cm}^{-2} \text{ sec}^{-1}$ for the region north of 20N which when extended over the whole earth is about 125×10^{20} ergs sec^{-1} . The numerical model results of Miyakoda et al. show somewhat larger values in middle and high latitudes but also illustrate that an appropriate value for the hemisphere is smaller than that for the region

north of 20N. Hence, there appears to be a reasonable compatibility between the present generation rates and the dissipation rates estimated from conversions to KE and KZ.

As with all studies there are some unresolved problems; one of these involves the surplus values of AZ which were evident. The apparent surplus probably arises because values of CA have been underestimated, particularly in the Southern Hemisphere. New values of the meridional heat flux by transient eddies are being calculated for the Southern Hemisphere and preliminary results indicate that the middle latitude poleward fluxes are considerably larger than the present results. Another outstanding problem is the lack of daily values of vertical velocity on a global basis. These are particularly needed in order to compute CE which is a missing link in the present study. As noted in Chapter 5 values of the vertical heat flux would also provide more useful information concerning the heat balance of the atmosphere. Still another outstanding problem is the absence of radiational heating rates in the Southern Hemisphere.

With today's increased observations, satellites and high speed computers, these problems will eventually be solved and a more complete understanding of the atmospheric general circulation and the heat and energy budgets will become available.

TABLE 3.1

NET RADIATIVE HEATING (deg day⁻¹)

(a) January

<u>P(mb)</u>	<u>90N</u>	<u>80N</u>	<u>70N</u>	<u>60N</u>	<u>50N</u>	<u>40N</u>	<u>30N</u>	<u>20N</u>	<u>10N</u>	<u>0</u>
10	-1.20	-1.30	-1.26	-1.10	-0.81	-0.42	-0.25	-0.13	0.45	0.80
20	-0.95	-1.04	-1.06	-0.98	-0.79	-0.49	-0.25	-0.05	0.27	0.32
30	-0.76	-0.84	-0.87	-0.82	-0.68	-0.40	-0.33	0.01	0.22	0.25
50	-0.52	-0.60	-0.63	-0.54	-0.47	-0.19	0.10	0.20	0.03	0.10
70	-0.45	-0.52	-0.55	-0.48	-0.41	-0.16	0.13	0.30	0.15	0.16
100	-0.43	-0.46	-0.50	-0.46	-0.41	-0.21	0.01	0.16	0.20	0.20
150	-0.43	-0.43	-0.39	-0.33	-0.28	-0.31	-0.23	-0.13	-0.12	-0.14
200	-0.45	-0.45	-0.40	-0.35	-0.33	-0.45	-0.46	-0.40	-0.50	-0.52
300	-0.75	-0.75	-0.75	-0.75	-0.75	-0.92	-1.00	-1.00	-1.07	-1.09
400	-1.20	-1.20	-1.25	-1.33	-1.35	-1.35	-1.40	-1.44	-1.48	-1.43
500	-0.95	-0.95	-1.00	-1.05	-1.31	-1.50	-1.65	-1.65	-1.56	-1.48
700	-2.00	-2.00	-2.00	-2.00	-1.90	-1.75	-1.70	-1.55	-1.42	-1.30
850	-1.85	-1.85	-1.85	-1.80	-1.90	-1.65	-1.45	-1.36	-1.25	-1.10
1000	-0.90	-0.90	-0.85	-0.75	-0.90	-1.10	-1.15	-1.20	-1.10	-0.95

(b) April

10	-0.45	-0.45	-0.30	-0.05	0.30	0.75	0.95	0.85	1.05	1.05
20	-0.70	-0.70	-0.55	-0.38	-0.16	0.00	0.23	0.27	0.31	0.18
30	-0.55	-0.55	-0.40	-0.26	-0.12	-0.10	0.14	0.22	0.22	0.07
50	-0.30	-0.30	-0.21	-0.12	-0.03	0.09	0.24	0.26	0.15	0.06
70	-0.20	-0.20	-0.15	-0.08	-0.06	0.05	0.21	0.28	0.21	0.16
100	-0.20	-0.20	-0.15	-0.09	-0.08	-0.03	0.09	0.20	0.23	0.24
150	-0.20	-0.20	-0.15	-0.09	-0.03	-0.05	-0.05	0.00	0.00	0.00
200	-0.20	-0.20	-0.20	-0.18	-0.10	-0.17	-0.22	-0.30	-0.40	-0.50
300	-0.50	-0.50	-0.58	-0.65	-0.65	-0.65	-0.70	-0.85	-1.05	-1.25
400	-0.90	-0.90	-0.98	-1.04	-1.08	-1.07	-1.18	-1.35	-1.51	-1.53
500	-1.02	-1.02	-1.06	-1.10	-1.12	-1.08	-1.14	-1.31	-1.47	-1.49
700	-1.35	-1.35	-1.30	-1.25	-1.21	-1.05	-1.09	-1.25	-1.37	-1.40
850	-1.05	-1.05	-1.00	-0.90	-0.90	-0.80	-1.00	-1.08	-1.26	-1.30
1000	-0.50	-0.50	-0.50	-0.50	-0.50	-0.50	-0.60	-0.75	-0.85	-1.00

TABLE 3.1

(continued)

(c) July

<u>P(mb)</u>	<u>90N</u>	<u>80N</u>	<u>70N</u>	<u>60N</u>	<u>50N</u>	<u>40N</u>	<u>30N</u>	<u>20N</u>	<u>10N</u>	<u>0</u>
10	0.20	0.20	0.30	0.40	0.55	0.75	0.85	0.70	0.70	0.80
20	-0.20	-0.20	-0.21	-0.24	-0.16	-0.03	0.20	0.17	0.17	0.32
30	-0.05	-0.05	-0.10	-0.20	-0.12	-0.04	0.10	0.15	0.11	0.25
50	0.05	0.05	0.02	-0.08	0.02	0.12	0.19	0.19	0.07	0.10
70	0.00	0.00	-0.01	-0.02	0.03	0.19	0.27	0.25	0.18	0.16
100	-0.10	-0.10	-0.07	-0.05	0.00	0.15	0.23	0.20	0.20	0.20
150	0.03	0.03	-0.03	-0.11	-0.02	-0.04	-0.07	-0.07	-0.07	-0.14
200	0.10	0.10	-0.10	-0.30	-0.25	-0.33	-0.47	-0.47	-0.45	-0.52
300	-0.55	-0.55	-0.65	-0.75	-0.70	-0.95	-1.10	-1.10	-1.05	-1.09
400	-1.15	-1.15	-1.09	-0.94	-0.80	-1.30	-1.40	-1.38	-1.38	-1.43
500	-1.00	-1.00	-0.95	-0.88	-0.85	-1.35	-1.43	-1.39	-1.34	-1.48
700	-1.35	-1.35	-1.30	-1.27	-1.24	-1.34	-1.35	-1.30	-1.25	-1.30
850	-1.05	-1.05	-1.08	-1.10	-1.00	-1.12	-1.25	-1.18	-1.15	-1.10
1000	-0.40	-0.40	-0.40	-0.55	-0.40	-0.65	-0.90	-1.00	-0.95	-0.95

(d) October

10	-1.05	-1.05	-0.85	-0.50	-0.25	0.00	0.30	0.30	0.70	1.05
20	-1.20	-1.20	-1.00	-0.75	-0.55	-0.00	-0.15	-0.10	-0.05	0.18
30	-0.95	-0.95	-0.80	-0.65	-0.45	-0.25	-0.19	-0.06	-0.04	0.07
50	-0.70	-0.70	-0.60	-0.48	-0.32	-0.09	0.00	0.04	-0.02	0.06
70	-0.70	-0.70	-0.58	-0.45	-0.29	-0.04	0.13	0.18	0.12	0.16
100	-0.70	-0.70	-0.55	-0.40	-0.26	-0.07	0.09	0.20	0.23	0.24
150	-0.50	-0.50	-0.42	-0.32	-0.28	-0.17	-0.12	-0.05	-0.00	0.00
200	-0.45	-0.45	-0.44	-0.41	-0.40	-0.40	-0.38	-0.39	-0.45	-0.50
300	-1.10	-1.10	-1.00	-0.90	-0.90	-0.95	-0.98	-1.00	-1.10	-1.25
400	-1.65	-1.65	-1.53	-1.38	-1.38	-1.48	-1.48	-1.55	-1.54	-1.53
500	-1.90	-1.90	-1.75	-1.55	-1.55	-1.55	-1.46	-1.51	-1.50	-1.49
700	-2.10	-2.10	-2.00	-1.81	-1.83	-1.52	-1.43	-1.44	-1.44	-1.40
850	-1.50	-1.50	-1.50	-1.50	-1.40	-1.25	-1.30	-1.35	-1.30	-1.30
1000	-0.70	-0.70	-0.70	-0.70	-0.70	-0.65	-0.95	-1.00	-1.00	-1.00

TABLE 3.2

VERTICAL DISTRIBUTION OF LATENT HEAT RELEASE (deg day⁻¹)

(a) December-February

<u>P(mb)</u>	<u>1000-900</u>		<u>900-800</u>		<u>800-700</u>		<u>700-600</u>		<u>600-500</u>		<u>500-400</u>		<u>400-300</u>		<u>300-200</u>		<u>200-100</u>	
	<u>Lat.</u>	<u>%</u>	<u>LHR</u>	<u>%</u>	<u>LHR</u>	<u>%</u>	<u>LHR</u>	<u>%</u>	<u>LHR</u>	<u>%</u>	<u>LHR</u>	<u>%</u>	<u>LHR</u>	<u>%</u>	<u>LHR</u>	<u>%</u>	<u>LHR</u>	
80N	25	0.33	50	0.65	25	0.33	0	0.00	0	0.00	0	0.00	0	0.00	0	0.00	0	0.00
70N	10	0.19	50	0.95	30	0.57	10	0.19	0	0.00	0	0.00	0	0.00	0	0.00	0	0.00
60N	4	0.14	50	1.73	30	1.04	11	0.38	5	0.17	0	0.00	0	0.00	0	0.00	0	0.00
50N	0	0.00	33	1.68	33	1.68	20	1.02	10	0.51	4	0.20	0	0.00	0	0.00	0	0.00
40N	0	0.00	15	0.86	31	1.77	31	1.77	15	0.86	6	0.35	2	0.11	0	0.00	0	0.00
30N	0	0.00	10	0.48	26	1.25	34	1.64	20	0.97	7	0.34	3	0.15	0	0.00	0	0.00
20N	0	0.00	8	0.35	22	0.97	32	1.40	24	1.05	9	0.40	4	0.17	1	0.04	0	0.00
10N	0	0.00	6	0.58	14	1.36	22	2.13	23	2.22	19	1.83	12	1.16	4	0.39	0	0.00
0	0	0.00	6	0.91	11	1.66	15	2.26	18	2.71	19	2.86	18	2.71	12	1.81	1	0.15
10S	0	0.00	6	0.71	11	1.30	15	1.77	18	2.13	19	2.24	18	2.13	12	1.42	1	0.12
20S	0	0.00	7	0.57	15	1.23	21	1.72	24	1.97	18	1.48	11	0.90	4	0.33	0	0.00
30S	0	0.00	7	0.43	19	1.18	26	1.61	23	1.42	16	0.98	7	0.43	2	0.12	0	0.00
40S	0	0.00	8	0.54	22	1.49	29	1.95	21	1.42	13	0.87	6	0.41	1	0.07	0	0.00
50S	0	0.00	15	1.13	29	2.18	29	2.18	15	1.13	7	0.53	4	0.30	1	0.08	0	0.00
60S	0	0.00	25	1.71	37	2.52	24	1.64	10	0.68	3	0.21	1	0.07	0	0.00	0	0.00
70S	2	0.09	35	1.54	35	1.54	21	0.92	6	0.27	1	0.04	0	0.00	0	0.00	0	0.00
80S	4	0.06	42	0.61	36	0.53	17	0.25	1	0.02	0	0.00	0	0.00	0	0.00	0	0.00

TABLE 3.2

(continued)

(b) March-May

<u>P(mb)</u>	<u>1000-900</u>		<u>900-800</u>		<u>800-700</u>		<u>700-600</u>		<u>600-500</u>		<u>500-400</u>		<u>400-300</u>		<u>300-200</u>		<u>200-100</u>	
<u>Lat.</u>	<u>%</u>	<u>LHR</u>	<u>%</u>	<u>LHR</u>	<u>%</u>	<u>LHR</u>	<u>%</u>	<u>LHR</u>	<u>%</u>	<u>LHR</u>	<u>%</u>	<u>LHR</u>	<u>%</u>	<u>LHR</u>	<u>%</u>	<u>LHR</u>	<u>%</u>	<u>LHR</u>
80N	15	0.17	46	0.52	30	0.34	9	0.10	0	0.00	0	0.00	0	0.00	0	0.00	0	0.00
70N	6	0.10	43	0.74	32	0.55	16	0.28	3	0.05	0	0.00	0	0.00	0	0.00	0	0.00
60N	2	0.07	38	1.28	33	1.11	18	0.60	8	0.27	1	0.03	0	0.00	0	0.00	0	0.00
50N	0	0.00	24	1.24	31	1.61	25	1.30	13	0.67	5	0.26	2	0.10	0	0.00	0	0.00
40N	0	0.00	12	0.67	27	1.52	30	1.68	18	1.01	9	0.50	4	0.22	0	0.00	0	0.00
30N	0	0.00	8	0.37	22	1.01	30	1.38	22	1.01	12	0.55	5	0.23	1	0.04	0	0.00
20N	0	0.00	8	0.32	20	0.81	27	1.09	23	0.93	13	0.53	7	0.29	2	0.08	0	0.00
10N	0	0.00	6	0.52	13	1.12	19	1.64	22	1.90	19	1.64	14	1.21	7	0.60	0	0.00
0	0	0.00	6	0.86	11	1.58	15	2.16	18	2.59	19	2.73	18	2.59	12	1.73	1	0.15
10S	0	0.00	6	0.65	13	1.40	19	2.05	22	2.38	19	2.05	14	1.51	7	0.75	0	0.00
20S	0	0.00	8	0.52	20	1.30	27	1.76	23	1.49	13	0.85	7	0.46	2	0.13	0	0.00
30S	0	0.00	8	0.48	22	1.33	30	1.82	22	1.33	12	0.73	5	0.30	1	0.06	0	0.00
40S	0	0.00	12	0.81	27	1.82	30	2.02	18	1.21	9	0.60	4	0.27	0	0.00	0	0.00
50S	0	0.00	24	1.81	31	2.33	25	1.88	13	0.98	5	0.38	2	0.15	0	0.00	0	0.00
60S	2	0.14	38	2.66	33	2.31	18	1.26	8	0.56	1	0.07	0	0.00	0	0.00	0	0.00
70S	6	0.28	43	1.97	32	1.47	16	0.73	3	0.14	0	0.00	0	0.00	0	0.00	0	0.00
80S	15	0.22	46	0.67	30	0.44	9	0.13	0	0.00	0	0.00	0	0.00	0	0.00	0	0.00

TABLE 3.2

(continued)

(c) June-August

<u>P(mb)</u>	<u>1000-900</u>		<u>900-800</u>		<u>800-700</u>		<u>700-600</u>		<u>600-500</u>		<u>500-400</u>		<u>400-300</u>		<u>300-200</u>		<u>200-100</u>	
	<u>Lat.</u>	<u>%</u>	<u>LHR</u>	<u>%</u>	<u>LHR</u>	<u>%</u>	<u>LHR</u>	<u>%</u>	<u>LHR</u>	<u>%</u>	<u>LHR</u>	<u>%</u>	<u>LHR</u>	<u>%</u>	<u>LHR</u>	<u>%</u>	<u>LHR</u>	
80N	4	0.05	42	0.54	36	0.47	17	0.22	1	0.02	0	0.00	0	0.00	0	0.00	0	0.00
70N	2	0.05	35	0.97	35	0.97	21	0.58	6	0.16	1	0.03	0	0.00	0	0.00	0	0.00
60N	0	0.00	25	1.23	37	1.82	24	1.18	10	0.49	3	0.15	1	0.05	0	0.00	0	0.00
50N	0	0.00	15	0.85	29	1.62	29	1.62	15	0.85	7	0.40	4	0.22	1	0.05	0	0.00
40N	0	0.00	8	0.41	22	1.11	29	1.47	21	1.06	13	0.66	6	0.30	1	0.05	0	0.00
30N	0	0.00	7	0.36	19	0.98	26	1.34	23	1.19	16	0.83	7	0.36	2	0.10	0	0.00
20N	0	0.00	7	0.57	15	1.23	21	1.72	24	1.97	18	1.48	11	0.90	4	0.33	0	0.00
10N	0	0.00	6	0.77	11	1.41	15	1.92	18	2.31	19	2.44	18	2.31	12	1.54	1	0.13
0	0	0.00	6	0.80	11	1.47	15	2.00	18	2.40	19	2.54	18	2.40	12	1.61	1	0.13
10S	0	0.00	6	0.54	14	1.26	22	1.98	23	2.06	19	1.71	12	1.08	4	0.36	0	0.00
20S	0	0.00	8	0.43	22	1.18	32	1.73	24	1.30	9	0.48	4	0.22	1	0.05	0	0.00
30S	0	0.00	10	0.60	26	1.55	34	2.02	20	1.19	7	0.41	3	0.18	0	0.00	0	0.00
40S	0	0.00	15	1.01	31	2.09	31	2.09	15	1.01	6	0.41	2	0.14	0	0.00	0	0.00
50S	0	0.00	33	2.19	33	2.19	20	1.33	10	0.67	4	0.27	0	0.00	0	0.00	0	0.00
60S	4	0.22	50	2.81	30	1.68	11	0.62	5	0.28	0	0.00	0	0.00	0	0.00	0	0.00
70S	10	0.35	50	1.73	30	1.04	10	0.35	0	0.00	0	0.00	0	0.00	0	0.00	0	0.00
80S	25	0.36	50	0.73	25	0.36	0	0.00	0	0.00	0	0.00	0	0.00	0	0.00	0	0.00

TABLE 3.2

(continued)

(d) September-November

<u>P(mb)</u>	<u>1000-900</u>		<u>900-800</u>		<u>800-700</u>		<u>700-600</u>		<u>600-500</u>		<u>500-400</u>		<u>400-300</u>		<u>300-200</u>		<u>200-100</u>	
	<u>Lat.</u>	<u>%</u>	<u>LHR</u>	<u>%</u>	<u>LHR</u>	<u>%</u>	<u>LHR</u>	<u>%</u>	<u>LHR</u>	<u>%</u>	<u>LHR</u>	<u>%</u>	<u>LHR</u>	<u>%</u>	<u>LHR</u>	<u>%</u>	<u>LHR</u>	
80N	15	0.09	46	0.52	30	0.34	9	0.10	0	0.00	0	0.00	0	0.00	0	0.00	0	0.00
70N	6	0.15	43	1.08	32	0.80	16	0.40	3	0.08	0	0.00	0	0.00	0	0.00	0	0.00
60N	2	0.10	38	1.81	33	1.57	18	0.86	8	0.38	1	0.05	0	0.00	0	0.00	0	0.00
50N	0	0.00	24	1.35	31	1.75	25	1.40	13	0.73	5	0.28	2	0.11	0	0.00	0	0.00
40N	0	0.00	12	0.67	27	1.49	30	1.66	18	0.99	9	0.50	4	0.22	0	0.00	0	0.00
30N	0	0.00	8	0.40	22	1.09	30	1.49	22	1.09	12	0.60	5	0.25	1	0.05	0	0.00
20N	0	0.00	8	0.47	20	1.17	27	1.58	23	1.34	13	0.76	7	0.41	2	0.12	0	0.00
10N	0	0.00	6	0.67	13	1.46	19	2.13	22	2.47	19	2.13	14	1.57	7	0.79	0	0.00
0	0	0.00	6	0.78	11	1.42	15	1.94	18	2.32	19	2.45	18	2.32	12	1.55	1	0.13
10S	0	0.00	6	0.50	13	1.10	19	1.60	22	1.85	19	1.60	14	1.18	7	0.59	0	0.00
20S	0	0.00	8	0.41	20	1.03	27	1.39	23	1.18	13	0.67	7	0.36	2	0.10	0	0.00
30S	0	0.00	8	0.47	22	1.29	30	1.75	22	1.29	12	0.70	5	0.29	1	0.06	0	0.00
40S	0	0.00	12	0.81	27	1.82	30	2.02	18	1.21	9	0.60	4	0.27	0	0.00	0	0.00
50S	0	0.00	24	1.54	31	1.98	25	1.60	13	0.83	5	0.32	2	0.13	0	0.00	0	0.00
60S	2	0.10	38	1.97	33	1.71	18	0.93	8	0.41	1	0.05	0	0.00	0	0.00	0	0.00
70S	6	0.20	43	1.41	32	1.05	16	0.53	3	0.10	0	0.00	0	0.00	0	0.00	0	0.00
80S	15	0.22	46	0.67	30	0.44	9	0.13	0	0.00	0	0.00	0	0.00	0	0.00	0	0.00

TABLE 3.3
LATENT HEAT RELEASE (deg day⁻¹)

<u>P(mb)</u>	<u>(a) December-February</u>							<u>(b) March-May</u>						
	<u>850</u>	<u>700</u>	<u>500</u>	<u>400</u>	<u>300</u>	<u>200</u>	<u>150</u>	<u>850</u>	<u>700</u>	<u>500</u>	<u>400</u>	<u>300</u>	<u>200</u>	<u>150</u>
<u>Lat.</u>														
90N	0.33	0.02	0.00	0.00	0.00	0.00	0.00	0.22	0.10	0.00	0.00	0.00	0.00	0.00
80N	0.65	0.16	0.00	0.00	0.00	0.00	0.00	0.52	0.22	0.00	0.00	0.00	0.00	0.00
70N	0.95	0.33	0.00	0.00	0.00	0.00	0.00	0.74	0.41	0.02	0.00	0.00	0.00	0.00
60N	1.64	0.75	0.10	0.00	0.00	0.00	0.00	0.17	0.83	0.16	0.02	0.00	0.00	0.00
50N	1.60	1.42	0.35	0.12	0.00	0.00	0.00	1.21	1.47	0.43	0.17	0.04	0.00	0.00
40N	0.86	1.81	0.60	0.20	0.04	0.00	0.00	0.69	1.62	0.73	0.35	0.12	0.00	0.00
30N	0.48	1.45	0.67	0.22	0.05	0.00	0.00	0.43	1.25	0.76	0.39	0.15	0.00	0.00
20N	0.35	1.17	0.78	0.29	0.11	0.02	0.00	0.32	0.93	0.73	0.40	0.18	0.03	0.00
10N	0.58	1.73	1.99	1.47	0.82	0.17	0.02	0.52	1.43	1.81	1.47	0.91	0.26	0.04
0	0.91	1.99	2.81	2.81	2.25	0.86	0.15	0.87	1.86	2.72	2.64	2.20	0.86	0.15
10S	0.71	1.56	2.20	2.20	1.73	0.60	0.12	0.65	1.73	2.16	1.73	1.12	0.39	0.07
20S	0.56	1.47	1.73	1.19	0.60	0.18	0.00	0.60	1.56	1.14	0.65	0.30	0.05	0.00
30S	0.43	1.47	1.20	0.76	0.32	0.03	0.00	0.52	1.57	1.10	0.56	0.22	0.01	0.00
40S	0.56	1.73	1.12	0.59	0.22	0.00	0.00	0.82	1.92	0.95	0.41	0.12	0.00	0.00
50S	1.12	2.33	0.82	0.40	0.16	0.00	0.00	1.86	1.34	0.67	0.26	0.04	0.00	0.00
60S	1.73	2.16	0.48	0.14	0.03	0.00	0.00	2.59	1.86	0.35	0.02	0.00	0.00	0.00
70S	1.51	1.34	0.15	0.02	0.00	0.00	0.00	1.86	1.17	0.04	0.00	0.00	0.00	0.00
80S	0.62	0.39	0.01	0.00	0.00	0.00	0.00	0.71	0.32	0.00	0.00	0.00	0.00	0.00
90S	0.13	0.09	0.00	0.00	0.00	0.00	0.00	0.19	0.03	0.00	0.00	0.00	0.00	0.00

TABLE 3.3

(continued)

<u>P(mb)</u>	<u>(c) June-August</u>							<u>(d) September-November</u>						
	<u>850</u>	<u>700</u>	<u>500</u>	<u>400</u>	<u>300</u>	<u>200</u>	<u>150</u>	<u>850</u>	<u>700</u>	<u>500</u>	<u>400</u>	<u>300</u>	<u>200</u>	<u>150</u>
<u>Lat.</u>														
90N	0.11	0.11	0.00	0.00	0.00	0.00	0.00	0.19	0.08	0.00	0.00	0.00	0.00	0.00
80N	0.54	0.36	0.00	0.00	0.00	0.00	0.00	0.52	0.22	0.00	0.00	0.00	0.00	0.00
70N	0.97	0.86	0.09	0.00	0.00	0.00	0.00	1.08	0.56	0.02	0.00	0.00	0.00	0.00
60N	1.21	1.51	0.29	0.10	0.02	0.00	0.00	1.81	1.23	0.19	0.02	0.00	0.00	0.00
50N	0.86	1.64	0.60	0.31	0.15	0.00	0.00	1.35	1.64	0.47	0.19	0.03	0.00	0.00
40N	0.41	1.30	0.86	0.47	0.19	0.01	0.00	0.67	1.56	0.73	0.35	0.09	0.00	0.00
30N	0.36	1.17	1.04	0.62	0.28	0.03	0.00	0.40	1.30	0.82	0.43	0.14	0.00	0.00
20N	0.57	1.43	1.73	1.17	0.56	0.16	0.01	0.47	1.38	1.04	0.60	0.28	0.06	0.00
10N	0.77	1.77	2.42	2.38	1.90	0.78	0.13	0.67	1.81	2.29	1.88	1.30	0.35	0.06
0	0.80	1.81	2.51	2.42	1.94	0.86	0.13	0.78	1.73	2.40	2.35	1.90	0.86	0.13
10S	0.54	1.51	1.88	1.38	0.73	0.19	0.02	0.50	1.34	1.73	1.43	0.86	0.26	0.03
20S	0.43	1.43	0.86	0.35	0.10	0.02	0.00	0.41	1.21	0.99	0.52	0.22	0.02	0.00
30S	0.65	1.86	0.76	0.33	0.09	0.00	0.00	0.47	1.56	1.04	0.52	0.17	0.00	0.00
40S	1.04	2.11	0.69	0.29	0.05	0.00	0.00	0.81	1.99	0.98	0.43	0.13	0.00	0.00
50S	2.16	1.86	0.46	0.13	0.00	0.00	0.00	1.54	1.86	0.59	0.21	0.03	0.00	0.00
60S	2.76	1.25	0.15	0.00	0.00	0.00	0.00	1.90	1.34	0.24	0.02	0.00	0.00	0.00
70S	1.68	0.67	0.00	0.00	0.00	0.00	0.00	1.41	0.73	0.03	0.00	0.00	0.00	0.00
80S	0.73	0.19	0.00	0.00	0.00	0.00	0.00	0.67	0.29	0.00	0.00	0.00	0.00	0.00
90S	0.29	0.00	0.00	0.00	0.00	0.00	0.00	0.24	0.04	0.00	0.00	0.00	0.00	0.00

TABLE 3.4
BOUNDARY LAYER HEATING (deg day⁻¹)

(a) January

P(mb)	1000-950		950-900		900-850		850-800		800-750		750-700	
	Lat.	%	BLH	%	BLH	%	BLH	%	BLH	%	BLH	%
60N	67	0.66	33	0.32	--	----	--	----	--	----	--	----
50N	67	1.70	33	0.84	--	----	--	----	--	----	--	----
40N	49	2.05	36	1.51	15	0.63	--	----	--	----	--	----
30N	49	2.37	36	1.74	15	0.73	--	----	--	----	--	----
20N	38	1.74	31	1.42	22	1.01	9	0.41	--	----	--	----
10N	31	1.22	27	1.06	22	0.87	15	0.59	5	0.20	--	----
0	26	0.72	24	0.67	20	0.56	16	0.45	11	0.31	3	0.08
10S	26	0.60	24	0.55	20	0.46	16	0.37	11	0.25	3	0.07
20S	26	0.87	24	0.81	20	0.67	16	0.54	11	0.37	3	0.10
30S	31	1.27	27	1.11	22	0.90	15	0.62	5	0.21	--	----
40S	38	0.09	31	0.08	22	0.05	9	0.02	--	----	--	----
50S	49	-0.84	36	-0.62	15	-0.26	--	----	--	----	--	----
60S	49	0.08	36	0.06	15	0.02	--	----	--	----	--	----

(b) April

60N	67	0.71	33	0.35	--	----	--	----	--	----	--	----
50N	49	1.21	36	0.89	15	0.37	--	----	--	----	--	----
40N	49	1.57	36	1.15	15	0.48	--	----	--	----	--	----
30N	38	1.96	31	1.60	22	1.14	9	0.46	--	----	--	----
20N	31	1.60	27	1.39	22	1.14	15	0.77	5	0.26	--	----
10N	26	0.94	24	0.87	20	0.72	16	0.58	11	0.40	3	0.11
0	26	0.62	24	0.57	20	0.48	16	0.38	11	0.26	3	0.07
10S	26	0.55	24	0.51	20	0.43	16	0.34	11	0.23	3	0.06
20S	31	0.94	27	0.82	22	0.67	15	0.46	5	0.15	--	----
30S	38	1.31	31	1.07	22	0.76	9	0.31	--	----	--	----
40S	49	1.53	36	1.12	15	0.47	--	----	--	----	--	----
50S	49	1.53	36	1.12	15	0.47	--	----	--	----	--	----
60S	67	2.42	33	1.19	--	----	--	----	--	----	--	----

TABLE 3.4

(continued)

(c) July

<u>P(mb)</u>	<u>1000-950</u>		<u>950-900</u>		<u>900-850</u>		<u>850-800</u>		<u>800-750</u>		<u>750-700</u>	
	<u>Lat.</u>	<u>%</u>	<u>BLH</u>	<u>%</u>	<u>BLH</u>	<u>%</u>	<u>BLH</u>	<u>%</u>	<u>BLH</u>	<u>%</u>	<u>BLH</u>	<u>%</u>
60N	49	1.00	36	0.74	15	0.31	--	----	--	----	--	----
50N	49	1.85	36	1.36	15	0.57	--	----	--	----	--	----
40N	38	1.96	31	1.60	22	1.14	9	0.46	--	----	--	----
30N	31	1.80	27	1.57	22	1.28	15	0.87	5	0.29	--	----
20N	26	0.87	24	0.81	20	0.67	16	0.54	11	0.37	3	0.10
10N	26	0.47	24	0.43	20	0.36	16	0.29	11	0.20	3	0.05
0	26	0.55	24	0.51	20	0.43	16	0.34	11	0.23	3	0.06
10S	31	0.92	27	0.80	22	0.65	15	0.44	5	0.15	--	----
20S	38	1.34	31	1.09	22	0.78	9	0.32	--	----	--	----
30S	49	1.93	36	1.42	15	0.59	--	----	--	----	--	----
40S	49	2.09	36	1.54	15	0.64	--	----	--	----	--	----
50S	67	2.80	33	1.38	--	----	--	----	--	----	--	----
60S	67	2.80	33	1.38	--	----	--	----	--	----	--	----

(d) October

60N	67	1.26	33	0.62	--	----	--	----	--	----	--	----
50N	49	1.25	36	0.92	15	0.38	--	----	--	----	--	----
40N	49	1.77	36	1.30	15	0.54	--	----	--	----	--	----
30N	38	1.84	31	1.50	22	1.06	9	0.44	--	----	--	----
20N	31	1.30	27	1.13	22	0.92	15	0.63	5	0.21	--	----
10N	26	0.70	24	0.65	20	0.54	16	0.43	11	0.30	3	0.08
0	26	0.64	24	0.59	20	0.49	16	0.39	11	0.27	3	0.07
10S	26	0.77	24	0.71	20	0.59	16	0.47	11	0.32	3	0.09
20S	31	1.12	27	0.97	22	0.79	15	0.54	5	0.18	--	----
30S	38	1.22	31	0.99	22	0.70	9	0.29	--	----	--	----
40S	49	1.00	36	0.74	15	0.31	--	----	--	----	--	----
50S	49	0.68	36	0.50	15	0.21	--	----	--	----	--	----
60S	67	0.82	33	0.41	--	----	--	----	--	----	--	----

TABLE 3.5
BOUNDARY LAYER HEATING (deg day⁻¹)

<u>P(mb)</u>	<u>January</u>		<u>April</u>		<u>July</u>		<u>October</u>	
	<u>1000</u>	<u>850</u>	<u>1000</u>	<u>850</u>	<u>1000</u>	<u>850</u>	<u>1000</u>	<u>850</u>
<u>Lat.</u>								
90N	0.00	0.00	0.00	0.00	0.00	0.00	0.00	0.00
80N	0.00	0.00	0.00	0.00	0.00	0.00	0.00	0.00
70N	-0.25	0.00	-0.25	0.00	0.25	0.00	0.30	0.00
60N	0.75	0.00	0.75	0.00	1.00	0.05	1.10	0.00
50N	1.70	0.00	1.25	0.05	1.90	0.25	1.30	0.05
40N	2.15	0.20	1.60	0.25	2.00	0.75	1.75	0.30
30N	2.45	0.45	2.00	0.70	1.75	1.05	1.85	0.70
20N	1.95	0.70	1.60	0.90	0.88	0.65	1.35	0.80
10N	1.25	0.75	0.96	0.67	0.55	0.33	0.75	0.50
0	0.75	0.55	0.62	0.44	0.65	0.39	0.67	0.45
10S	0.62	0.40	0.56	0.40	0.95	0.55	0.80	0.55
20S	0.90	0.60	0.95	0.57	1.40	0.55	1.15	0.65
30S	1.35	0.72	1.35	0.54	1.90	0.30	1.25	0.50
40S	0.12	0.04	1.55	0.22	2.15	0.15	1.10	0.25
50S	-0.90	-0.12	1.65	0.05	2.80	0.00	0.85	0.05
60S	0.10	0.00	2.40	0.00	2.80	0.00	0.95	0.00
70S	0.30	0.00	1.50	0.00	2.00	0.00	1.00	0.00
80S	0.30	0.00	1.00	0.00	1.40	0.00	0.70	0.00
90S	0.40	0.00	0.70	0.00	0.90	0.00	0.50	0.00

TABLE 4.1
ZONAL MEAN TEMPERATURES (°C)
(a) December-February

<u>P(mb)</u>	<u>1000</u>	<u>850</u>	<u>700</u>	<u>500</u>	<u>400</u>	<u>300</u>	<u>200</u>	<u>150</u>	<u>100</u>	<u>70</u>	<u>50</u>	<u>30</u>	<u>20</u>	<u>10</u>
<u>Lat.</u>														
90N	-39.0	-24.0	-28.0	-41.0	-51.0	-61.0	-61.0	-65.0	-69.0	-72.0	-74.0	-74.0	-72.0	-69.0
80N	-33.6	-21.0	-26.3	-39.4	-48.5	-58.9	-59.4	-61.4	-63.7	-67.2	-69.3	-69.4	-67.8	-65.0
70N	-26.4	-18.0	-24.2	-37.7	-46.5	-57.2	-58.2	-58.1	-59.0	-62.2	-64.1	-64.5	-63.0	-60.7
60N	-16.2	-13.0	-19.9	-34.1	-43.0	-54.4	-56.0	-54.5	-54.8	-57.4	-58.7	-59.3	-57.8	-55.1
50N	- 6.6	- 7.9	-15.3	-29.2	-39.0	-51.3	-55.1	-52.8	-53.4	-55.5	-56.3	-56.1	-54.2	-50.7
40N	7.2	- 0.2	- 7.1	-22.9	-33.5	-46.8	-56.1	-56.1	-58.8	-58.2	-58.7	-56.3	-53.8	-49.3
30N	14.7	7.7	0.8	-14.9	-26.3	-40.0	-55.1	-60.9	-67.5	-66.0	-61.6	-55.8	-52.2	-45.7
20N	20.8	14.7	7.1	- 7.9	-19.4	-34.4	-53.9	-64.9	-74.5	-72.6	-64.3	-55.3	-50.5	-43.1
10N	24.4	17.1	9.3	- 5.8	-16.9	-32.2	-53.6	-66.6	-78.7	-74.6	-66.6	-57.4	-51.6	-43.2
0	25.9	17.6	9.4	- 5.6	-16.1	-31.6	-53.7	-67.4	-80.5	-73.9	-68.1	-56.8	-50.4	-43.5
10S	25.4	17.4	9.5	- 5.6	-16.0	-31.2	-53.6	-67.1	-80.2	-73.5	-66.4	-58.6	-51.4	-43.5
20S	23.0	17.5	9.4	- 6.0	-16.7	-32.0	-53.3	-65.6	-76.7	-71.2	-64.8	-54.8	-51.4	-43.0
30S	20.3	15.1	7.0	- 9.3	-20.6	-35.9	-53.7	-62.0	-68.9	-66.1	-60.9	-53.4	-48.4	-42.0
40S	16.0	9.0	1.0	-14.9	-26.5	-41.2	-54.4	-56.6	-58.2					
50S	7.8	1.5	- 6.1	-21.3	-31.4	-44.5	-49.0	-49.1	-49.1					
60S	- 1.3	- 6.6	-12.2	-27.0	-37.0	-49.5	-49.2	-48.0	-46.2					
70S	- 6.6	-11.8	-17.9	-31.9	-41.3	-52.8	-45.8	-44.3	-42.7					
80S	-10.5	-13.9	-21.8	-35.5	-45.0	-55.2	-43.4	-42.5	-41.4					
90S	-15.0	-16.0	-25.0	-38.0	-48.0	-55.5	-41.0	-41.0	-40.5					

TABLE 4.1
 (continued)
 (b) March-May

<u>P(mb)</u>	<u>1000</u>	<u>850</u>	<u>700</u>	<u>500</u>	<u>400</u>	<u>300</u>	<u>200</u>	<u>150</u>	<u>100</u>	<u>70</u>	<u>50</u>	<u>30</u>	<u>20</u>	<u>10</u>
<u>Lat.</u>														
90N	-23.5	-20.5	-27.0	-40.0	-47.0	-55.0	-46.5	-47.0	-48.5	-48.5	-48.5	-47.0	-44.0	-39.0
80N	-16.7	-17.0	-23.5	-37.1	-44.3	-53.4	-47.6	-46.8	-46.7	-48.7	-48.8	-47.8	-45.1	-40.4
70N	- 9.9	-12.5	-19.6	-33.8	-42.0	-52.1	-48.6	-47.0	-46.7	-48.9	-49.0	-48.5	-46.2	-41.4
60N	- 1.2	- 6.5	-14.4	-29.0	-38.0	-50.3	-50.2	-48.4	-49.1	-50.6	-50.7	-49.9	-47.0	-42.1
50N	6.1	- 1.0	- 9.3	-24.5	-35.0	-47.9	-53.0	-51.2	-51.9	-52.7	-53.1	-51.5	-48.0	-42.3
40N	13.0	5.7	- 2.4	-18.2	-30.0	-44.3	-56.6	-56.3	-58.1	-58.8	-56.6	-53.2	-50.6	-45.0
30N	18.0	12.2	6.5	-12.2	-24.0	-38.8	-55.6	-60.9	-66.4	-65.7	-59.3	-53.4	-49.1	-41.0
20N	23.4	17.5	9.1	- 7.4	-18.7	-33.7	-53.4	-64.6	-73.5	-72.2	-62.9	-53.4	-48.6	-38.8
10N	25.7	18.5	9.4	- 5.7	-16.1	-31.4	-52.9	-66.2	-78.0	-73.9	-65.6	-55.3	-48.6	-38.8
0	26.0	18.1	9.1	- 5.5	-15.6	-31.0	-53.3	-67.3	-80.7	-74.4	-66.8	-54.9	-48.7	-39.6
10S	25.1	17.5	9.0	- 5.4	-15.9	-31.1	-53.2	-66.8	-79.7	-72.7	-65.7	-54.8	-48.8	-40.0
20S	21.8	15.9	7.7	- 6.6	-17.7	-33.3	-53.6	-65.0	-75.3	-70.1	-63.2	-53.8	-49.0	-41.0
30S	17.4	11.2	4.8	-11.9	-22.6	-38.0	-55.1	-61.3	-68.1	-65.4	-60.0	-53.4	-49.5	-42.0
40S	13.3	6.9	- 1.1	-18.2	-29.0	-42.9	-56.7	-57.9	-59.2					
50S	5.4	- 0.3	- 7.5	-24.0	-34.3	-47.8	-53.9	-53.4	-53.8					
60S	- 3.0	- 9.1	-12.4	-27.3	-36.8	-48.6	-51.9	-51.3	-50.7					
70S	- 9.5	-15.3	-19.1	-32.6	-41.8	-52.4	-52.5	-51.7	-50.9					
80S	-14.2	-20.3	-23.6	-38.0	-46.6	-55.1	-54.0	-53.8	-53.3					
90S	-20.0	-24.0	-28.0	-42.5	-51.5	-57.1	-56.0	-56.0	-55.0					

TABLE 4.1
 (continued)
 (c) June-August

<u>P(mb)</u>	<u>1000</u>	<u>850</u>	<u>700</u>	<u>500</u>	<u>400</u>	<u>300</u>	<u>200</u>	<u>150</u>	<u>100</u>	<u>70</u>	<u>50</u>	<u>30</u>	<u>20</u>	<u>10</u>
<u>Lat.</u>														
90N	- 7.0	- 3.0	- 9.5	-23.0	-33.0	-46.0	-42.0	-41.0	-41.0	-40.5	-40.5	-40.5	-37.5	-32.0
80N	0.2	0.5	- 7.0	-21.4	-31.5	-45.1	-43.9	-41.8	-41.7	-42.6	-42.4	-42.4	-38.9	-33.1
70N	6.6	3.5	- 4.3	-19.3	-30.0	-43.4	-46.5	-43.6	-43.7	-44.6	-44.5	-44.0	-40.2	-34.0
60N	13.9	7.0	- 1.4	-16.4	-27.0	-41.6	-48.9	-46.5	-46.3	-47.6	-47.5	-46.2	-42.0	-34.9
50N	18.7	11.0	2.3	-12.5	-24.0	-38.6	-50.7	-50.5	-50.3	-51.8	-51.3	-48.4	-43.8	-35.9
40N	21.0	16.1	7.3	- 8.9	-21.1	-34.4	-51.6	-57.8	-60.8	-60.2	-54.5	-49.5	-45.3	-39.2
30N	23.9	18.8	10.0	- 6.3	-17.1	-31.8	-51.8	-62.5	-68.4	-64.8	-57.6	-50.8	-46.2	-39.8
20N	26.1	19.5	10.6	- 5.9	-16.2	-31.3	-52.2	-65.2	-72.7	-67.1	-59.9	-51.9	-47.6	-40.0
10N	26.2	18.1	9.7	- 6.0	-16.4	-31.6	-53.5	-66.9	-75.9	-68.4	-61.8	-53.7	-48.6	-41.8
0	24.8	16.6	9.0	- 6.0	-16.5	-32.0	-54.0	-67.5	-77.1	-68.4	-62.9	-55.0	-50.7	-43.5
10S	22.6	15.4	8.6	- 6.1	-16.9	-32.6	-54.4	-67.4	-76.8	-68.6	-62.4	-55.0	-51.3	-43.5
20S	18.7	12.9	6.6	- 7.9	-19.2	-34.9	-54.0	-64.7	-72.8	-66.3	-60.8	-54.6	-50.8	-43.5
30S	14.9	7.9	0.3	-15.3	-26.7	-41.0	-53.1	-59.2	-63.3	-61.8	-59.0	-54.8	-52.0	-45.8
40S	10.6	2.9	- 6.0	-23.5	-35.8	-48.6	-53.8	-54.6	-55.8					
50S	3.0	- 3.9	-12.2	-28.0	-39.2	-53.1	-57.8	-56.0	-57.7					
60S	- 4.6	-10.0	-16.7	-32.6	-43.0	-55.8	-63.1	-63.0	-63.1					
70S	-11.2	-17.0	-23.5	-37.5	-47.0	-59.3	-68.4	-69.2	-70.3					
80S	-17.4	-23.0	-29.9	-42.1	-51.0	-62.3	-72.7	-74.0	-75.9					
90S	-22.0	-28.0	-35.0	-45.0	-54.5	-65.0	-75.0	-77.0	-79.0					

TABLE 4.1

(continued)

(d) September–November

<u>P(mb)</u>	<u>1000</u>	<u>850</u>	<u>700</u>	<u>500</u>	<u>400</u>	<u>300</u>	<u>200</u>	<u>150</u>	<u>100</u>	<u>70</u>	<u>50</u>	<u>30</u>	<u>20</u>	<u>10</u>
<u>Lat.</u>														
90N	-25.0	-18.0	-23.5	-37.0	-44.5	-54.5	-51.0	-50.5	-53.0	-56.0	-58.2	-62.0	-61.0	-59.5
80N	-16.7	-13.0	-19.7	-33.5	-42.1	-53.0	-51.0	-50.4	-52.1	-55.0	-57.2	-60.0	-57.8	-56.4
70N	- 9.9	- 8.0	-15.8	-29.7	-39.0	-51.1	-51.2	-50.3	-51.3	-54.2	-56.0	-57.8	-53.6	-53.2
60N	- 1.2	- 3.5	-11.0	-25.6	-35.5	-48.5	-52.2	-51.5	-52.0	-54.2	-55.4	-55.9	-56.2	-49.7
50N	6.1	2.0	- 6.2	-21.1	-31.5	-45.0	-53.3	-54.3	-54.7	-55.9	-56.0	-54.8	-58.6	-46.9
40N	16.0	8.8	1.4	-14.5	-25.6	-40.1	-54.8	-59.2	-61.9	-60.6	-58.1	-54.4	-51.1	-46.8
30N	20.9	14.4	4.2	- 9.1	-20.5	-35.2	-54.0	-63.3	-69.2	-65.3	-59.5	-53.4	-49.3	-43.6
20N	25.2	17.9	8.7	- 6.6	-17.5	-32.6	-53.7	-66.0	-74.1	-69.1	-61.1	-53.0	-48.1	-41.5
10N	25.7	18.1	10.0	- 6.0	-16.6	-31.8	-53.7	-67.3	-76.8	-70.3	-63.0	-55.0	-49.3	-41.5
0	25.3	17.1	9.6	- 5.9	-16.2	-31.6	-53.9	-67.9	-78.5	-69.9	-64.4	-56.0	-50.5	-41.5
10S	23.7	16.5	9.6	- 6.2	-16.6	-32.2	-54.2	-67.3	-77.2	-69.1	-62.5	-54.0	-50.0	-41.5
20S	20.1	15.0	7.9	- 8.0	-18.5	-34.4	-54.1	-64.9	-72.6	-67.4	-61.3	-54.4	-49.5	-42.5
30S	16.8	10.1	2.5	-13.2	-24.9	-39.2	-53.6	-59.3	-63.8	-62.0	-58.3	-52.0	-49.5	-42.5
40S	13.3	6.0	- 3.7	-18.8	-30.0	-44.3	-52.8	-53.5	-55.0					
50S	5.4	- 1.9	-11.2	-25.7	-36.4	-49.9	-53.7	-52.5	-51.5					
60S	- 3.0	- 9.4	-17.3	-32.3	-42.5	-55.8	-61.2	-61.0	-60.7					
70S	- 9.9	-16.0	-23.8	-37.3	-47.4	-60.4	-67.1	-67.8	-68.6					
80S	-17.0	-22.6	-29.4	-41.9	-51.2	-63.6	-70.5	-72.1	-74.2					
90S	-23.0	-28.0	-34.0	-45.5	-54.0	-66.0	-73.0	-75.0	-77.0					

TABLE 4.2
 MEAN ZONAL WIND (m sec⁻¹)
 (a) December-February

<u>P(mb)</u>	<u>1000</u>	<u>850</u>	<u>700</u>	<u>500</u>	<u>400</u>	<u>300</u>	<u>200</u>	<u>150</u>	<u>100</u>	<u>70</u>	<u>50</u>	<u>30</u>	<u>20</u>	<u>10</u>
<u>Lat.</u>														
90N	0.0	0.0	0.0	0.0	0.0	0.0	0.0	0.0	0.0	0.0	0.0	0.0	0.0	0.0
80N	- 0.1	- 0.2	1.1	1.6	2.3	3.4	3.2	4.2	6.6	10.0	13.5	17.9	21.0	24.7
70N	0.4	0.7	2.0	3.6	4.7	5.8	6.8	7.5	8.8	18.4	22.0	27.5	31.0	37.8
60N	0.7	3.0	5.0	7.5	8.7	10.5	11.3	11.6	11.0	19.5	21.7	26.0	29.5	35.7
50N	1.4	5.5	8.6	12.6	14.8	17.1	18.8	17.9	14.9	17.7	17.1	17.8	21.0	24.9
40N	1.8	5.9	10.1	16.0	19.8	25.2	28.7	28.7	21.0	15.6	10.5	8.0	9.0	13.5
30N	0.3	4.2	8.3	17.7	23.9	31.5	38.6	35.5	25.1	13.0	7.3	3.2	5.0	8.1
20N	- 2.4	- 1.6	2.8	8.7	14.3	19.9	25.9	22.6	13.8	6.4	0.2	- 3.0	- 2.5	- 1.9
10N	- 2.9	- 5.4	- 3.4	- 3.1	0.2	3.0	7.8	6.8	2.1	2.4	- 1.3	- 6.2	- 8.4	-10.7
0	- 1.7	- 2.1	- 3.1	- 3.3	- 2.1	- 1.3	- 1.4	- 0.1	- 1.0	0.4	- 1.5	- 7.9	-10.6	-15.0
10S	- 1.1	- 0.9	- 0.8	- 1.1	- 0.9	- 0.4	- 1.4	- 0.7	- 2.6	- 5.5	- 9.9	-16.2	-19.2	-20.0
20S	- 1.2	- 2.0	- 0.4	2.2	3.2	7.5	9.8	9.7	2.9	- 4.8	-10.3	-16.9	-20.4	-23.0
30S	- 0.3	0.5	4.5	9.0	12.0	16.0	21.0	20.7	10.0	0.0	- 6.5	-11.1	-12.8	-19.5
40S	1.5	6.3	9.5	14.5	17.5	21.0	22.4	21.0	14.5	6.0	0.8	- 4.6	- 8.0	-16.0
50S	6.0	10.5	14.5	18.8	23.0	25.5	25.0	22.0	15.5	8.0	3.2	- 3.0	- 6.5	-12.5
60S	3.0	5.7	8.0	12.0	14.2	16.0	16.5	15.0	11.0	6.0	2.3	- 2.5	- 5.0	- 9.5
70S	- 2.0	- 2.0	0.0	3.0	4.5	7.5	8.0	7.0	5.0	3.5	1.2	- 2.0	- 3.5	- 5.5
80S	- 2.0	- 2.5	0.5	2.0	3.0	4.0	4.0	4.0	3.0	2.5	1.4	0.0	- 2.0	- 3.5
90S	0.0	0.0	0.0	0.0	0.0	0.0	0.0	0.0	0.0	0.0	0.0	0.0	0.0	0.0

TABLE 4.2
(continued)
(b) March-May

<u>P(mb)</u>	<u>1000</u>	<u>850</u>	<u>700</u>	<u>500</u>	<u>400</u>	<u>300</u>	<u>200</u>	<u>150</u>	<u>100</u>	<u>70</u>	<u>50</u>	<u>30</u>	<u>20</u>	<u>10</u>
<u>Lat.</u>														
90N	0.0	0.0	0.0	0.0	0.0	0.0	0.0	0.0	0.0	0.0	0.0	0.0	0.0	0.0
80N	- 0.7	0.3	1.4	2.5	3.2	3.8	4.0	3.7	3.2	4.0	4.9	4.3	4.5	6.9
70N	- 0.3	0.7	2.3	4.8	5.9	6.8	6.5	5.5	4.3	7.2	6.6	5.4	4.5	3.5
60N	0.0	2.2	3.6	6.2	7.5	8.9	9.1	7.8	5.5	7.2	5.9	3.9	3.0	2.0
50N	0.9	3.3	5.8	9.2	11.4	13.7	14.3	12.7	9.3	8.0	5.0	1.9	0.8	- 0.2
40N	1.7	4.3	8.0	14.1	16.0	21.1	23.6	23.0	16.6	9.1	3.5	0.6	2.0	8.0
30N	- 0.3	2.6	6.5	13.2	16.9	22.6	30.0	28.8	18.6	8.5	2.0	- 1.8	- 0.5	8.3
20N	- 2.1	- 1.3	1.3	5.9	10.2	15.2	21.8	18.8	10.8	1.9	- 3.0	- 6.5	- 6.8	- 7.3
10N	- 2.1	- 4.1	- 4.3	- 2.4	- 0.2	3.0	7.5	5.2	1.9	- 0.2	- 4.8	- 9.5	-12.5	-15.0
0	- 1.6	- 2.8	- 3.7	- 4.1	- 3.6	- 2.6	- 1.2	0.8	- 0.1	- 0.1	- 6.0	-11.0	-13.5	-16.0
10S	- 1.6	- 2.6	- 1.8	- 1.5	- 0.6	0.5	2.5	3.6	0.8	- 2.6	- 6.5	-11.5	-13.5	-16.5
20S	- 1.7	- 1.5	1.5	5.9	8.7	12.5	16.0	15.0	9.8	0.5	- 5.0	-10.0	-11.5	-15.0
30S	- 0.6	1.6	4.5	11.0	14.3	18.2	24.0	23.0	14.2	4.8	- 1.5	- 4.5	- 5.5	- 8.0
40S	0.4	4.0	8.8	13.8	17.3	20.0	23.0	22.0	17.2	10.0	7.0	6.0	5.5	2.0
50S	7.5	10.2	13.2	17.2	21.0	23.1	24.2	22.2	18.7	15.2	14.7	14.5	13.5	11.0
60S	6.0	7.5	10.0	13.0	15.0	17.0	19.0	19.5	18.5	18.0	19.5	20.0	20.5	20.0
70S	0.0	- 1.0	2.0	6.0	8.4	10.5	12.8	14.0	15.5	16.5	17.5	20.8	22.0	22.0
80S	- 1.0	0.2	1.8	4.8	6.5	8.0	8.8	9.5	10.5	12.0	12.5	14.0	14.0	14.0
90S	0.0	0.0	0.0	0.0	0.0	0.0	0.0	0.0	0.0	0.0	0.0	0.0	0.0	0.0

TABLE 4.2

(continued)

(c) June-August

<u>P(mb)</u>	<u>1000</u>	<u>850</u>	<u>700</u>	<u>500</u>	<u>400</u>	<u>300</u>	<u>200</u>	<u>150</u>	<u>100</u>	<u>70</u>	<u>50</u>	<u>30</u>	<u>20</u>	<u>10</u>
<u>Lat.</u>														
90N	0.0	0.0	0.0	0.0	0.0	0.0	0.0	0.0	0.0	0.0	0.0	0.0	0.0	0.0
80N	0.0	1.9	2.5	3.5	3.3	2.9	2.7	2.2	1.3	0.0	- 1.2	- 2.1	- 2.5	- 3.6
70N	- 0.2	0.9	2.5	3.8	4.4	4.7	4.9	4.0	2.3	- 0.3	- 2.0	- 4.0	- 5.0	- 6.2
60N	0.4	1.9	3.2	5.2	6.5	7.9	8.7	7.6	4.1	1.1	- 1.6	- 4.5	- 6.0	- 7.4
50N	0.9	3.7	5.8	9.0	11.0	13.7	15.7	13.9	7.7	3.2	- 1.3	- 5.1	- 7.0	- 9.1
40N	0.8	2.7	4.7	8.8	10.7	14.7	17.9	15.5	8.7	1.0	- 4.2	- 8.0	-10.0	-12.0
30N	- 0.9	0.1	1.5	2.7	4.2	5.5	6.9	4.4	- 1.6	- 7.5	-10.3	-14.5	-15.6	-17.3
20N	- 1.5	- 2.1	- 2.1	- 3.2	- 2.5	- 0.9	- 1.7	- 4.7	-10.6	-12.7	-16.5	-20.3	-21.2	-24.1
10N	- 1.0	- 1.4	- 3.2	- 4.4	- 5.0	- 5.6	- 7.7	- 9.2	-11.3	-11.0	-12.2	-17.0	-19.7	-24.4
0	- 1.4	- 1.8	- 3.4	- 5.1	- 6.0	- 6.6	- 7.8	- 5.3	- 4.4	- 1.6	- 5.0	- 9.5	-12.1	-16.0
10S	- 2.5	- 3.8	- 2.0	- 2.8	- 1.3	1.9	3.3	4.5	1.2	1.1	- 1.3	- 3.0	- 5.0	- 9.0
20S	- 1.6	- 1.9	2.3	10.0	15.0	20.6	22.3	20.5	11.4	4.6	2.5	2.0	2.0	- 2.3
30S	0.0	4.5	7.5	16.0	22.0	29.0	33.5	31.0	22.5	12.0	8.0	9.0	10.0	10.0
40S	5.0	6.5	9.0	14.0	16.8	20.0	24.5	26.0	22.5	20.0	19.5	23.0	26.0	28.0
50S	8.0	10.0	12.5	16.0	19.0	22.0	25.0	27.5	29.0	33.0	33.5	40.0	43.0	44.0
60S	5.0	6.5	7.5	9.5	13.5	16.5	20.0	23.0	28.0	33.0	38.0	44.0	49.0	50.0
70S	- 2.0	- 0.5	2.5	6.0	8.0	10.5	14.5	17.0	22.0	26.5	31.0	41.0	44.0	44.0
80S	- 2.0	- 0.5	1.0	4.0	5.0	6.5	8.0	9.5	12.0	15.0	17.5	24.0	25.0	25.0
90S	0.0	0.0	0.0	0.0	0.0	0.0	0.0	0.0	0.0	0.0	0.0	0.0	0.0	0.0

TABLE 4.2

(continued)

(d) September–November

<u>P(mb)</u>	<u>1000</u>	<u>850</u>	<u>700</u>	<u>500</u>	<u>400</u>	<u>300</u>	<u>200</u>	<u>150</u>	<u>100</u>	<u>70</u>	<u>50</u>	<u>30</u>	<u>20</u>	<u>10</u>
<u>Lat.</u>														
90N	0.0	0.0	0.0	0.0	0.0	0.0	0.0	0.0	0.0	0.0	0.0	0.0	0.0	0.0
80N	- 0.2	- 0.0	0.5	2.1	3.1	3.9	4.6	4.8	4.4	4.0	4.6	6.1	7.5	9.7
70N	0.1	0.7	2.0	4.4	5.6	7.1	8.1	8.0	6.2	7.7	8.3	9.7	12.0	15.5
60N	0.7	3.7	5.2	7.9	9.0	10.7	12.2	11.9	8.7	10.5	10.0	10.7	13.5	16.2
50N	1.7	5.6	8.7	13.0	15.5	18.3	20.2	18.5	13.0	12.9	10.3	9.8	11.5	14.4
40N	1.0	3.6	7.0	12.8	15.3	21.7	23.7	20.2	15.0	9.0	5.0	4.0	6.0	10.0
30N	- 1.0	0.0	2.7	7.7	10.4	14.3	18.3	15.8	9.2	2.3	- 1.0	- 1.0	0.0	5.0
20N	- 1.9	- 2.8	- 1.5	0.1	2.3	5.3	7.2	7.1	0.4	- 3.2	- 7.0	-11.0	-10.0	- 7.5
10N	- 1.4	- 3.6	- 3.8	- 3.8	- 3.3	- 1.8	- 1.2	- 1.2	- 3.8	- 5.2	- 8.5	-12.5	-14.6	-16.0
0	- 1.5	- 2.3	- 3.2	- 4.1	- 4.0	- 3.8	- 3.4	- 0.9	- 1.4	- 0.7	- 8.0	-12.0	-14.0	-15.5
10S	- 2.5	- 3.5	- 2.6	- 1.7	- 0.4	1.3	4.1	5.0	0.1	- 0.9	- 5.5	-10.0	-12.0	-14.0
20S	- 2.6	- 1.5	3.0	9.0	13.0	17.5	21.5	19.6	10.0	2.0	- 2.0	- 5.5	- 8.0	-12.0
30S	- 0.8	2.2	7.0	13.9	18.8	24.0	28.2	26.0	16.6	8.0	2.5	- 1.5	- 3.0	- 5.0
40S	5.2	6.9	9.8	14.6	17.7	20.2	23.0	22.5	19.2	16.0	14.5	13.0	11.5	8.5
50S	7.5	9.8	12.8	17.2	20.8	23.0	25.5	26.5	26.5	27.0	27.0	26.5	25.0	22.5
60S	5.5	7.8	10.5	14.0	15.5	18.0	20.5	23.5	26.5	29.5	32.5	36.0	37.5	37.0
70S	- 2.5	- 1.0	2.0	5.0	6.8	9.5	12.5	15.5	19.0	22.5	25.5	30.0	31.0	32.5
80S	- 1.5	- 0.4	0.6	2.3	3.0	4.0	5.0	6.1	8.5	11.2	13.5	16.3	16.5	16.3
90S	0.0	0.0	0.0	0.0	0.0	0.0	0.0	0.0	0.0	0.0	0.0	0.0	0.0	0.0

TABLE 4.3
 MEAN MERIDIONAL WIND (m sec⁻¹)
 (a) December-February

<u>P(mb)</u>	<u>1000</u>	<u>850</u>	<u>700</u>	<u>500</u>	<u>400</u>	<u>300</u>	<u>200</u>	<u>150</u>	<u>100</u>	<u>70</u>	<u>50</u>	<u>30</u>	<u>20</u>	<u>10</u>	<u>Vert. Avg.</u>
<u>Lat.</u>															
90N	0.00	0.00	0.00	0.00	0.00	0.00	0.00	0.00	0.00	0.00	0.00	0.00	0.00	0.00	0.00
80N	-0.15	-0.09	-0.01	0.06	0.08	0.09	0.09	0.09	0.16	0.25	0.33	0.30	0.16	-0.18	0.03
70N	-0.10	-0.06	-0.03	0.01	0.05	0.07	0.08	0.07	0.08	0.07	0.06	-0.10	-0.30	-0.67	-0.00
60N	0.12	0.09	0.06	0.01	-0.02	-0.05	-0.07	-0.08	-0.05	-0.05	-0.10	-0.25	-0.40	-0.54	-0.00
50N	0.80	0.50	0.10	-0.08	-0.26	-0.32	-0.35	-0.34	-0.23	-0.15	-0.13	-0.10	-0.09	0.01	0.02
40N	0.65	0.30	0.06	-0.05	-0.15	-0.28	-0.32	-0.30	-0.16	-0.07	0.00	0.08	0.15	0.26	0.01
30N	0.08	0.06	0.05	0.04	0.04	-0.02	-0.16	-0.24	-0.06	0.04	0.05	0.10	0.15	0.23	0.01
20N	-1.50	-0.43	-0.05	0.09	0.00	0.08	1.25	1.20	0.66	0.14	0.07	0.02	0.06	0.10	0.02
10N	-1.58	-1.20	-0.26	-0.04	-0.34	0.41	2.88	2.14	0.57	-----	-----	-----	-----	-----	0.00
0	-0.40	-0.93	-0.45	-0.21	-0.47	0.60	2.47	1.52	0.17	-----	-----	-----	-----	-----	0.00
10S	0.45	-0.24	-0.33	-0.21	-0.23	0.27	0.70	0.58	0.30	-----	-----	-----	-----	-----	0.01
20S	0.31	-0.07	-0.11	-0.03	-0.03	0.00	-0.03	0.13	0.27	-----	-----	-----	-----	-----	0.00
30S	0.04	0.03	0.04	0.00	-0.04	-0.06	-0.08	0.00	0.02	-----	-----	-----	-----	-----	-0.00
40S	-0.08	-0.06	-0.06	-0.02	0.02	0.12	0.17	0.10	-0.04	-----	-----	-----	-----	-----	0.00
50S	-0.08	-0.06	-0.05	-0.00	0.04	0.09	0.12	0.06	-0.03	-----	-----	-----	-----	-----	0.00
60S	-0.04	-0.02	-0.01	-0.00	0.01	0.02	0.05	0.03	0.01	-----	-----	-----	-----	-----	0.00
70S	0.02	0.01	0.02	-0.01	-0.03	-0.05	-0.03	0.02	0.05	-----	-----	-----	-----	-----	0.00
80S	0.02	0.01	0.01	0.01	-0.01	-0.02	-0.03	0.01	0.04	-----	-----	-----	-----	-----	0.00
90S	0.00	0.00	0.00	0.00	0.00	0.00	0.00	0.00	0.00	-----	-----	-----	-----	-----	0.00

TABLE 4.3

(continued)

(b) March-May

<u>P(mb)</u>	<u>1000</u>	<u>850</u>	<u>700</u>	<u>500</u>	<u>400</u>	<u>300</u>	<u>200</u>	<u>150</u>	<u>100</u>	<u>70</u>	<u>50</u>	<u>30</u>	<u>20</u>	<u>10</u>	<u>Vert. Avg.</u>
<u>Lat.</u>															
90N	0.00	0.00	0.00	0.00	0.00	0.00	0.00	0.00	0.00	0.00	0.00	0.00	0.00	0.00	0.00
80N	0.01	0.02	0.04	0.05	0.08	0.06	-0.04	-0.05	-0.05	-0.01	-0.02	-0.03	-0.05	-0.07	0.02
70N	-0.06	-0.03	0.00	0.02	0.04	0.04	0.02	-0.01	-0.01	-0.01	-0.02	-0.05	-0.08	-0.11	-0.00
60N	-0.05	0.01	0.05	0.01	-0.01	-0.02	-0.02	-0.03	-0.02	-0.02	-0.02	-0.03	-0.04	-0.05	-0.00
50N	0.50	0.30	0.08	-0.08	-0.20	-0.24	-0.24	-0.18	-0.09	-0.02	-0.01	0.01	0.02	0.03	0.01
40N	0.40	0.25	0.01	-0.08	-0.12	-0.15	-0.18	-0.18	-0.12	-0.04	-0.01	0.01	0.02	0.02	0.00
30N	0.05	0.10	0.12	0.03	0.00	-0.13	-0.25	-0.28	-0.20	-0.04	-0.01	0.01	0.02	0.02	-0.01
20N	-0.83	0.03	0.09	-0.01	-0.11	-0.06	0.45	0.38	0.11	0.00	-0.03	-0.02	0.01	0.06	-0.00
10N	-1.20	-0.12	-0.17	0.00	-0.11	0.10	1.19	0.88	0.11	----	----	----	----	----	-0.00
0	-0.16	0.19	-0.29	-0.10	-0.04	0.24	0.38	0.16	-0.17	----	----	----	----	----	0.00
10S	1.08	0.68	-0.15	-0.21	-0.04	0.06	-0.99	-0.94	-0.24	----	----	----	----	----	-0.00
20S	0.71	0.30	-0.07	-0.08	-0.05	-0.04	-0.60	-0.41	0.01	----	----	----	----	----	-0.00
30S	0.02	0.01	0.01	0.00	0.00	-0.02	-0.06	-0.01	0.01	----	----	----	----	----	-0.00
40S	-0.08	-0.06	-0.07	0.00	0.07	0.12	0.13	0.06	-0.05	----	----	----	----	----	0.00
50S	-0.08	-0.06	-0.05	0.00	0.04	0.12	0.11	0.04	-0.04	----	----	----	----	----	0.00
60S	-0.05	-0.04	0.00	-0.01	0.01	0.06	0.07	0.03	-0.01	----	----	----	----	----	0.00
70S	0.02	0.02	0.02	-0.05	-0.04	-0.03	0.04	0.04	0.03	----	----	----	----	----	0.00
80S	0.03	0.02	-0.02	-0.04	-0.03	-0.03	0.03	0.08	0.08	----	----	----	----	----	0.00
90S	0.00	0.00	0.00	0.00	0.00	0.00	0.00	0.00	0.00	----	----	----	----	----	0.00

TABLE 4.3

(continued)

(c) June-August

<u>P(mb)</u>	<u>1000</u>	<u>850</u>	<u>700</u>	<u>500</u>	<u>400</u>	<u>300</u>	<u>200</u>	<u>150</u>	<u>100</u>	<u>70</u>	<u>50</u>	<u>30</u>	<u>20</u>	<u>10</u>	<u>Vert.</u> <u>Avg.</u>
<u>Lat.</u>															
90N	0.00	0.00	0.00	0.00	0.00	0.00	0.00	0.00	0.00	0.00	0.00	0.00	0.00	0.00	0.00
80N	0.01	0.01	0.02	0.03	0.04	0.01	-0.03	-0.06	-0.02	0.01	0.01	0.01	0.01	0.01	0.01
70N	0.02	0.03	0.04	0.03	0.02	-0.01	-0.05	-0.06	-0.03	-0.01	-0.01	-0.01	-0.01	-0.01	0.01
60N	0.10	0.08	0.05	0.01	-0.01	-0.07	-0.11	-0.11	-0.05	0.00	0.00	0.00	0.00	0.00	0.01
50N	0.30	0.18	0.02	-0.01	-0.05	-0.11	-0.16	-0.17	-0.05	0.02	0.01	0.01	0.01	0.01	0.01
40N	0.15	0.06	0.02	0.01	0.00	-0.04	-0.09	-0.12	-0.06	-0.01	0.00	0.00	0.00	0.00	0.01
30N	-0.10	-0.02	0.08	0.02	-0.05	-0.05	0.00	0.08	-0.04	-0.08	-0.04	-0.01	0.00	0.01	-0.00
20N	-0.05	0.20	0.13	0.08	-0.05	-0.17	-0.33	-0.35	-0.23	-0.12	-0.05	0.00	0.02	0.03	-0.02
10N	0.38	0.75	0.06	0.05	0.12	-0.30	-1.30	-1.20	0.28	-----	-----	-----	-----	-----	-0.01
0	1.40	1.61	0.33	-0.26	0.21	-0.70	-2.70	-2.20	0.17	-----	-----	-----	-----	-----	0.01
10S	2.31	1.88	0.31	-0.56	0.00	-0.85	-2.83	-2.35	-0.39	-----	-----	-----	-----	-----	-0.01
20S	1.07	0.68	0.01	-0.26	-0.09	-0.33	-0.91	-0.74	-0.08	-----	-----	-----	-----	-----	-0.01
30S	0.02	0.02	0.00	-0.01	-0.01	-0.01	-0.01	-0.01	-0.01	-----	-----	-----	-----	-----	0.00
40S	-0.11	-0.08	-0.06	0.02	0.08	0.14	0.12	0.02	-0.06	-----	-----	-----	-----	-----	0.00
50S	-0.11	-0.08	-0.03	0.03	0.08	0.14	0.06	0.00	-0.06	-----	-----	-----	-----	-----	0.00
60S	-0.07	-0.04	-0.00	0.01	0.04	0.06	0.02	0.00	-0.03	-----	-----	-----	-----	-----	0.00
70S	0.01	0.03	0.04	-0.02	-0.05	-0.07	-0.03	0.02	0.02	-----	-----	-----	-----	-----	0.00
80S	0.05	0.00	-0.06	-0.02	-0.04	-0.06	0.02	0.19	0.13	-----	-----	-----	-----	-----	0.00
90S	0.00	0.00	0.00	0.00	0.00	0.00	0.00	0.00	0.00	-----	-----	-----	-----	-----	0.00

TABLE 4.3

(continued)

(d) September–November

<u>P(mb)</u>	<u>1000</u>	<u>850</u>	<u>700</u>	<u>500</u>	<u>400</u>	<u>300</u>	<u>200</u>	<u>150</u>	<u>100</u>	<u>70</u>	<u>50</u>	<u>30</u>	<u>20</u>	<u>10</u>	<u>Vert. Avg.</u>
<u>Lat.</u>															
90N	0.00	0.00	0.00	0.00	0.00	0.00	0.00	0.00	0.00	0.00	0.00	0.00	0.00	0.00	0.00
80N	-0.20	-0.15	-0.06	0.03	0.10	0.10	0.09	0.07	0.01	-0.04	-0.04	-0.03	-0.02	0.00	-0.02
70N	-0.07	-0.02	0.01	0.02	0.02	0.02	0.02	0.00	0.00	0.01	0.00	-0.03	-0.05	-0.09	0.00
60N	0.25	0.18	0.12	0.01	-0.08	-0.14	-0.18	-0.17	-0.10	-0.02	-0.01	-0.03	-0.05	-0.08	0.02
50N	0.65	0.35	0.07	-0.06	-0.19	-0.26	-0.28	-0.26	-0.14	-0.03	-0.01	0.00	0.00	0.01	0.02
40N	0.25	0.15	0.00	-0.01	-0.03	-0.09	-0.15	-0.18	-0.09	-0.01	0.01	0.04	0.06	0.09	0.01
30N	-0.40	-0.20	0.03	0.10	0.12	0.07	0.15	0.25	0.15	0.03	0.04	0.07	0.10	0.13	0.01
20N	-0.75	-0.32	-0.04	0.17	0.19	0.18	0.30	0.37	0.40	0.00	0.01	0.03	0.07	0.08	0.01
10N	-0.03	0.04	-0.17	0.10	0.23	0.04	-0.18	-0.02	0.16	-----	-----	-----	-----	-----	0.01
0	0.95	0.64	0.00	-0.11	0.20	-0.27	-1.25	-0.91	-0.10	-----	-----	-----	-----	-----	0.00
10S	1.33	0.73	0.15	-0.22	0.08	-0.35	-1.48	-1.24	-0.14	-----	-----	-----	-----	-----	-0.00
20S	0.68	0.35	0.06	-0.10	-0.04	-0.26	-0.56	-0.40	0.02	-----	-----	-----	-----	-----	0.01
30S	0.05	0.06	0.03	-0.02	-0.06	-0.10	-0.03	0.02	0.04	-----	-----	-----	-----	-----	-0.00
40S	-0.09	-0.07	-0.06	-0.00	0.06	0.16	0.10	0.04	-0.04	-----	-----	-----	-----	-----	0.00
50S	-0.13	-0.11	-0.06	0.02	0.09	0.17	0.12	0.03	-0.07	-----	-----	-----	-----	-----	0.00
60S	-0.08	-0.06	-0.03	0.01	0.04	0.08	0.09	0.02	-0.05	-----	-----	-----	-----	-----	0.00
70S	0.03	0.02	0.02	-0.01	-0.04	-0.05	0.00	0.01	0.00	-----	-----	-----	-----	-----	0.00
80S	0.09	0.03	0.02	-0.00	-0.04	-0.09	-0.07	-0.00	0.06	-----	-----	-----	-----	-----	0.00
90S	0.00	0.00	0.00	0.00	0.00	0.00	0.00	0.00	0.00	-----	-----	-----	-----	-----	0.00

TABLE 4.4
 MEAN VERTICAL VELOCITY (mm sec⁻¹)
 (a) December-February

<u>P(mb)</u>	<u>1000</u>	<u>850</u>	<u>700</u>	<u>500</u>	<u>400</u>	<u>300</u>	<u>200</u>	<u>150</u>	<u>100</u>	<u>70</u>	<u>50</u>	<u>30</u>	<u>20</u>	<u>10</u>
<u>Lat.</u>														
85N	-0.43	-0.81	-1.11	-1.34	-1.41	-1.48	-1.71	-1.92	-2.16	-2.10	-1.69	-0.61	0.29	0.96
75N	0.17	0.17	0.17	0.15	0.17	0.26	0.50	0.74	1.14	1.51	1.85	2.23	2.24	2.10
65N	-0.02	0.20	0.41	0.67	0.76	0.79	0.81	0.80	0.81	0.85	0.88	0.75	0.52	0.28
55N	-0.16	0.59	1.08	1.38	1.38	1.18	0.82	0.50	-0.01	-0.42	-0.80	-1.24	-1.38	-1.38
45N	0.05	-0.04	-0.16	-0.22	-0.19	-0.17	-0.31	-0.46	-0.66	-0.82	-0.94	-1.02	-0.93	-0.80
35N	-0.02	-0.49	-0.75	-0.87	-0.83	-0.62	-0.35	-0.32	-0.31	-0.22	-0.13	-0.06	-0.03	-0.01
25N	-0.09	-1.50	-2.24	-3.03	-3.61	-4.47	-4.00	-2.45	-0.61	0.09	0.28	0.39	0.37	0.34
15N	0.15	-0.47	-1.36	-2.28	-3.12	-3.92	-2.43	-0.60	0.37	-----	-----	-----	-----	-----
5N	0.01	0.96	1.18	1.05	1.00	1.32	1.56	1.09	0.30	-----	-----	-----	-----	-----
5S	-0.04	0.99	1.82	2.59	3.32	4.07	2.50	0.67	-0.10	-----	-----	-----	-----	-----
15S	0.04	0.06	0.39	1.10	1.64	1.99	1.25	0.48	0.03	-----	-----	-----	-----	-----
25S	0.01	-0.11	0.08	0.35	0.44	0.49	0.52	0.50	0.21	-----	-----	-----	-----	-----
35S	-0.01	-0.15	-0.32	-0.59	-0.68	-0.60	-0.24	0.01	0.05	-----	-----	-----	-----	-----
45S	0.00	0.02	0.05	0.14	0.19	0.20	0.11	0.02	-0.02	-----	-----	-----	-----	-----
55S	0.00	0.07	0.14	0.25	0.27	0.22	0.08	-0.03	-0.04	-----	-----	-----	-----	-----
65S	0.01	0.07	0.13	0.20	0.21	0.18	0.05	-0.02	-0.02	-----	-----	-----	-----	-----
75S	-0.02	-0.03	-0.06	-0.10	-0.08	-0.02	0.06	0.08	0.04	-----	-----	-----	-----	-----
85S	0.04	0.00	-0.02	-0.07	-0.08	-0.04	0.08	0.14	0.06	-----	-----	-----	-----	-----

TABLE 4.4

(continued)

(b) March-May

<u>P(mb)</u>	<u>1000</u>	<u>850</u>	<u>700</u>	<u>500</u>	<u>400</u>	<u>300</u>	<u>200</u>	<u>150</u>	<u>100</u>	<u>70</u>	<u>50</u>	<u>30</u>	<u>20</u>	<u>10</u>
<u>Lat.</u>														
85N	-0.30	-0.32	-0.29	-0.17	-0.01	0.25	0.45	0.42	0.34	0.33	0.39	0.46	0.46	0.42
75N	0.11	0.04	-0.01	-0.06	-0.07	-0.08	-0.02	0.05	0.13	0.21	0.27	0.33	0.33	0.30
65N	0.01	0.02	0.09	0.19	0.20	0.15	0.09	0.05	0.02	-0.01	-0.05	-0.08	-0.09	-0.08
55N	-0.08	0.48	0.84	1.04	1.01	0.82	0.48	0.23	-0.03	-0.15	-0.21	-0.26	-0.26	-0.24
45N	0.05	0.04	-0.00	-0.10	-0.09	-0.01	0.10	0.13	0.08	0.02	-0.00	-0.00	0.01	0.02
35N	0.10	-0.18	-0.22	0.01	0.19	0.35	0.36	0.27	0.09	0.00	-0.01	-0.01	-0.01	-0.01
25N	-0.04	-0.70	-0.89	-1.26	-1.63	-2.10	-1.81	-1.06	-0.26	0.02	0.05	-0.02	-0.08	-0.13
15N	-0.02	-0.40	-0.80	-1.41	-1.68	-1.95	-1.33	-0.50	-0.02	----	----	----	----	----
5N	-0.01	0.88	1.19	1.26	1.49	2.09	1.91	1.04	0.20	----	----	----	----	----
5S	0.03	1.18	1.88	2.55	2.98	3.55	2.62	1.07	0.05	----	----	----	----	----
15S	-0.03	-0.57	-0.93	-0.92	-1.00	-1.36	-1.40	-0.87	-0.20	----	----	----	----	----
25S	0.01	-0.66	-0.95	-1.03	-1.12	-1.33	-1.00	-0.38	0.00	----	----	----	----	----
35S	-0.03	-0.14	-0.28	-0.47	-0.51	-0.44	-0.16	0.02	0.05	----	----	----	----	----
45S	0.01	0.03	0.07	0.13	0.12	0.10	0.05	0.00	-0.02	----	----	----	----	----
55S	-0.01	0.04	0.12	0.21	0.22	0.16	0.03	-0.04	-0.03	----	----	----	----	----
65S	0.02	0.11	0.18	0.23	0.22	0.14	-0.00	-0.05	-0.03	----	----	----	----	----
75S	0.00	-0.01	-0.05	-0.07	-0.03	0.02	0.01	-0.02	-0.01	----	----	----	----	----
85S	-0.01	-0.07	-0.08	0.04	0.15	0.30	0.46	0.40	0.14	----	----	----	----	----

TABLE 4.4
 (continued)
 (c) June-August

<u>P(mb)</u>	<u>1000</u>	<u>850</u>	<u>700</u>	<u>500</u>	<u>400</u>	<u>300</u>	<u>200</u>	<u>150</u>	<u>100</u>	<u>70</u>	<u>50</u>	<u>30</u>	<u>20</u>	<u>10</u>
<u>Lat.</u>														
85N	-0.14	-0.14	-0.12	-0.03	0.07	0.19	0.23	0.12	-0.06	-0.11	-0.10	-0.09	-0.08	-0.06
75N	-0.04	-0.02	0.03	0.12	0.16	0.18	0.17	0.14	0.12	0.11	0.10	0.09	0.08	0.06
65N	0.01	0.12	0.21	0.30	0.33	0.31	0.21	0.11	-0.01	-0.04	-0.04	-0.04	-0.03	-0.02
55N	-0.08	0.16	0.27	0.30	0.31	0.27	0.18	0.07	-0.06	-0.07	-0.06	-0.05	-0.04	-0.04
45N	0.05	-0.08	-0.17	-0.19	-0.18	-0.12	-0.01	0.05	0.08	0.06	0.04	0.04	0.03	0.02
35N	0.08	-0.13	-0.16	-0.11	-0.16	-0.27	-0.28	-0.10	0.14	0.13	0.06	-0.01	-0.02	-0.04
25N	0.10	0.30	0.58	0.93	1.17	1.33	1.14	0.73	0.21	0.02	-0.04	-0.08	-0.08	-0.06
15N	-0.08	0.58	1.09	1.31	1.70	2.16	1.31	-0.06	-0.58	----	----	----	----	----
5N	-0.12	1.13	2.24	2.92	3.32	3.83	2.61	1.07	0.08	----	----	----	----	----
5S	0.12	0.88	1.22	1.17	0.99	0.87	0.86	0.90	0.43	----	----	----	----	----
15S	0.00	-1.70	-3.24	-4.28	-4.94	-5.71	-4.19	-1.97	-0.25	----	----	----	----	----
25S	-0.04	-1.21	-1.97	-2.27	-2.44	-2.63	-1.86	-0.83	-0.07	----	----	----	----	----
35S	-0.01	-0.16	-0.30	-0.43	-0.42	-0.30	-0.05	0.08	0.06	----	----	----	----	----
45S	-0.00	0.02	0.06	0.13	0.14	0.14	0.06	-0.01	-0.01	----	----	----	----	----
55S	0.00	0.09	0.16	0.24	0.23	0.15	-0.00	-0.06	-0.03	----	----	----	----	----
65S	0.02	0.12	0.23	0.30	0.27	0.13	-0.06	-0.10	-0.05	----	----	----	----	----
75S	-0.00	-0.02	-0.12	-0.25	-0.26	-0.25	-0.22	-0.17	-0.04	----	----	----	----	----
85S	-0.05	-0.11	-0.06	0.10	0.22	0.47	0.79	0.68	0.19	----	----	----	----	----

TABLE 4.4

(continued)

(d) September–November

<u>P(mb)</u>	<u>1000</u>	<u>850</u>	<u>700</u>	<u>500</u>	<u>400</u>	<u>300</u>	<u>200</u>	<u>150</u>	<u>100</u>	<u>70</u>	<u>50</u>	<u>30</u>	<u>20</u>	<u>10</u>
<u>Lat.</u>														
85N	0.20	-0.17	-0.50	-0.74	-0.70	-0.50	-0.22	0.02	0.26	0.30	0.24	0.13	0.06	0.00
75N	-0.08	-0.02	0.07	0.17	0.17	0.14	0.11	0.06	0.02	0.06	0.16	0.28	0.33	0.34
65N	-0.14	0.19	0.48	0.81	0.88	0.83	0.64	0.44	0.19	0.09	0.07	0.08	0.07	0.06
55N	-0.04	0.42	0.65	0.73	0.70	0.58	0.37	0.21	0.00	-0.10	-0.16	-0.22	-0.23	-0.24
45N	0.08	-0.21	-0.42	-0.57	-0.54	-0.40	-0.24	-0.19	-0.18	-0.20	-0.24	-0.29	-0.28	-0.26
35N	-0.07	-0.74	-1.12	-1.28	-1.31	-1.33	-1.20	-0.87	-0.37	-0.20	-0.20	-0.21	-0.19	-0.16
25N	0.02	-0.34	-0.56	-0.73	-0.74	-0.72	-0.57	-0.44	-0.09	0.15	0.15	0.14	0.12	0.12
15N	0.02	0.72	1.02	1.08	1.28	1.52	1.20	0.74	0.27	-----	-----	-----	-----	-----
5N	0.06	1.13	1.94	2.51	2.82	3.18	2.35	1.17	0.20	-----	-----	-----	-----	-----
5S	0.03	0.33	0.57	0.81	0.78	0.77	0.64	0.33	0.03	-----	-----	-----	-----	-----
15S	-0.08	-0.83	-1.37	-1.77	-2.12	-2.67	-2.12	-1.02	-0.13	-----	-----	-----	-----	-----
25S	0.07	-0.56	-0.92	-1.15	-1.32	-1.49	-1.04	-0.42	-0.01	-----	-----	-----	-----	-----
35S	-0.02	-0.19	-0.39	-0.60	-0.61	-0.40	-0.02	0.10	0.06	-----	-----	-----	-----	-----
45S	-0.00	-0.03	-0.04	-0.01	0.03	0.04	0.05	0.05	0.02	-----	-----	-----	-----	-----
55S	0.01	0.11	0.21	0.31	0.30	0.19	0.02	-0.04	-0.03	-----	-----	-----	-----	-----
65S	0.01	0.13	0.25	0.36	0.35	0.24	0.02	-0.08	-0.05	-----	-----	-----	-----	-----
75S	0.00	0.01	-0.01	-0.01	0.02	0.05	0.01	-0.04	-0.03	-----	-----	-----	-----	-----
85S	-0.03	-0.17	-0.27	-0.39	-0.41	-0.28	0.02	0.16	0.09	-----	-----	-----	-----	-----

REFERENCES

- Berggren, R. and A. Nyberg, 1967: Eddy vertical transport of latent and sensible heat. Tellus, 19, 18-23.
- Bjerknes, J., 1969: Atmospheric teleconnections from the equatorial Pacific. Mon. Wea. Rev., 97, 163-172.
- Brown, J.A., Jr., 1967: On atmospheric zonal to eddy kinetic energy exchange for January 1963. Tellus, 19, 14-17.
- Brunt, D., 1926: Energy of the earth's atmosphere. Phil. Mag., 7(1), 523-532.
- Buch, H., 1954: Hemispheric wind conditions during the year 1950. Final Rep., part 2, M.I.T., Depart. of Meteorology, Planetary Circulations Project, Contract No. AF 19(122)-153, 126 pp.
- Budyko, M.I., 1963: Atlas of heat balance of the globe. Moscow.
- Budyko, M.I. and K.Y. Kondratiev, 1964: The heat balance of the earth. Research in Geophysics, Vol. 2: Solid earth and interface phenomena, 529-554.
- Crutcher, H.L., 1959: Upper wind statistics charts of the Northern Hemisphere (850, 700 and 500 mb levels). Office of the Chief of Naval Operations, Navaer 50-1C-535, Vols. I and II.
- _____, 1961: Meridional cross-sections. Upper winds over the Northern Hemisphere. U.S. Dept. of Commerce, National Weather Records Center, U.S. Weather Bureau, Technical paper, No. 41, 307 pp.
- _____, 1966: Components of the 1000 mb winds (or surface winds) of the Northern Hemisphere. Navair 50-1C-51, published by direction of the Chief of Naval Operations, U.S. Govt. Printing Office, Washington, D.C.
- Davis, P.A., 1961: A re-examination of the heat budget of the troposphere and lower stratosphere. Sci. Rep. No. 3, New York Univ., College of Engineering, AF 19(604)-6146.
- _____, 1963: An analysis of the atmospheric heat budget. J. Atmos. Sci., 20, 5-22.
- Dutton, J.A. and D.R. Johnson, 1967: The theory of available potential energy and a variation approach to atmospheric energetics.

- Advances in Geophysics; 12, New York, Academic Press, 333-436.
- Ellsaesser, H.W., 1969: A climatology of epsilon (Atmospheric Dissipation). Mon. Wea. Rev., 97, 415-423.
- Garstang, M., 1967: Sensible and latent heat exchange in low latitude synoptic scale systems. Tellus, 19, 492-508.
- Gilman, P.A., 1965: The mean meridional circulation of the Southern Hemisphere inferred from momentum and mass balance. Tellus, 17, 277-284.
- Goldie, N., J.G. Moore and E.E. Austin, 1958: Geophys. Mem., 13, No. 101, London, 101 pp.
- Gordon, A.H., 1953: Seasonal changes in the mean pressure distribution over the world and some inferences about the general circulation. Bull. Amer. Met. Soc., 34, 357-367.
- Hadley, G., 1735: Concerning the cause of the general trade winds. Phil. Trans., 29, 58-62.
- Halley, E., 1686: An historical account of the trade-winds and monsoons observable in the seas between and near the tropics with an attempt to assign the physical cause of said winds. Phil. Trans., 26, 153-168.
- Hann, J. and R. Süring, 1943: Lehrbuch der meteorologie. 1, lief 15, publ. by Willibald Keller, Leipzig, Germany.
- Heastie, H. and P.M. Stephenson, 1960: Upper winds over the world. Geophys. Mem., 13, No. 103, London, 213 pp.
- Hering, W.S. and T.R. Borden, 1964: Ozonesonde observations over North America. Vol. 2. Environmental Research Papers. No. 38, AFCRL-64-30(11).
- Holopainen, E.O., 1963: On the dissipation of kinetic energy in the atmosphere. Tellus, 15, 26-32.
- _____, 1967: On the mean meridional circulation and the flux of angular momentum over the northern hemisphere. Tellus, 19, 1-13.
- Houghton, H.G., 1950: A preliminary quantitative analysis of precipitation mechanisms. J. Meteor., 7, 363-369.
- _____, 1968: On precipitation mechanisms and their artificial modification. J. Appl. Meteor., 7, 851-859.

- Jensen, C.E., 1961: Energy transformation and vertical flux processes over the Northern Hemisphere. J. Geophys. Res., 66, 1145-1156.
- Katayama, A., 1967: On the radiation budget of the troposphere over the Northern Hemisphere, II and III. J. Met. Soc. Japan, 45, 1-39.
- Keshava Murty, R.N., 1968: On the maintenance of the mean zonal motion in the Indian summer monsoon. Mon. Wea. Rev., 96, 23-31.
- Kidson, J.W., D.G. Vincent and R.E. Newell, 1969: Observational Studies of the general circulation of the tropics: Long term mean values. Quart. J. Roy. Meteor. Soc., 95, 258-287.
- Kung, E.C., 1966a: Kinetic energy generation and dissipation in the large-scale atmospheric circulations. Mon. Wea. Rev., 94, 67-82.
- _____, 1966b: Large scale balance of kinetic energy in the atmosphere. Mon. Wea. Rev., 94, 627-640.
- _____, 1967: Diurnal and long-term variations of the kinetic energy generation and dissipation for a five-year period. Mon. Wea. Rev., 95, 593-606.
- _____, 1969: Further study on the kinetic energy balance. Mon. Wea. Rev., 97, 573-581.
- Lettau, H., 1954: A study of the mass, momentum and energy budget of the atmosphere. Arch. Met. Geophys. Bioklima, 7, 133-157.
- London, J., 1957: A study of the atmospheric heat balance. Final Rep., College of Engineering, Research Division, Dept. of Meteorology and Oceanography, New York Univ., AFC-TR-57-287, OTS PB 129551, 99 pp.
- Lorenz, E.N., 1955a: Available potential energy and the maintenance of the general circulation. Tellus, 7, 157-167.
- _____, 1955b: Generation of available potential energy and the intensity of the general circulation. Large scale synoptic processes. Final Rep., Univ. of California (Los Angeles), Dept. of Meteorology.
- _____, 1967: The nature and theory of the general circulation of the atmosphere. World Meteor. Org., 161 pp.
- Malkus, J.S., and H. Riehl, 1964: Cloud structure and distributions over the tropical Pacific Ocean. Univ. of California Press,

- Berkeley and Los Angeles, 229 pp.
- Malkus, J.S. and C. Ronne, 1954: On the structure of some cumulonimbus clouds which penetrated the high tropical troposphere. Tellus, 6, 351-366.
- Malkus, J.S. and R.T. Williams, 1963: On the interaction between severe storms and large cumulus clouds. Met. Monographs, 5, No. 27, Publ. by Amer. Meteor. Soc., 59-64.
- Manabe, S. and B.G. Hunt, 1968: Experiments with a stratospheric general circulation model: I. Radiative and dynamical aspects. Mon. Wea. Rev., 96, 477-502.
- Manabe, S. and J. Smagorinsky, 1967: Simulated climatology of a general circulation model with a hydrological cycle, Part II: Analysis of the tropical atmosphere. Mon. Wea. Rev., 95, 155-169.
- Margules, M., 1903: Über die Energie der Stürme. Jahrb Zentralanst. Vienna, 1-26. English trans. Abbe, C., 1910: The mechanics of the Earth's atmosphere, 3rd Coll., Washington, Smithsonian Inst., 533-595.
- Mason, B.J., 1962: Clouds, Rain and Rainmaking. Cambridge Univ. Press, London, England, 145 pp.
- Miyakoda, K., 1963: Some characteristic features of the winter circulation in the troposphere and lower stratosphere. Tech. Rep. No. 14, Grant NSF-GP-4710, Univ. of Chicago, 93 pp.
- Miyakoda, K., J. Smagorinsky, R.F. Strickler, and G.O. Hembree, 1969: Experimental extended predictions with a nine-level hemispheric model. Mon. Wea. Rev., 97, 1-76.
- Morin, M., 1966: Mean 200 and 100 mb charts for the Southern Hemisphere, contours and isotherms for the months July, October, and April, from July 1959 to April 1961, Tech. Rep. No. 5, Commonwealth Bureau of Meteorology (reprint in English from Monographic No. 40, Meteorologie Nationale Paris, 1965).
- Muench, H.S., 1965: On the dynamics of the wintertime stratospheric circulation. J. Atmos. Sci., 22, 349-360.
- Murakami, T., 1962: Stratospheric wind, temperature and isobaric height conditions during the IGY period, Part I. Rep. No. 5, M.I.T. Dept. of Meteorology, Planetary Circulations Project, AT (30-1)2241 and AF 19(604)-5223.
- Murgatroyd, R.J., 1969: A note on the contributions of the mean and

eddy terms to the momentum and heat balances of the troposphere and lower stratosphere. Quart. J. Roy. Meteor. Soc., 95, 194-202.

Newell, R.E., J.W. Kidson and D.G. Vincent, 1969: Annual and biennial modulations in the tropical Hadley cell circulation. Nature, 222, No. 5188, 76-78.

_____, 1970a: The general circulation of the tropical atmosphere and interactions with extra-tropical latitudes. (To be published by M.I.T. Press).

Newell, R.E. and M.E. Richards, 1969: Energy flux and convergence patterns in the lower and middle stratosphere during the IQSY. Quart. J. Roy. Meteor. Soc., 95, 310-328.

Newell, R.E., D.G. Vincent, T.G. Dopplick, D. Ferruzza and J.W. Kidson, 1970b: The energy balance of the global atmosphere. Paper presented at the Conference on the Global Circulation of the Atmosphere, London, August 1969, Proceedings to be published by the Roy. Meteor. Soc.

Obasi, G.O.P., 1963a: Atmospheric momentum and energy calculations for the Southern Hemisphere during the IGY. Rep. No. 6, M.I.T. Dept. of Meteorology, Planetary Circulations Project, 353 pp.

_____, 1963b: Poleward flux of atmospheric angular momentum in the Southern Hemisphere. J. Atmos. Sci., 20, 516-528.

_____, 1965: On the maintenance of the kinetic energy of mean zonal flow in the Southern Hemisphere. Tellus, 17, 95-105.

Oort, A.H., 1964: On estimates of the atmosphere energy cycle. Mon. Wea. Rev., 92, 483-493.

Palmen, E., H. Riehl and L.A. Vuorela, 1958: On the meridional circulation and release of kinetic energy in the tropics. J. Meteor., 15, 271-277.

Palmen, E. and L.A. Vuorela, 1963: On the mean meridional circulations in the Northern Hemisphere during the winter season. Quart J. Roy. Meteor. Soc., 89, 131-138.

Peixoto, J.P., 1960a: Hemispheric temperature conditions during the year 1950. Rep. No. 4, M.I.T. Dept. of Meteorology, Planetary Circulations Project, 211 pp.

_____, 1960b: Contribucao para o estudo dos campos medios da distribucao e do fluxo meridional da entalpia na atmosfera. Prize essay 'Artur Malheiros', Academy of Science, Lisbon, 39 pp.

- _____, 1965: On the role of water vapor in the energetics of the general circulation of the atmosphere. Portugaliae Physica, 4, fasc. 2, 135-170.
- Peng, L., 1963: Stratospheric wind, temperature and isobaric height conditions during the IGY period, Part II. Rep. No. 10, M.I.T. Dept. of Meteorology, Planetary Circulations Project, AT (30-1) 2241 and AF 19(604)-5225.
- _____, 1965: A simple numerical experiment concerning the general circulation in the lower stratosphere. Pure and Appl. Geophys. 61, 197-218.
- Perry, J.S., 1967: Long-wave energy processes in the 1963 sudden stratosphere warming. J. Atmos. Sci., 24, 539-550.
- Priestley, C.H.B., 1949: Heat transport and zonal stress between latitudes. Quart. J. Roy. Meteor. Soc., 75, 28-40.
- Reed, R.J. and C.L. Vleck, 1969: The annual temperature variation in the lower tropical stratosphere. J. Atmos. Sci., 26, 163-167.
- Richards, M.E., 1967: The energy budget of the stratosphere during 1965. Rep. No. 21, M.I.T., Dept. of Meteorology, Planetary Circulations Project, 171 pp.
- Riehl, H., 1950: On the role of the tropics in the general circulation of the atmosphere. Tellus, 2, 1-17.
- _____, 1954: Tropical Meteorology. McGraw-Hill Book Company, Inc., New York, 392 pp.
- _____, 1969: On the role of the tropics in the general circulation of the atmosphere. Weather, 288-308.
- Riehl, H. and J.S. Malkus, 1958: On the heat balance in the equatorial trough zone. Geophysica, 6:3-4, 503-538.
- Robinson, J.B., 1968: Mean meridional eddy flux of enthalpy in the Southern Hemisphere during the IGY. Master's thesis, M.I.T., Dept. of Meteorology, 77 pp.
- Rodgers, C.D., 1967: The radiative heat budget of the troposphere and lower stratosphere. Rep. No. A2, M.I.T., Dept. of Meteorology, Planetary Circulations Project, NSF Grant No. GA-400, 99 pp.
- Schwerdtfeger, W. and D.W. Martin, 1964: The zonal flow of the free atmosphere between 10N and 80S, in the South American sector.

- J. Appl. Meteor., 3, 726-733.
- Smith, F.B., 1955: Geostrophic and ageostrophic wind analysis. Quart. J. Roy. Meteor. Soc., 81, 403-413.
- Smith, P.J., 1969: On the contribution of a limited region to the global energy budget. Tellus, 21, 202-207.
- Solot, S.B., and J.K. Angell, 1969: Temperate latitude 200 mb zonal winds from GHOST balloon flights in the Southern Hemisphere. J. Atmos. Sci., 26, 574-579.
- Starr, V.P. and B. Saltzman, 1966: A compilation of journal articles on observational studies of the atmospheric general circulation. Sci. Rep. No. 2, M.I.T., Dept. of Meteorology, Planetary Circulations Project, AF 19(628)-5816.
- Starr, V.P. and J.M. Wallace, 1964: Mechanics of eddy processes in the tropical troposphere. Pure and Appl. Geophys., 58, 138-144.
- Starr, V.P. and R.M. White, 1954: Balance requirement of the general circulation. Geophys. Res. papers, No. 35. Geophys. Res. Directorate, AFCRL, Cambridge, 57 pp.
- Streten, N.A., 1969: A case study of the winter circulation at 700 and 500 mb in middle and high southern latitudes. Mon. Wea. Rev., 97, 193-199.
- Telegades, K. and J. London, 1954: A physical model of the northern hemisphere troposphere for winter and summer. Sci. Rep. No. 1, New York Univ., College of Engineering, AF 19(122)-165.
- Thompson, B.W., 1965: The Climate of Africa. Oxford Univ. Press, Nairobi. 132 pp (atlas).
- Trout, D. and H.A. Panofsky, 1969: Energy dissipation near the tropopause. Tellus, 21, 355-358.
- Tucker, G.B., 1959: Mean meridional circulations in the atmosphere. Quart. J. Roy. Meteor. Soc., 85, 209-224.
- _____, 1965: The equatorial tropospheric wind regime. Quart. J. Roy. Meteor. Soc., 91, 140-150.
- Tuller, S.E., 1968: World distribution of mean monthly and annual precipitable water. Mon. Wea. Rev., 96, 785-797.
- U.S. Navy Marine Climatic Atlas of the World, Volume VII, Antarctica, 1965: NAVWEPS 50-1C-50.

- Vernekar, A.D., 1966: On mean meridional circulations in the atmosphere. Tech. Rep. No. 1, Univ. of Michigan, Dept. of Meteorology and Oceanography, U.S. Weather Bureau Grant No. WBG-44.
- _____, 1967: On mean meridional circulations in the atmosphere. Mon. Wea. Rev., 95, 705-721.
- Vincent, D.G., 1968: Mean meridional circulations in the Northern Hemisphere lower stratosphere during 1964 and 1965. Quart. J. Roy. Meteor. Soc., 94, 333-349.
- Vuorela, L.A. and I. Tuominen, 1964: On the mean zonal and meridional circulations and the flux of moisture in the Northern Hemisphere during the summer season. Pure and Appl. Geophys., 57, 167-180.
- Weyant, W.S., 1966: The Antarctic Atmosphere: Climatology of the Troposphere and Lower Stratosphere, Antarctic Map Folio Series, No. 4, AGU publication.
- White, R.M., 1954: The counter-gradient flux of sensible heat in the lower stratosphere, Tellus, 6, 177-179.
- Wiin-Nielsen, A., 1967: On the annual variation and spectral distribution of atmospheric energy. Tellus, 19, 540-559.

BIOGRAPHICAL NOTE

Dayton G. Vincent was born in Hornell, New York on April 23, 1936. He received an A.B. degree from the University of Rochester in 1958 and was commissioned a second lieutenant in the United States Air Force. He completed a basic meteorology course at St. Louis University in 1959 and served as a weather officer in France until 1962. He received an M.Sc. degree from the University of Oklahoma in 1964. He worked as a research meteorologist at the University of Oklahoma and at the United States Naval Weapons Laboratory in Dahlgren, Virginia until he was awarded a research assistantship at M.I.T. He published technical reports at Oklahoma and Virginia; while at M.I.T. he has published an article in the Quarterly Journal, Royal Meteorological Society, 1968, entitled, "Mean Meridional Circulations in the Northern Hemisphere Stratosphere During 1964-1965" and has been a co-author in other papers. He is married to the former Carol Sue Dressler of Hornell, New York and they have two children.